JOURNAL OF PROPULSION AND POWER
Vol. 22, No. 2, March–April 2006

Sealing in Turbomachinery

Raymond E. Chupp
General Electric Global Research, Niskayuna, New York 12302
Robert C. Hendricks
NASA John H. Glenn Research Center at Lewis Field, Cleveland, Ohio 44135
Scott B. Lattime
The Timken Company, North Canton, Ohio 44720
and
Bruce M. Steinetz
NASA John H. Glenn Research Center at Lewis Field, Cleveland, Ohio 44135

Dr. Chupp's career spans nearly 40 years in gas turbine design and development. In his current mechanical engineering position at GE Global Research, he has led several efforts to develop abradable tip seals for GE Energy gas-turbine product line. Previous work includes developing brush and other type advanced seals to significantly reduce leakage for expendable and long-life gas turbine engines; design of internal flow systems for various advanced aircraft and industrial gas turbines; leading experimental studies of impingement heat transfer and applying the results to airfoil design; and developing a thermal remote sensing technique for semitransparent materials. Dr. Chupp received his undergraduate degree from Kettering University and his MS and PhD degrees from Purdue University. He has worked at four different gas turbine manufactures during his career. He has authored 34 publications in gas turbine sealing and heat transfer, and has been granted 9 patents, with additional applications being reviewed.

Mr. Hendricks began his career solving combustion problems in the NACA X-15 LOX-ammonia rocket engine. His attention then turned to fluid hydrogen heat transfer data used in all LOX-Hydrogen engine designs. He also provided fundamental understanding for boiling, two-phase flows, supercritical and near-critical fluid behavior and produced the thermophysical property codes GASP and WASP. Analyzed and validated cryogenic two-phase choked flows and the extended theory of corresponding states for fluid flow. His data showed SSME failures were caused by seal instabilities leading to research in sealing and rotordynamics. This work on a variety of seals and secondary cavity flows resulted in the design codes SCISEAL and INDSEAL and conclusively demonstrated that small changes in leakage can enhance engine performance by altering flows throughout the entire engine, prompting interactive analyses of turbomachine sealing with demonstrated increases in engine performance. His research work also includes TBC's, component life prediction, trapped vortex combustors, water injection of turbomachines. He has authored some 300 publications, and has received several NASA and paper presentation awards.

Dr. Lattime has over nine years of experience as a research engineer in the industrial rotating machinery and aerospace markets with a focus on advanced bearing and seal design. For the past five years, Dr. Lattime has been a member of the Seal Team at the NASA Glenn Research Center. His research included the development of innovative seals, actuators, and kinematic designs to manage blade tip clearance in the high-pressure turbine for aero-based gas turbine engines. Presently, Dr. Lattime is a Product Development Specialist at the Timken Research Center in Canton, Ohio where his research is focused on the development of advanced seals, bearings, and power transmissions for new products supporting the industrial rotating machinery market. Dr. Lattime earned both a Master's Degree and doctorate in Mechanical Engineering from the University of Akron. He has authored over twenty technical papers including six journal publications and one book chapter.

Dr. Steinetz serves as NASA Glenn's Seal Team Leader. He technically directs the development of advanced turbomachinery seals (shaft seals, active mechanical tip clearance control, regenerative seals, etc), hypersonic engine and re-entry vehicle seals, and vehicle docking and berthing seals for NASA's Space Exploration Initiative. Notable projects include development and test of seals for the X-38 and X-37 (test vehicles for future re-entry systems); solid rocket motor thermal barriers (Shuttle and Atlas V), and evaluation of Shuttle Discovery main-landing gear door seals for return-to-flight. Dr. Steinetz patented and led the development of the carbon thermal barrier that prevents superheated (5500°F) rocket combustion gas within the Space Shuttle and Atlas V motors from reaching the temperature-limited elastomeric O-rings. The Glenn thermal barriers have successfully flown on three Atlas 5 missions helping enable safe delivery of three satellites into orbit. The Glenn thermal barriers will be flown on future Shuttle missions starting with STS-122. Dr. Steinetz received his degrees from Case Western Reserve University. His career at NASA spans 21 years. Dr. Steinetz has been granted 9 advanced seal patents.

Received 23 May 2005; revision received 29 August 2005; accepted for publication 30 August 2005.

Clearance control is of paramount importance to turbomachinery designers and is required to meet today's aggressive power output, efficiency, and operational life goals. Excessive clearances lead to losses in cycle efficiency, flow instabilities, and hot gas ingestion into disk cavities. Insufficient clearances limit coolant flows and cause interface rubbing, overheating downstream components and damaging interfaces, thus limiting component life. Designers have put renewed attention on clearance control, as it is often the most cost-effective method to enhance system performance. Advanced concepts and proper material selection continue to play important roles in maintaining interface clearances to enable the system to meet design goals. This work presents an overview of turbomachinery sealing to control clearances. Areas covered include characteristics of gas and steam turbine sealing applications and environments, benefits of sealing, types of standard static and dynamics seals, advanced seal designs, as well as life and limitations issues.

I. Introduction

CONTROLLING interface clearances is the most cost-effective method of enhancing turbomachinery performance. Seals control turbomachinery leakages, coolant flows and contribute to overall system rotordynamic stability. In many instances, sealing interfaces and coatings are sacrificial, like lubricants, giving up their integrity for the benefit of the component. They are subjected to abrasion, erosion, oxidation, incursive rubs, foreign object damage (FOD) and deposits, and extremes in thermal, mechanical, aerodynamic and impact loadings. Tribological pairing of materials control how well and how long these interfaces will be effective in controlling flow.

A variety of seal types and materials is required to satisfy turbomachinery sealing demands. These seals must be properly designed to maintain the interface clearances. In some cases, this will mean machining adjacent surfaces, yet in many other applications coatings are employed for optimum performance. Many seals are coating composites fabricated on superstructures or substrates that are coated with sacrificial materials, which can be refurbished either in situ or by removal, stripping, recoating, and replacing until substrate life is exceeded.

For blade and knife tip sealing, an important class of materials known as abradables permit blade or knife rubbing without significant damage or wear to the rotating element while maintaining an effective sealing interface. Most such tip interfaces are passive, yet some, as for the high-pressure turbine (HPT) case or shroud, are actively controlled.

This work presents an overview of turbomachinery sealing. Areas covered include characteristics of gas and steam turbine sealing applications and environments, benefits of sealing, types of standard static and dynamics seals, advanced seal designs, as well as life and limitations issues.

II. Sealing in Gas and Steam Turbines

A. Clearance Control Characteristics

Turbomachines range in size from centimeters (size of a penny) to ones you can almost walk through. The problem is how to control the large changes in geometry between adjacent rotor/stator components from cold build to operation. The challenge is to provide geometric control while maintaining efficiency, integrity, and long service life (e.g., estimated time to failure or maintenance and low cost[1]). Figure 1 shows the relative clearance between the rotor tip and case for a HPT during takeoff, climb, and cruise conditions.[2] The figure shows the dramatic effect of clearance control via applied cooling to the casing. A critical clearance requirement occurs at "cutback" (about 1000 s into climb-out) when takeoff thrust is reduced. Using thermal active clearance control (ACC), the running clearance is drastically reduced, producing significant cost savings in fuel reduction and increased service life. However, designers must note that changing parameters in critical seals can change the dynamics of the entire engine.[3] These effects are not always positive.

B. Sealing Benefits

Performance issues are closely tied to engine clearances. Ludwig[4] determined that improvements in fluid film sealing resulting from a proposed research program could lead to an annual energy saving, on a national basis, equivalent to about 37 million barrels (1.554 billion U.S. gallons) of oil or 0.3% of the total U.S. energy consumption (1977 statistics). In terms of engine bleed, Moore[5] cited that a 1% reduction in engine bleed gives a 0.4% reduction in specific fuel consumption (SFC), which translates into nearly 0.033 (1977 statistics) to 0.055 (2004 statistics) billion gallons of U.S. airlines fuel savings and nearly 0.28 billion gallons worldwide (2004 statistics), annually. In terms of clearance changes, Lattime and Steinetz[6] cite a 0.0254-mm (0.001-in.) change in HPT tip clearance,

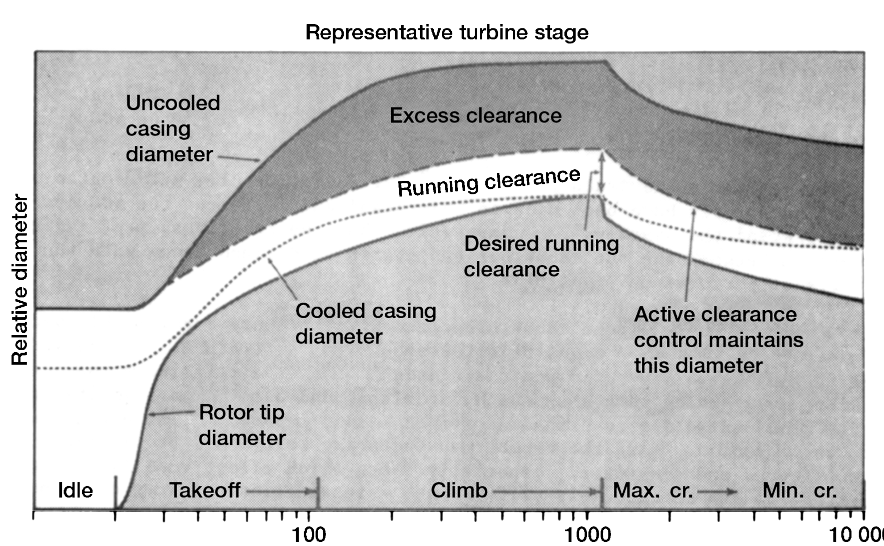

Fig. 1 Effects of case cooling on HPT blade-tip clearance during takeoff.[2]

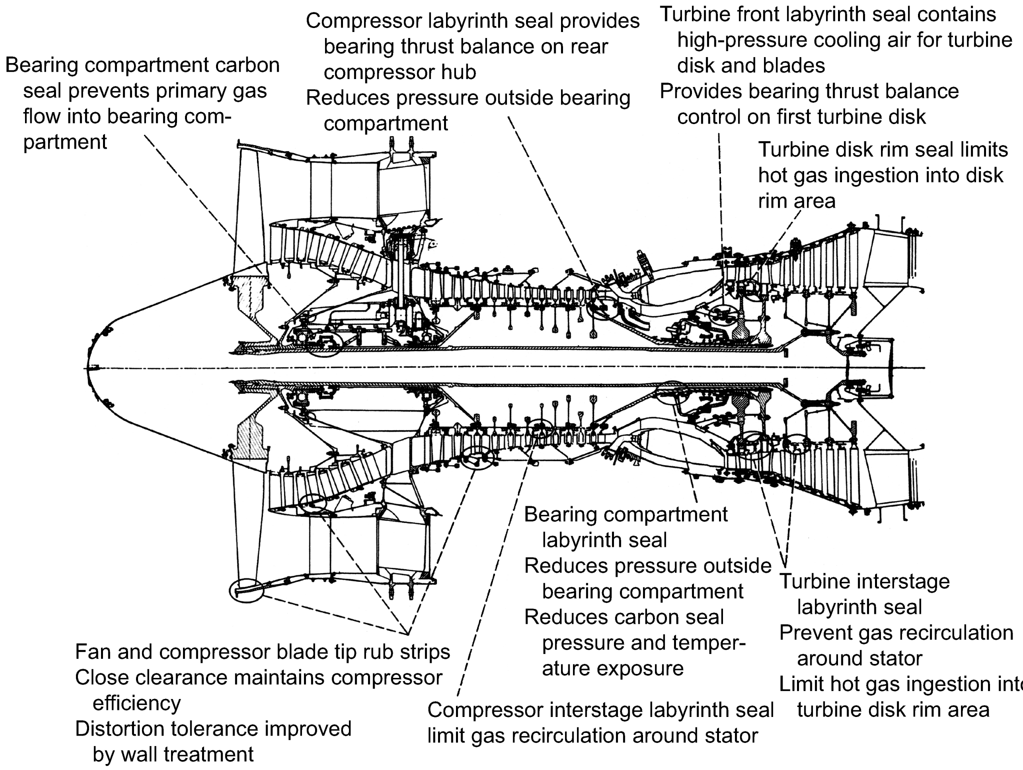

Fig. 2 Key aeroengine sealing and thermal restraint locations.[9]

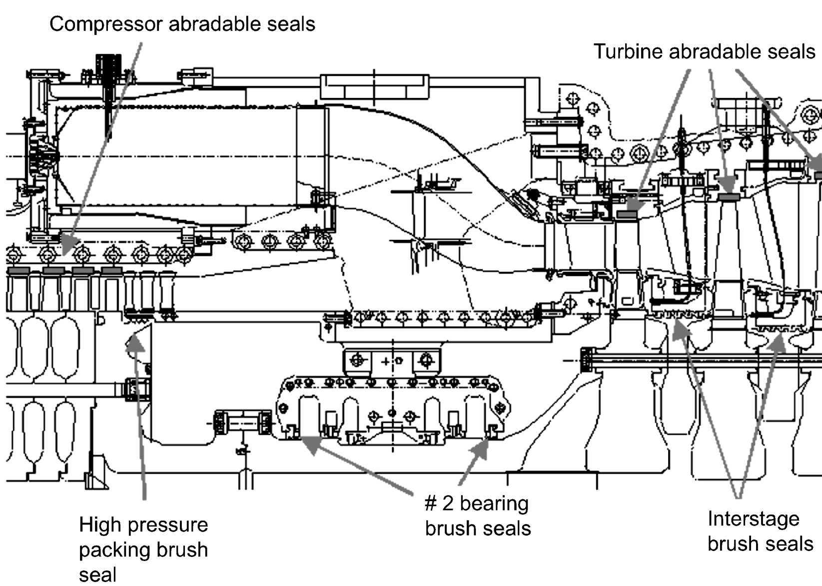

Fig. 3 Advanced seals locations in a Frame 7EA gas turbine.[10]

decreases SFC by 0.1% and exhaust gas temperature by 1°C, producing an annual savings of 0.02 billion gallons for U.S. airlines. In terms of advanced sealing, Munson et al.[7] estimate savings of over 0.5 billion gallons of fuel. Chupp et al.[8] estimated that refurbishing compressor seals would yield impressive improvements across the fleet ranging from 0.2 to 0.6% reduction in heat rate and 0.3 to 1% increase in power output. For these large, land-based gas turbines, the percentages represent huge fuel savings and monetary returns with the greatest returns cited for aging power systems.

C. Sealing Environment

1. Seal Types and Locations

Key aeroengine sealing and thermal restraint locations cited by Bill[9] are shown in Fig. 2. These include the fan and compressor shroud seals (rub strips), compressor interstage and discharge seals (labyrinth), combustor static seals, balance piston sealing, turbine shroud and rim-cavity sealing. Industrial engines have similar sealing requirements. Key sealing locations for the compressor and turbine in an industrial engine are cited by Aksit et al.[10] and Camatti et al.[11,12] and are shown in Figs. 3 and 4. Figure 3 shows high-pressure compressor (HPC) and HPT tip seal (abradable) and interstage seal (brush seal) locations, whereas Fig. 4 shows impeller shroud (labyrinth) and interstage seal (honeycomb) locations for the compressor. Compressor interstage platform seals are of the shrouded type (Figs. 5 and 6). These seals are used to minimize backflow, stage pressure losses, and reingested passage flow. Turbine stators, also of the shrouded type, prevent hot gas ingestion into the cavities that house the rotating disks and control blade and disk coolant flows. Designers need to carefully consider the differences

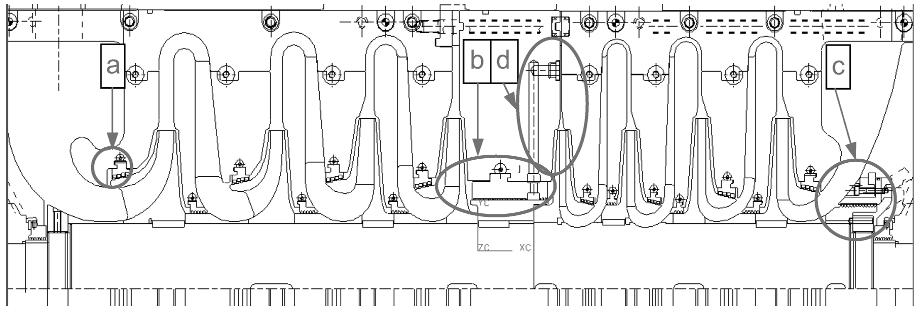

Fig. 4 Compressor cross-sectional drawing showing detail of rotor and seals: a) impeller shroud labyrinth seal, b) honeycomb interstage seal, c) abradable seal, and d) honeycomb interstage seal.[12]

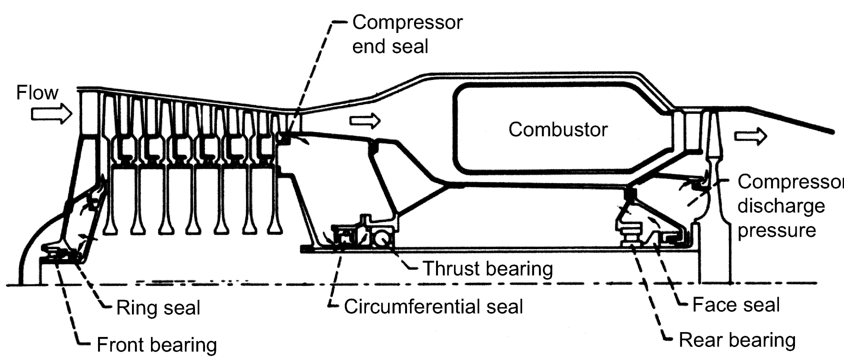

Fig. 5 Engine schematic showing main-shaft seal locations.[4]

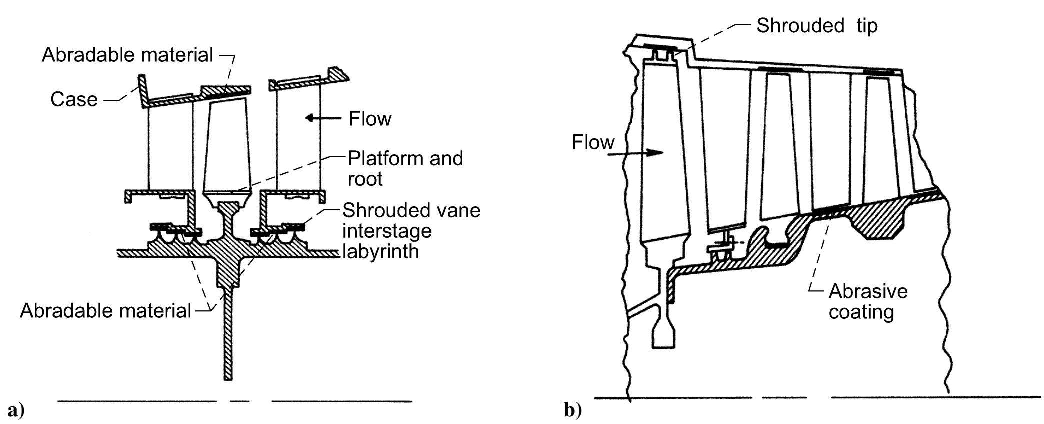

Fig. 6 Compressor sealing locations: a) blade tip and interstage and b) drum rotor.[4]

in thermal and structural characteristics, pressure gradient differences, and blade rub interfaces.

Characteristically the industrial gas turbine can be thought of as a heavy-duty derivative of an aeroengine. Still industrial and aeroturbomachines have many differences. The most notable are the fan, spools, and combustor. Aeroengines derive a large portion of their thrust though the bypass fan and usually have inline combustors, high- and low-pressure spools, drum rotors, and high exhaust velocities, all subject to flight constraints. Large industrial engines (Fig. 7) have plenum inlets, can-combustors, single spools, through-bolted-stacked disc rotors, and exhaust systems constrained by 640°C (1180°F) combined-cycle (steam-reheat-turbine) requirements. In both types of engines, core requirements are similar, yet materials restraints differ.

2. *Materials and Environmental Conditions*

Over the years, advances in new base materials, notably Ni-based single crystal alloys, and coatings have allowed increased operating temperatures of turbine engine components. Complementary to the thermal and pressure profiles, materials used range from steel to superalloys coated with metallics and ceramics. Variations in engine pressure and temperature of the Rolls-Royce Trent gas turbine[¶] are illustrated in Fig. 8. The lower-temperature blades in the fan and low-pressure compressor (LPC) sections are made of titanium, or composite materials, with corrosion-resistant coatings due to their high strength and low density. The elevated temperatures of the HPC, HPT and low-pressure turbine (LPT) require the use of nickel-based superalloys. In the HPT of aeroengines, for example, the first-stage turbine blades can see gas path temperatures around 1400°C (2550°F). To withstand these punishing temperatures for the 20,000-h and more service lives, aeroengine designers have turned to single crystal blades, with thermal barrier coatings generally using yttria-stabilized zirconia (YSZ).[2] In this configuration,

[¶]Data available online: Sourmail, T., "Coatings for Turbine Blades," University of Cambridge, URL: http://www.msm.cam.ac.uk/phase-trans/2003/Superalloys/coatings/ [cited 18 May 2005].

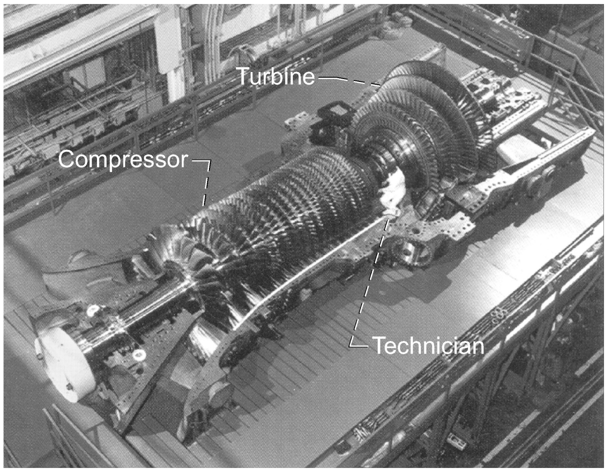

Fig. 7 General Electric's H System gas turbine, showing an 18-stage compressor and four-stage turbine.

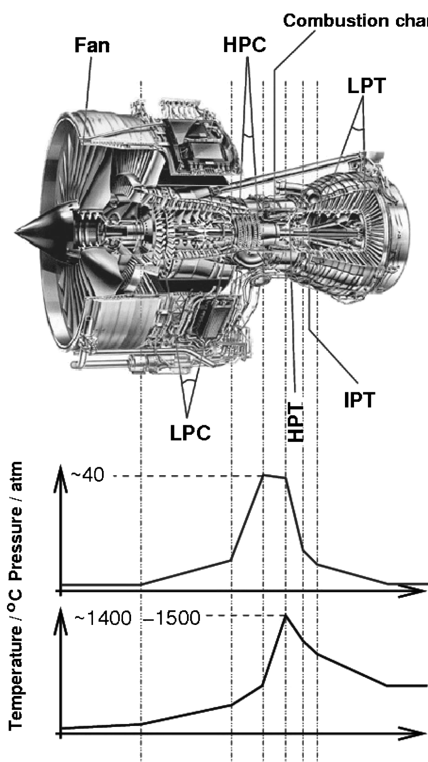

Fig. 8 Temperature and pressure profiles of a Rolls-Royce Trent gas turbine engine.¶

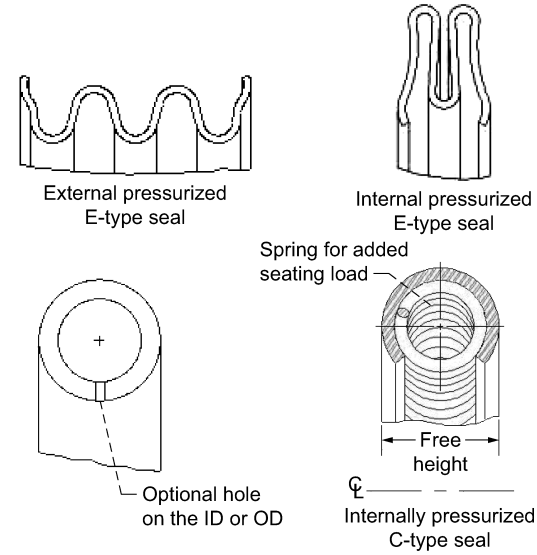

Fig. 9 Some types of metallic seals used in turbomachinery.

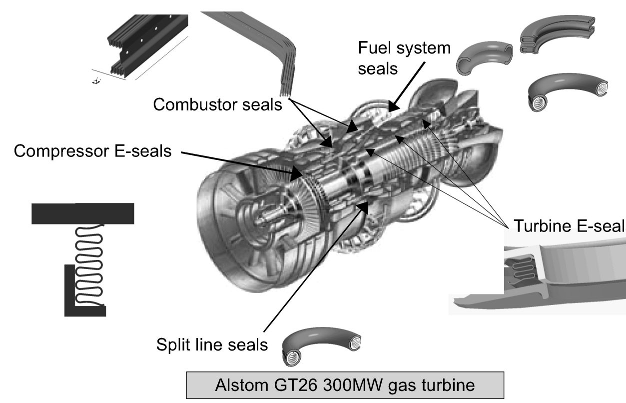

Fig. 10 Typical gas-turbine seal locations (courtesy of Advanced Products, Parker Hannifin Corporation).

blade metal temperatures reach 982°C (1800°F), and ceramic surface temperatures reach 1100°C (2010°F).

To improve blade-tip sealing effectiveness, squealer tips [approximately 0.8 mm (0.03 in.) high] are integrated into the blade. Depending on engine design, adjacent shroud seals are made of either directionally solidified cast superalloy materials coated with sprayed abradable coatings (YSZ based)[13] or single crystal shroud segments capable of the required operating temperatures.

III. Static Sealing

Sealing in static or slow interface relative movement locations in turbomachinery includes the interfaces or junctions between the stationary components (combustors, nozzles, shrouds, etc.) throughout the internal cooling flowpath to minimize or control parasitic leakage flows between turbine components. Typically, adjacent members have to sustain relative vibratory motion with minimal wear or loss of sealing over the design life of the seal. In addition, they must be compliant to accommodate thermal growth and misalignment. Effective sealing at these static interface locations not only increases turbine efficiency and output, but also improves the main gas-path temperature profile. Various compliant-interface seals have been developed to address these issues as discussed in the following sections.

A. Metallic Seals

For smaller gap movements, more conventional seals are used. These seals are metallic for higher temperature and pressure environments where rubber and polymer seals are not suitable. The wide range of applications in turbomachinery drive the need for multiple configurations, such as the O-, C-, and E-type cross section (see Fig. 9). The type of seal that is best suited for a particular application depends on operating variables such as temperature, pressure, required leakage rate, flange separation, fatigue life, and the load available to seat the seal. Figure 10 shows an example of where some metal seals are used in an industrial gas turbine. There are many smaller "feather" seals (thin sheet metal) used throughout; all interfaces require sealing of some nature.

In higher temperature environments, a large amount of thermal growth in surrounding structures is typical. This makes it necessary for the metal seal to maintain contact with the sealing surfaces while the structure moves. A seal's ability to follow the moving structure is caused by its spring back and system pressure to seat the seal. In general, E-type seals (alternatively called W seals) provide the largest amount of spring back. For this reason, the majority of

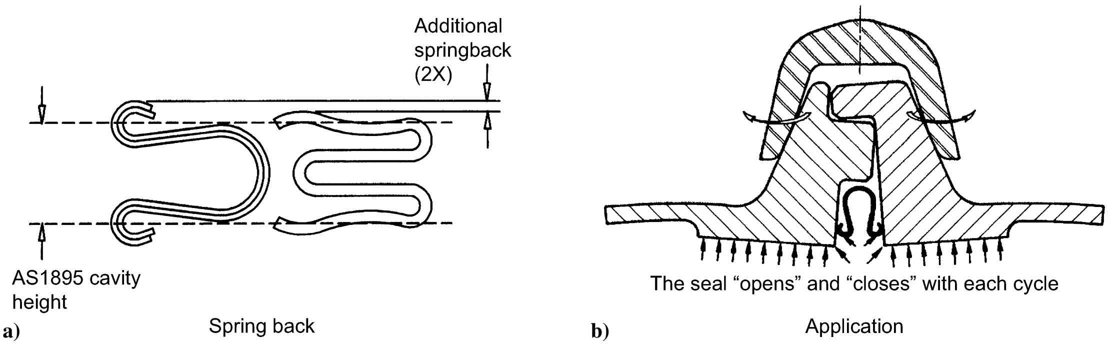

Fig. 11 U-Plex and E-seal geometry: a) spring-back comparison and b) U-Plex application.[15]

metal seals found in steam, gas, and jet engines are of the E-type configuration.

The ability of a seal to maintain a low leakage rate is mostly caused by the force the seal exerts on the mating flange, also called the "seating load." Typically speaking, the leakage rate of a seal will decrease as the seal seating load increases. C-type seals have higher seating loads than E-type seals. To further increase a C-type seal load and spring back, a spring can be inserted around the circumference on the inside of the cross section. The high load of a C seal can be used to enhance sealing performance by the addition of plating such as silver, nickel, gold, and copper. The simple geometry of a C-type seal limits further design possibilities.

The relative complexity and adaptability of the E-type seal cross sections allows for increased design variations with somewhat increased leakage rates compared to C seals. The number of convolutions, material thickness, convolution depth, and free height all play a major roll in seal performance. Despite the large thermal growth common in turbine engines, a properly designed E-type seal can have millions-of-cycles fatigue life. A majority of the E-type seals used in turbine engines is located between engine case segments, such as the horizontal joint in the combustion section on steam and gas turbines. E-type seals can also be found in the cartridge assemblies of a turbine fuel nozzle. The seal can be cut axially in one or more circumferential locations to accommodate radial growth difference or assembly requirements. Small "caps" can be placed on the seal to span the circumferential gaps to control leakage.

Currently metallic seals for higher-temperature applications are made from Inconel 718 and Waspaloy with a temperature limit of about 730°C (1350°F) (Ref. 14). Above this temperature, such seals under compressive and tensile stresses relax as a result of creep with an attendant loss in sealing performance. Development is in progress to increase the operating temperature range using strengthened [e.g., oxide-dispersion strengthened (ODS)] and refractory alloys. In laboratory tests, new superalloy Rene 41 seals have exhibited superior performance at 815–870°C (1500–1600°F) compared to standard Waspaloy seals with the same design. ODS alloys are being tested for temperatures above 870°C (1600°F) (Ref. 14).

The U-Plex seal (Fig. 11) is another self-energized static seal, similar to a multi-element E seal.[15] The E seal is a single "folded" element. The U-Plex seal consists of two or more plies of materials nested together that act independently when the seal is compressed, as does a leaf spring, yet function as one under sealing pressure. It will accommodate 2.5 to 5 times more deformation than a single ply E seal, is more compliant to surface irregularities, requires $\frac{1}{3}$ the compression force, and has enhanced high cycle fatigue resistance and comparable leakage rates.

B. Metallic Cloth Seals

For large interface gap relative movements, rigid metal strips, feather seals, and "dog-bone" shaped strips have been the primary sealing method. For applications with significant relative motion, these seals can rock and rotate or jam against the slots in the adjacent components to be sealed. A lack of flexibility can result in poor sealing and excessive wear. Compliance can be attempted by reducing the thickness of the seal strips. But the use of thinner foil seals in aircraft engine applications results in large stress levels and limited wear life. One approach to address seal compliance issues for large relative movements is the development of relatively low cost, flexible cloth seals.[10] Cloth seals are formed by combining thin sheet metals (shims) and layers of densely woven metal cloth. Whereas shims prevent through leakage and provide structural strength with flexibility, external cloth layers add sacrificial wear volume and seal thickness without adding significant stiffness. As illustrated in Fig. 12a, a typical design requires simply wrapping a layer of cloth around thin flexible shims. The assembly is held together by a number of spot welds along the seal centerline. Further leakage reduction can be achieved by a crimped design with exposed, contoured shim ends that enhance enwall sealing (Fig. 12b) (Refs. 16 and 17) or, combined with added compliance (Fig. 12c). Demonstrated leakage reductions up to 30% have been achieved in combustors and 70% in nozzle segments. The flow savings achieved in nozzle-shroud cloth seal applications translates to large performance gains of up to a 0.50% output increase and 0.25% heat rate reduction in an industrial gas turbine.

C. Cloth and Rope Seals

Rope or gasket seals can be used in various locations in turbomachinery. Table 1 lists the various materials being used. However, aircraft engine turbine inlet temperatures and industrial system temperatures continue to climb to meet aggressive cycle thermal efficiency goals. Advanced material systems, including monolithic/composites ceramics, intermetallic alloys (i.e., nickel aluminide), and carbon-carbon composites are being explored to meet aggressive temperature, durability, and weight requirements. To incorporate these materials in the high-temperature locations of the system, designers must overcome materials issues, such as differences in thermal expansion rates and lack of material ductility.[18]

Designers are finding that one way to avoid cracking and buckling of the high-temperature brittle components rigidly mounted in their support structures is to allow relative motion between the primary and supporting components.[19] Often this joint occurs in a location where differential pressures exist, requiring high-temperature seals. These seals or packings must exhibit the following important properties: operate hot [≥705°C (1300°F)]; exhibit low leakage; resist mechanical scrubbing caused by differential thermal growth and acoustic loads; seal complex geometries; retain resilience after cycling; and support structural loads.

Braided rope seals can be made with a variety of materials and combinations, each having their own strengths and weaknesses. All ceramic designs consist of a ceramic fiber, uniaxial core, overbraided with ceramic sheath layers.[20] This design offers the potential for very high-temperature 1150°C (2100°F) operation. However, researchers have determined that all ceramic seals are susceptible to the vibratory and acoustic loadings present in turbine engines. These seals can also be ejected from the seal gland because of dynamic loading.

To improve upon structural integrity, Steinetz and Adams[19] developed a hybrid braided rope seal design that consists of uniaxial ceramic core fibers overbraided with high-temperature superalloy

Table 1 Gasket/rope seal materials

Fiber material	Maximum working temperature °F	°C
Graphite		
Oxidizing environment	1000	540
Reducing	5400	2980
Fiberglass (glass dependent)	1000	540
Superalloy metals (depending on alloy)	1300–1600	705–870
Oxide ceramics (Thompkins, 1955)[18]		
Nextel 312 (62% Al_2O_3, 24% SiO_2, 14% B_2O_3)	1800[a]	980
Nextel 440 (70% Al_2O_3, 28% SiO_2, 2% B_2O_3)	2000[a]	1090
Nextel 550 (73% Al_2O_3, 27% SiO_2)	2100[a]	1150

[a]Temperature at which fiber retains 50% (nominal) room-temperature strength.

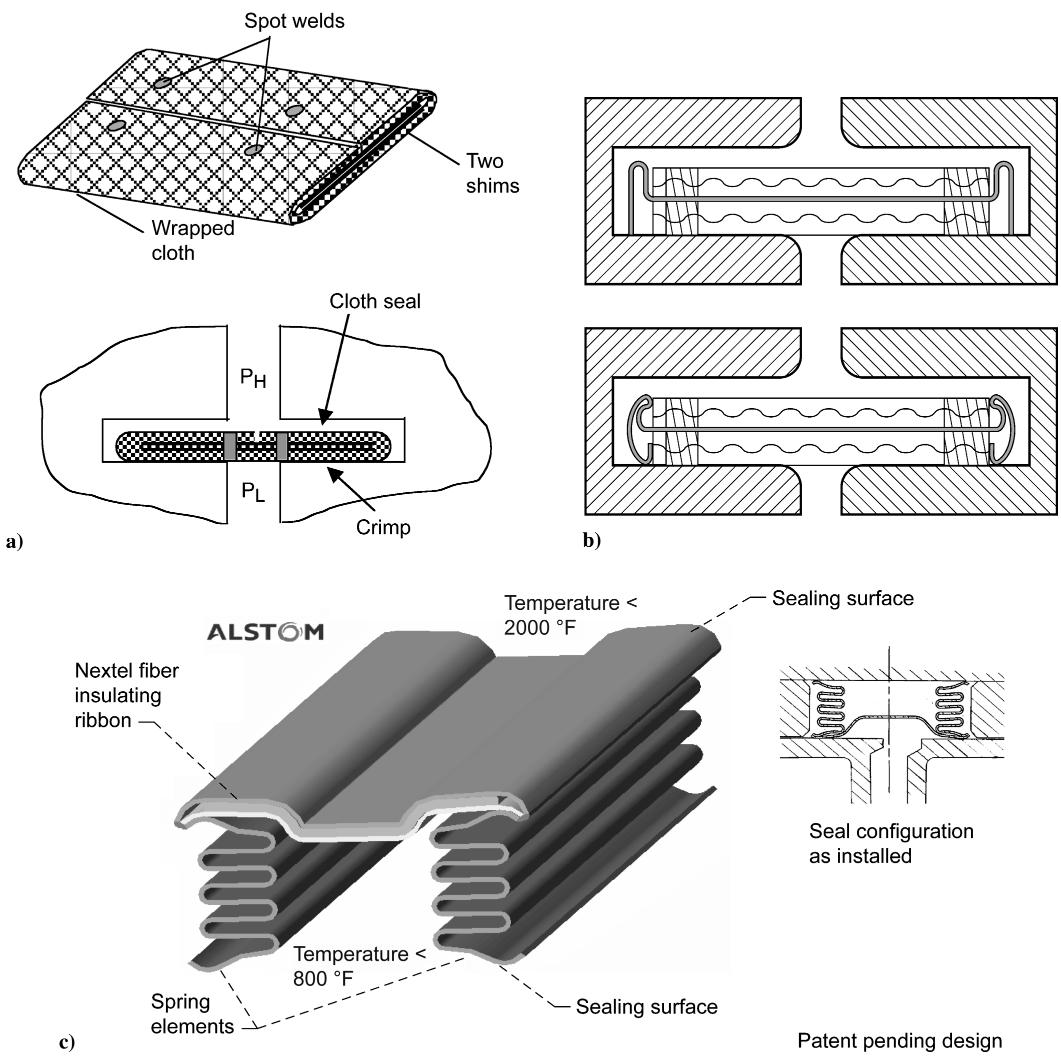

Fig. 12 Cloth seal approaches.[10,14]

wires. Tests have shown much greater resistance to abrasion and dynamic loadings. Wires made of HS-188 material show promise to 870°C (1600°F) temperatures. This hybrid construction was used to seal the last-stage articulated turning vane of the F119 turbine engine. The seal limits flow of fan cooling air past the turning vane flowpath (or power stream)/fairing interface and also prevents back-flow of potentially damaging high-temperature core air as shown in Fig. 13 (Ref. 19).

Researchers at NASA Glenn Research Center continue to strive for higher operating temperature hybrid seals. Recent oxidation studies by Opila et al.[21] showed that wires made from alumina forming scale base alloys (e.g., Plansee PM2000) could resist oxidation at temperatures to 1200°C (2200°F) for up to 70 h. Tests showed that alumina-forming alloys with reactive element additions performed best at 1200°C under all test conditions in the presence of oxygen, moisture, and temperature cycling. These wire samples exhibited slow growing and adherent oxide scales.

In other related developments, Hendricks et al.[22] discussed the modeling and application of several types of brush seals including hairpin woven or wrapped (see hybrid seal), taconite, self-purging, and buffer. Dunlap et al.[23] provide experimental data of a 0.62-in.-diam rope seal that consisted of an Inconel X 750 spring tube, filled with Saffil insulation, and covered by two layers of Nextel 312 fabric wrap for operational temperatures to 815°C (1500°F). Steinetz and Dunlap[24] developed a braided carbon-fiber thermal barrier that reduces solid-rocket combustion gas leakage [3038°C (5500°F), in a

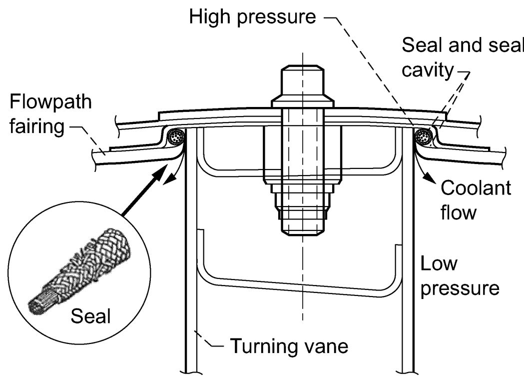

Fig. 13 Cross section of PW F119 engine showing last stage turning vane with hybrid braided rope seal around perimeter.[19]

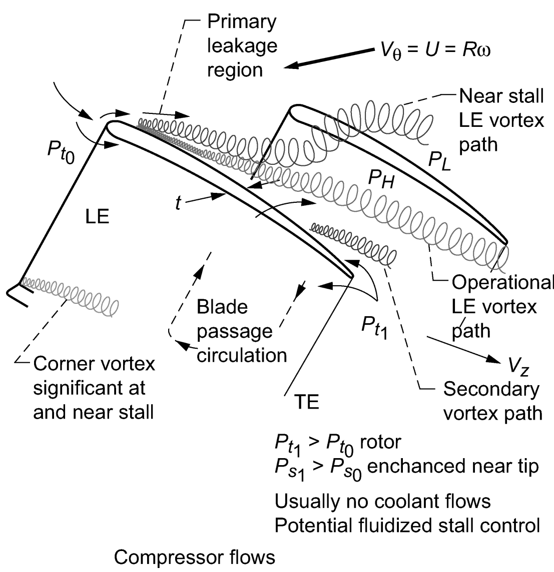

Fig. 14 Tip flow structure for an unshrouded compressor.[25]

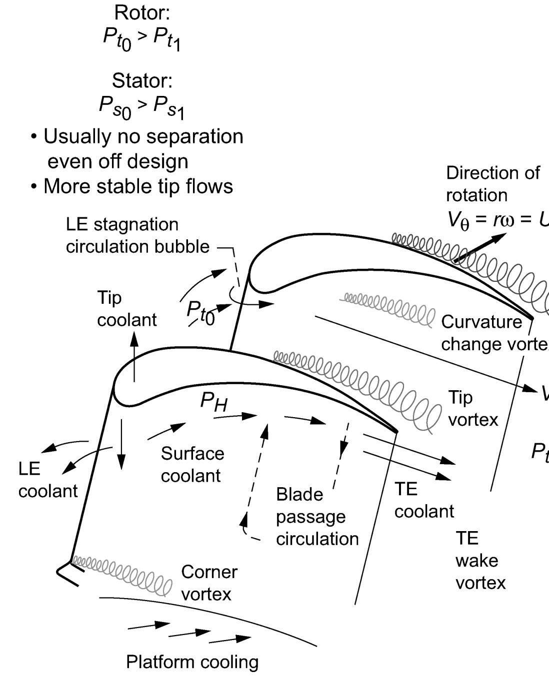

Fig. 15 Tip flow structure for an unshrouded turbine.[25]

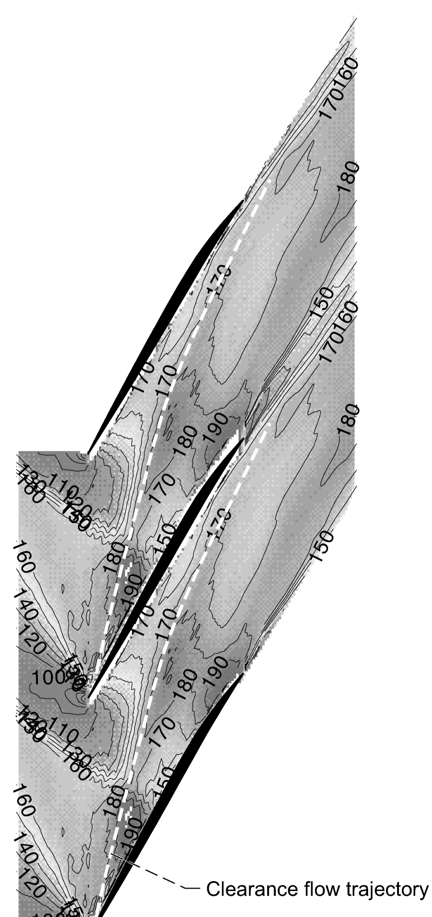

Fig. 16 Contours of axial velocity (m/s) on 92% span stream surface from LVD measurements of a transonic compressor rotor (no frame dependencies).[26]

nonoxidizing environment] and permits only relatively cool [<93°C (200°F)] gas to reach the elastomeric O-ring seals.

IV. Dynamic Seals

A. Tip Sealing

The flowfield about the tip of the blades is illustrated in Figs. 14 and 15 for the compressor and turbine, respectively. At the leading edge the flow is forced out and around the stagnation region, then joins with the primary leakage zone, and extends across the passage toward the low-pressure side and opposing the rotational velocity. These conditions are experimentally verified for tip clearance flows in the transonic compressor rotors and illustrated in Figs. 16 and 17.[26] Usually, the flow in transonic compressors is subsonic by the time it reaches the third or fourth stage.

Blade-tip flows and ensuing vortex patterns lead to flow losses, instabilities, and passage blockage. Without proper sealing, the flowfield can be reversed, resulting in compressor surge, and possible fire at the inlet. Flow losses in static elements such as vanes in the compressor and turbine have different sealing requirements as cited later. A few of these dynamic interfaces for aeroengine clearance control are illustrated in Fig. 2. More general flow details are found for example in Lakshminarayana[27] and for compressors in Copenhaver et al.,[28] Strazisar et al.,[29] and Wellborn and Okiishi.[30]

B. Abradables

Early on, researchers recognized the need for abradable materials for blade tip and vane sealing, for example, Ludwig,[4]

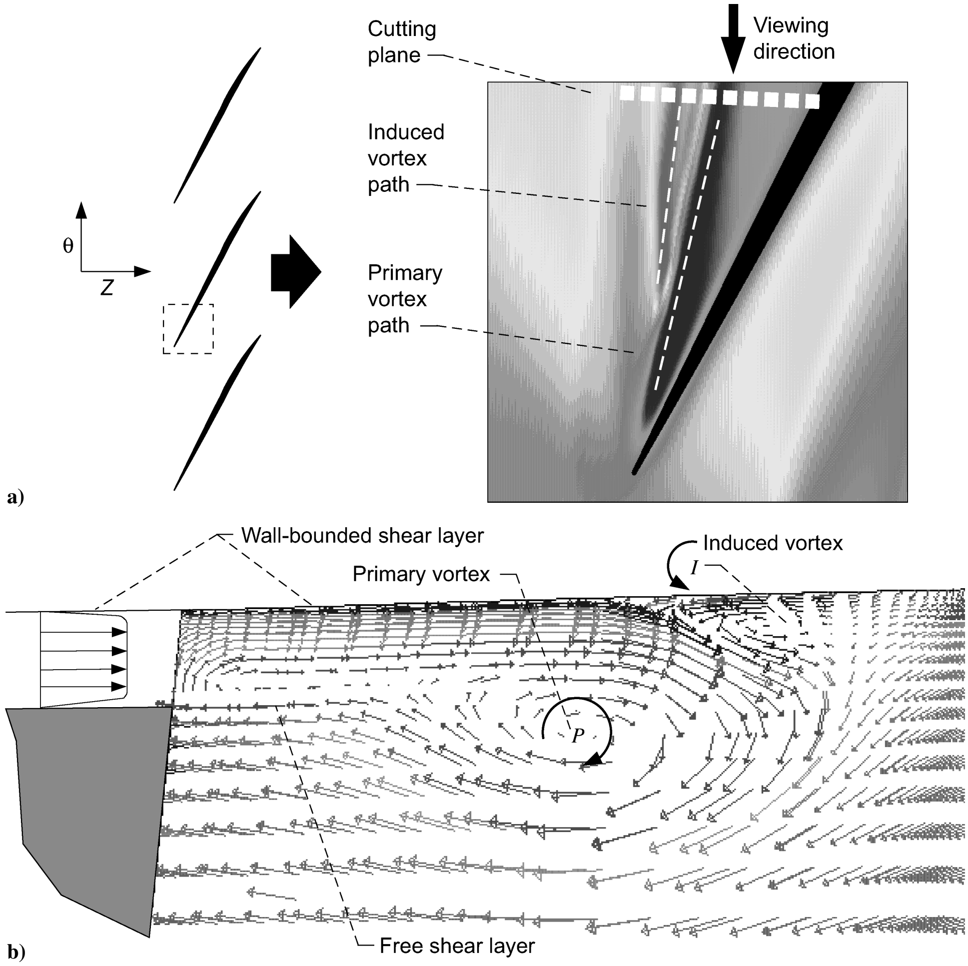

Fig. 17 Visualization of primary and induced clearance vortices in a transonic compressor rotor: a) axial velocity at 6% of clearance gap height from shroud and b) projection of relative velocity vectors on Z-r cutting plane as viewed in positive u direction, colored by u component of velocity. Suction surface at right edge of figure. Note that the velocity profile, upper left of figure, is valid only for cascades.[26]

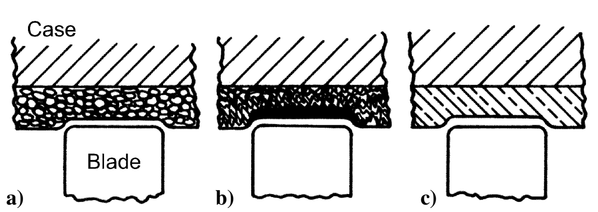

Fig. 18 Illustration of types of materials for interface outer air sealing: a) abradable (sintered or sprayed porous materials), b) compliant (porous material), and c) low shear strength (sprayed aluminum).[4]

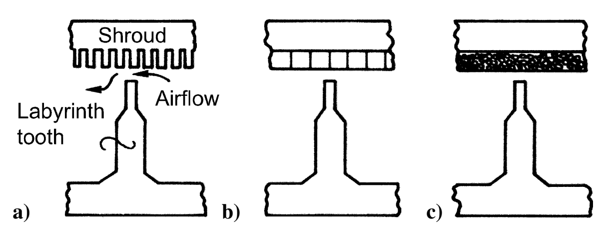

Fig. 19 Inner shrouds for compressor labyrinths: a) striated, b) honeycomb, and c) porous material (abradable or compliant).[4]

Bill and coworkers,[9,31,32] Shiembob,[13] Stocker and coworkers,[33,34] and Mahler.[35] Schematics of three types of abradable materials with associated incursion types are illustrated in Fig. 18 for outer air-blade-tip sealing interface in a compressor, for example. These types of materials usually differ from the platform or inner shroud-drum rotor interface sealing of the compressor, as illustrated in Fig. 19.

As the name suggests, abradable seal materials are worn in by the rotating blade during service. They are applied to the casing of compressors and gas and steam turbines to decrease clearances to levels difficult to achieve by mechanical means. Abradable seals are gaining appeal in gas turbines as a relatively simple means to reduce gas-path clearances in both the compressor and turbine. They offer clearance reductions at relatively low cost and minor engineering implications for the service fleet. Abradable seals have been in use in aviation gas turbines since the late 1960s and early 1970s.[36] Although low energy costs, materials and long cycle time have in the past limited applications of abradable seals in land-based gas turbines, current operation demands enhanced heat rate and reduced costs. With increasing fuel prices and advances in materials to allow extended service periods, abradable seals are gaining popularity within the power generation industry.[37]

Without abradable seals, the cold clearances between blade or bucket tips and shrouds must be large enough to prevent significant contact during operation. Use of abradable seals allows the cold clearances to be reduced with the assurance that if contact occurs the sacrificial part will be the abradable material on the stationary surface and not the blade or bucket tips. Also, abradable seals allow tighter clearances with common shroud or casing out-of-roundness and rotor misalignment.

1. *Interface Rub*

For properly designed abradables, if a rub occurs the blade cuts into the sacrificial seal material with minimal distress to the blade. The abradable seal material mitigates blade wear while providing a durable interface that enhances engine efficiency. Controlled porosity shroud seal materials provide for low-energy material removal without damaging the rotating blade while mitigating leakage and enhancing seal life. Material release, porosity, and structural strength can be controlled in both thermal sprayed coatings and fibermetals. Filler materials are often used to resist energy input to the shroud seal, mitigate case clearance distortion, and also lubricate the wear interface. Worn material must be released to escape sliding contact wear of the blade tip (vs cutting action for an abradable) and plowing of the interface.[38] Asymmetric rubs generate hot spots that can develop into destructive seal drum instabilities. Such modes have destroyed engines and have been known to destroy aircraft with loss of life.

Many attempts have been made to study the wear mechanisms of abradable structures using conventional tribometers[39] or specially designed test rigs.[40,41] However because of the high relative speeds, >100 m/s (>330 ft/s), between the abradable seal and the rotating blade-tip surface, the mechanisms of wear/cutting differ considerably from low-speed tribology normally associated with machining operations. At high speeds, the removal/cutting of a thermal spray abradable coating is done by release of small particle debris, that is, <0.1 mm (<0.004 in.). In contrast to conventional (low-speed) cutting in machine tools, the particle debris released in abradable materials is ejected at the rear of the moving blade.[42] This, therefore, partly sets the criteria for the design of such materials. It also sets a limiting design criterion for blade-tip thickness. Generally, a cutting element (blade-tip) thickness less than 1.3 mm (0.05 in.) allows release of the particles from the coating. Thicker tips tend to entrap the loose particles between the blade and the abradable material. As a result, special considerations have to be given to the design of the materials to allow for the cutting mechanisms (for example, altering the base material particle morphology and size).

Certain abradable materials rely more on densification (compaction) of the structure than on particle debris removal.[43] Material compaction limits the functional depth of the abradable material because the compacted material will increase the wear of the rotating blade tips as the porosity is reduced. These types of seal materials include some of the thermal spray coatings and porous metal fiber structures (fiber metals). Fiber metals can be designed and constructed with varying fiber sizes and densities to alter their tribological behavior.[44,45]

2. Interface Materials

There are different approaches used for a material to be abradable. Some have porosity built in so that the material wears away when rubbed by the blade tip. Some of these have a solid lubricant embedded to aid the wear process. Others abradables, such as honeycomb and fiber metal, deform at high speeds, and the cell walls rupture. For honeycomb, rotor wear is most pronounced at the brazed web where cell thickness doubles. Borel et al.[43] mapped incursion velocity as a function of tangential velocity as shown in Fig. 20. These parameters delineate regions of adhesive wear, melting wear, smearing, cutting, and adhesive titanium transfer from blade to interface. Abradable seals are generally classified according to their temperature capability,[46] but can also be characterized by method of application as shown in Table 2 (Ref. 38).

a) Low-temperature abradable seals. For thermally sprayed abradable coatings, different classes of coating materials behave

Table 2 Abradable material classification

Temperature	Location/material	Process
Low amb 400°C (750°F)	Fan or LPC AlSi + filler	Castings for polymer-based materials
Medium amb 760°C (1400°F)	LPC, HPC, LPT Ni or Co base	Brazing or diffusion bonding for honeycomb and/or fiber metals
High 760°C (1400°F)–1150°C (2100°F)	HPT YSZ and cBN or SiC	Thermal spray coatings for powdered composite materials

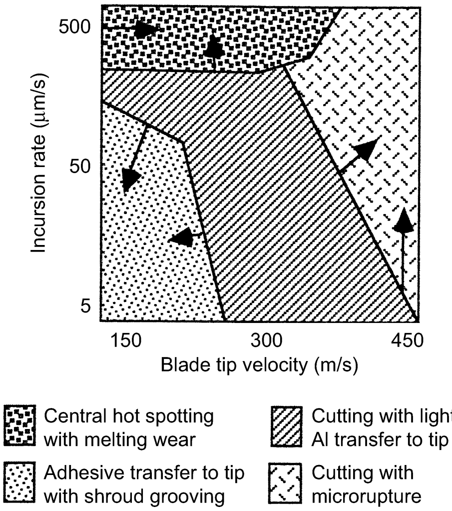

Fig. 20 Aluminum-silicon–polyester coating wear map using a 3-mm (0.12-in.) thick titanium blade at ambient temperature.[43]

tribologically differently. Traditionally, most of the powder metals available for low-temperature applications, that is, <400°C (<750°F), are aluminum-silicon based. To make them abradable, a second phase is added.[46] This phase is usually a polymeric material or a release agent and is often called a solid lubricant. The role of the second phase in aluminum-silicon-based abradable material is primarily to promote crack initiation within the structure. The size, morphology, quantity, and material of the second phase determine the wear mechanisms and abradability of the seal coating under various tribological conditions. The wear map in Fig. 20 is for an aluminum-silicon-polyester coating. The dominant wear mechanisms are different for various combinations of blade-tip velocity and incursion rate when rubbed by a 3-mm (0.12-in.)-thick titanium blade at ambient temperature. The arrows indicate the movement of wear-mechanism boundaries when a stiffer polymer than polyester is used as the second phase.

Low-temperature abradables (generally epoxy materials) are used for fan-tip sealing. Engine manufacturers' philosophy regarding fan rub strips is engine dependent. For example, the PW4090 uses a filled-honeycomb configuration, shown in Fig. 21a. The uneven rub, caused by in-flight maneuvers, can become, relatively speaking, quite deep (tens of mils), which is difficult to tell from the photo. The PW4000 and PW2000 have very similar labyrinth style rub strips (Fig. 21b). On the other hand, the CFM56 engine uses a smooth surface, which gets repotted during overhaul, and yet is usually not refurbished unless considerable damage has been incurred.

b) Midtemperature abradable seals. For temperature applications up to 760°C (1400°F), Ni- or Co-based alloy powders are commonly used as the basis of the abradable seal matrix. Other phases are added to the base metal powder to make the material abradable. These added phases are polymeric materials that are fugitive elements to generate coating porosity and act as release agents.[41,47]

Figure 22 displays a wear map of a midtemperature coating system abraded at 500°C (930°F) using titanium blades. The map shows the wear mechanism domains vs blade-tip velocity and incursion rate. The arrows indicate the movement of the wear regime boundaries as the polyester level increases. As polyester content and thus porosity increase, cutting becomes increasingly the predominant mechanism over the entire range of the speeds and incursion rates. However, increasing porosity has a negative effect on coating cohesive strength and erosion properties.

Fiber metals are a type of midtemperature abradable. Like other abradables, abradability and erosion resistance present conflicting design demands, as illustrated in Fig. 23, and provide the seal designer with some flexibility.[44] Chappel et al.[44,45] tested different fiber metals against other abradables for high- and low-speed abradability and erosion (see Table 3). The materials were then ranked per their

Table 3 Abradable materials used by Chappel et al.[44]

Fibermetal	Density, %	Ultimate tensile strength, psi
1	22	1050
2	23	2150

Honeycomb	Hastelloy-X, 0.05-mm foil, 1.59-mm cell
Nickel Graphite	Sulzer Metco 307NS (spray)
CoNiCrAlY/hBN/PE[a]	Sulzer Metco 2043 (spray)

[a]Hexagonal boron nitride (hBN) acts as a release agent; polyester (PE) controls porosity

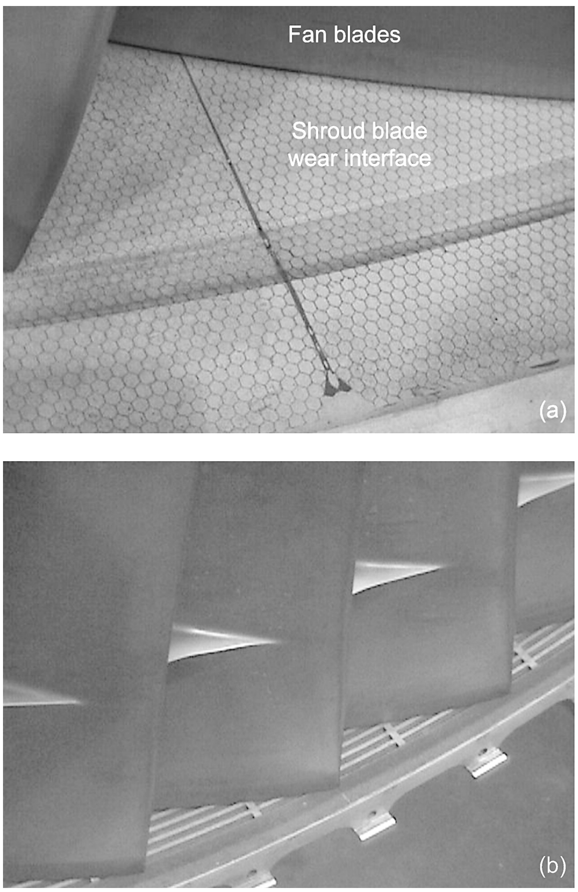

Fig. 21 Fan shroud rub strips: a) potted honeycomb PW4090 fan shroud and b) PW2000/4000 fan and rub strip interface (courtesy of Sherry Soditus, United Airlines Maintenance, San Francisco, CA).

Table 4 Wear-resistance performance rankings of abradable materials[44]

	Abradability		
Material	High speed[a]	Low speed[a]	Erosion[a]
1050-psi fiber metal	1	1	3
2150-psi fiber metal	1	1	1
Hastelloy-X honeycomb	2	3	2
Nickel graphite	3	1	2
CoNiCrAlY/ hBN/PE	3	3	1

[a]Where 1 = best and 3 = worst.

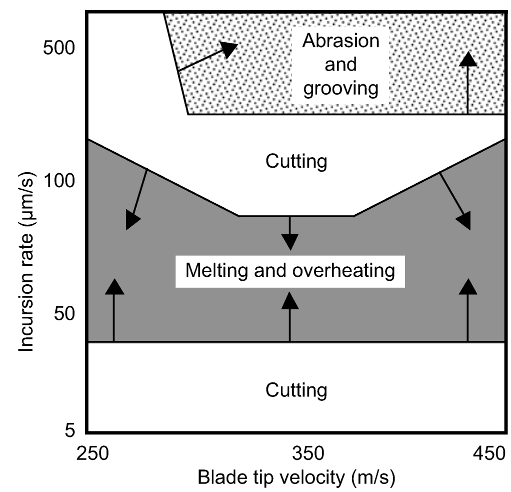

Fig. 22 Midtemperature abradable coating (CoNiCrAlY) wear map at 500°C (930°F) using titanium blades.[46]

performance (Table 4). Results showed that the high-strength fiber metal had the best performance overall with the highest abradability and lowest erosion.

c) High-temperature abradable seals. For operating temperatures above 760°C (1400°F), common practice is to use porous ceramics as the abradable material. The most widely used material is YSZ, which is usually mixed with a fugitive polymeric phase. There are a number of important considerations regarding porous ceramic abradable materials. To achieve an acceptable abradability, the cutting element/blade generally has to be reinforced with hard abrasive grits. Choosing these grits and processes to apply them has been the subject of numerous research activities. There are a number of patents that deal with this aspect of ceramic abradable materials.[48–52] Abrasive grits considered include cubic boron nitride (cBN), silicon carbide, aluminum oxide, and zirconium oxide. Published data suggest that cBN particles of a given size range tend to be the best abrasive medium against YSZ porous ceramics.[48,51] Cubic boron nitride poses a high hardness (second to diamond) and a high sublimation temperature, >2980°C (>5400°F), which makes it an ideal candidate to abrade ceramic abradable materials. But cBN's relatively low oxidation temperature, ∼850°C (∼1560°F), allows it to function for only a limited time. This has prompted the use of other abrasives such SiC.[49,52] Despite successful functionality of SiC against YSZ, SiC has been met with limited enthusiasm. SiC requires a diffusion barrier to prevent its reaction with transition metals at elevated temperatures.[53] This adds to the complexity and the cost of the abrasive system.

The ceramic abradable coating microstructure and its porosity are other essential considerations. Clearly, porosity increases the abradability of the coating. However, YSZ is strongly susceptible to high angle erosion because of its brittle nature,[54] and adding porosity makes it prone to low angle erosion. Thermally sprayed porous YSZ coatings show different tribological behavior when compared to metallic abradable materials. They tend to show a strong influence of blade-tip velocity on abradability[42] (see Fig. 24). Abradability tends to improve with increasing blade-tip velocity. On the other hand, porous YSZ coatings show less dependency on incursion rate. They tend to have poor abradability at very low incursion rates, <0.005 mm/s (<0.2 mils/s), thus requiring blade-tip treatments.

An example application of a high-temperature abradable has been reported where the bill-of-material first-stage turbine gas-path shroud seals were coated with a porosity-controlled plasma sprayed zirconia (PSZ) ceramic seal as shown in Fig. 25 (Ref. 55). The coating was a 1-mm (0.040-in.) layer of ZrO_2-$8Y_2O_3$ over a 1-mm (0.040-in.) NiCoCrAl-based bond coat onto a Haynes 25 substrate. Characteristic "mudflat" cracking of the ceramic occurred at the blade interface, but backside seal temperature reductions over BOM-seals of 78°C (140°F) were measured, with gas-path temperatures estimated over 1205°C (2200°F) (Ref. 37).

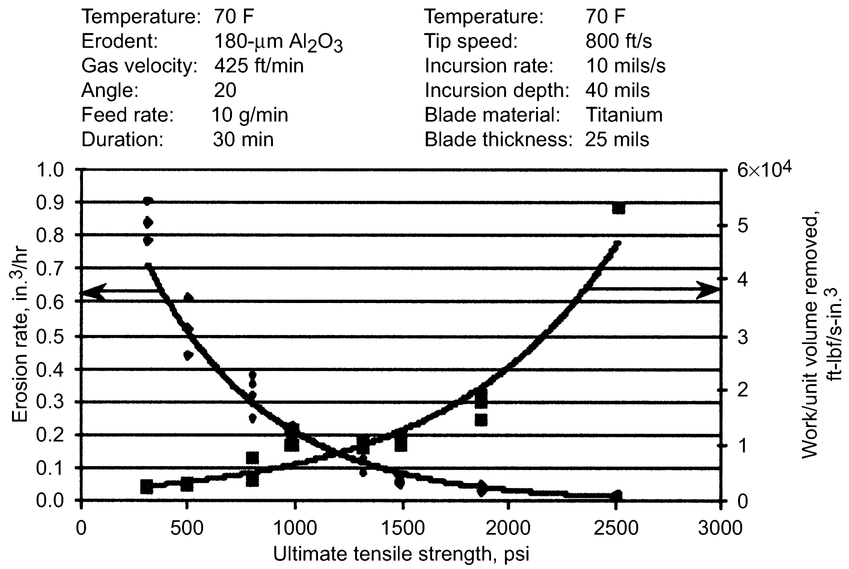

Fig. 23 Erosion and abradability as a function of ultimate tensile strength[44] (courtesy of Technetics Corporation).

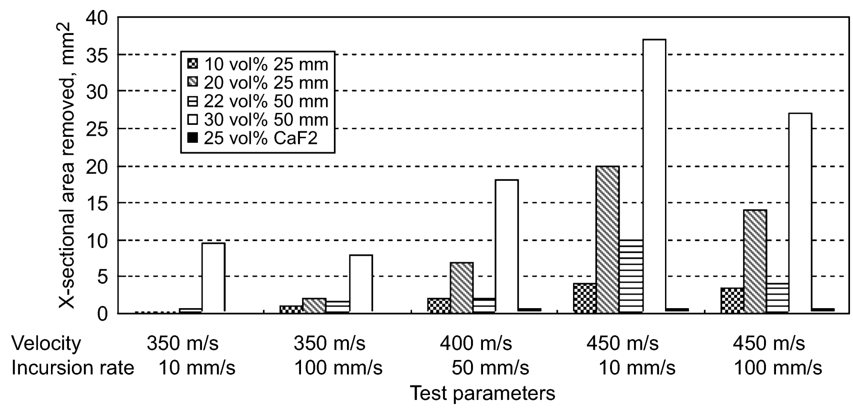

Fig. 24 Abradability of high-temperature materials by SiC tipped blades at 1025°C (1880°F). Right set of data (solid black bar) is for a CaF abradable; other data are for YSZ with polyamide. The *x* axis lists velocity and incursion rates. The legend gives porosity levels and average pore sizes after the polyamide is burned out.[53]

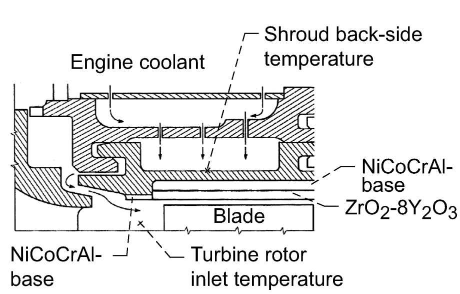

Fig. 25 Schematic of ceramic-coated shroud seal.[55]

3. *Designing Abradable Materials for Turbomachinery*

Because abradable seals are low-strength structures that wear without damaging the mating blade tips, they are also susceptible to gas and solid particle erosion. Abradable structures intended for use in harsh temperatures occurring in gas turbines can also be prone to oxidation because of the inherent material porosity. These conflicting properties need to be accounted for in designing abradable seals. Abradable seals then have to be considered as a complete tribological system that incorporates 1) relative motions and depth of cut—blade-tip speed and incursion rate; 2) environment temperature, fluid medium and contaminants; 3) cutting element geometry and material—blade-tip thickness, shrouded or unshrouded blades; and 4) counterelement—abradable seal material and structure. Manufacturing processes as well as microstructural consistency of abradable seals can have a profound effect on their properties.[44,56]

Another issue to consider in designing for abradables for compressors is the large changes in thermal environment and the fact that titanium fires are not contained. Therefore, rubbing must release particulate matter without engendering a fire or debris impacting downstream components. Also in compressors, an abradable can be combined with intentional grooving to enhance stall margins, yet clearance control or fluid injection might be better methods of controlling stall margin.

Considering all of the preceding design elements makes the abradable system quite unique, that is, designed to suit the particular application. Thus, despite the availability of many off-the-shelf materials, abradable seals have to be modified or redesigned in most applications to meet the design constraints. More extensive lists of references on abradable seals and their use have been published elsewhere.[42,44]

C. Labyrinth Seals

Labyrinth seals and their sealing principles are commonplace in turbomachinery and come in a variety of configurations. The most used configurations are straight, interlocking, slanted, stepped, and combinations (Fig. 26).[57] By their nature labyrinth seals, usually mounted on the rotor, are clearance seals that can rub against their shroud interface, such as abradables and honeycomb (Fig. 27).[58] They permit controlled leakages by dissipation of flow energy through a series of sequential aperture cavities (as sequential sharp edge orifices) with minimum heat rise and torque. The speed and pressure at which they operate is only limited by their structural design.

Principle design parameters include clearance and throttle (tooth or knife) and cavity geometry and tooth number (Fig. 28).[59] The clearance is set by aerothermomechanical conditions that preclude contact with the shroud allowing for radial and axial excursions. The throttle tip is as thin as structurally feasible to mitigate heat propagation through the throttle body into the shaft with a sharp leading edge (as an orifice) and is the primary flow restrictor. The angle at which the flow approaches the throttle is usually 90 deg, but slant throttles, into the flow, are more effective seals. {Borda

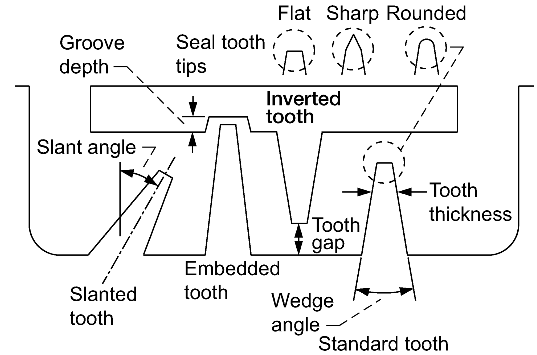

Fig. 28 Generalized schematics of labyrinth seal throttle configurations.[59]

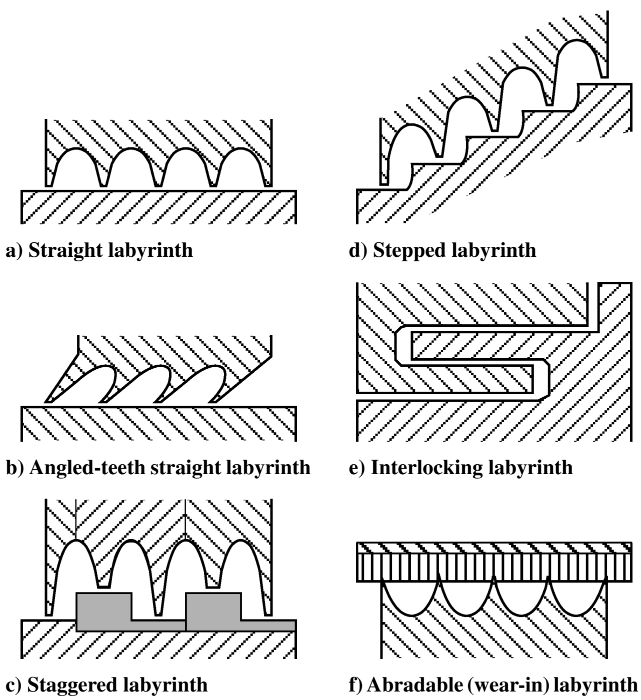

Fig. 26 Generalized labyrinth seal configurations.[57]

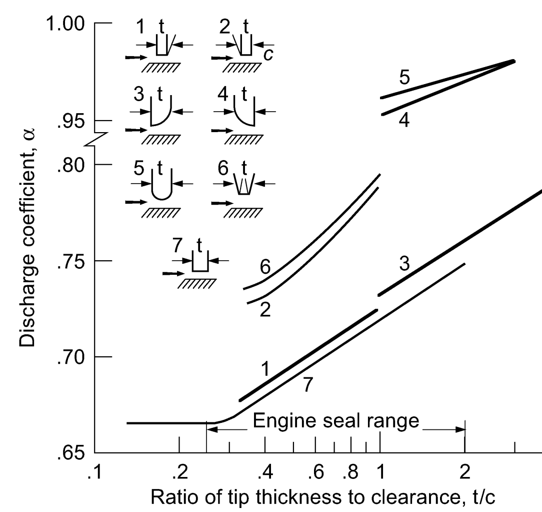

Fig. 29 Discharge coefficient as a function of knife-edge tooth shape.[35]

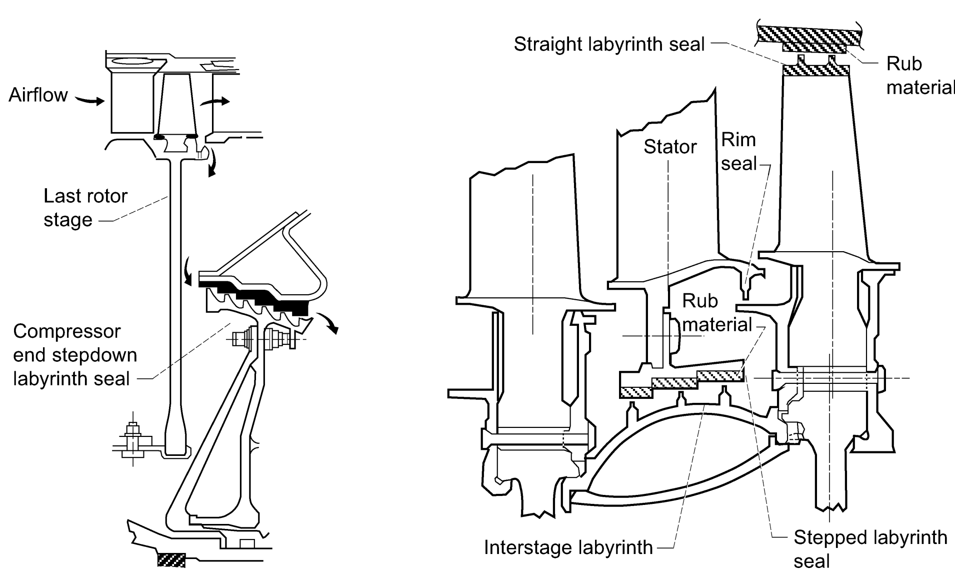

Fig. 27 Drum rotor labyrinth sealing configurations: a) compressor discharge stepdown labyrinth seal[58] and b) turbine interstage stepped labyrinth seal and shrouded-rotor straight labyrinth seal.[4]

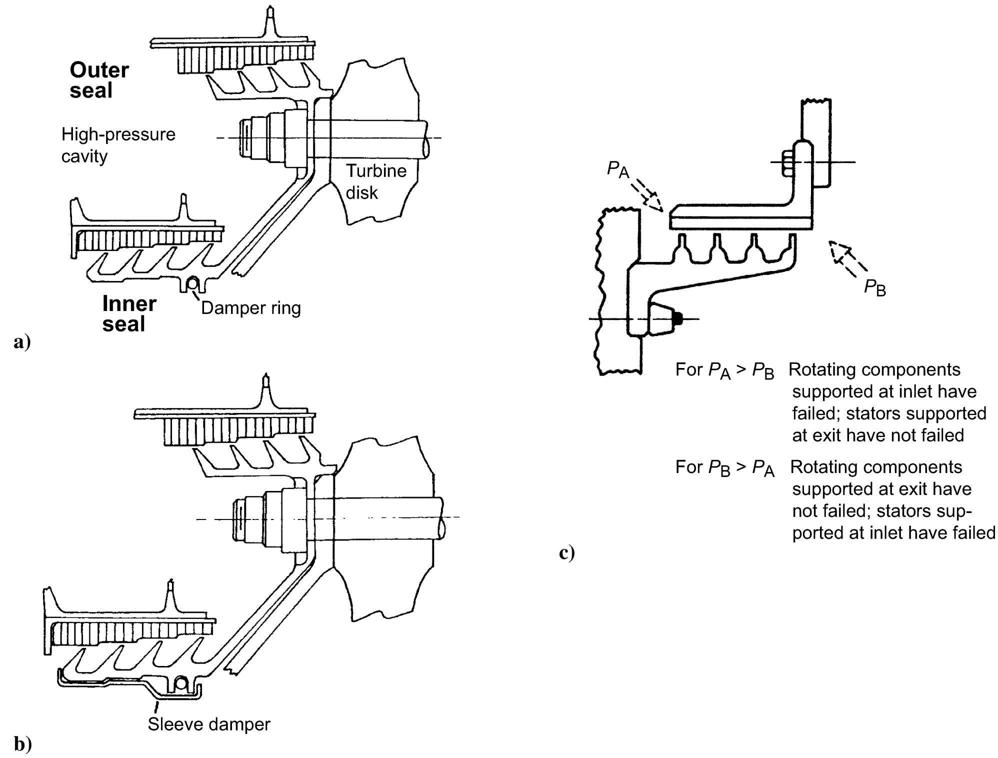

Fig. 30 Inner and outer labyrinth air seals: a) damper ring, b) damper drum (sleeve),[65] and c) effect of seal component support.[4]

inlets [$C_f = 0.5$ (C_f is the flow coefficient)] are more restrictive than orifice inlets $C_f = 0.63$.} One advantage of 90-deg throttles ($C_f = 0.63$) is the ability to seal flow reversals equally well; slant throttles are less effective handling flow reversals ($C_f = 0.8$ to 0.9). The cavity geometry is nearly 1:1 with axial spacing greater than six times the clearance and often shaped to enhance flow dissipation through generation of vortices. A relation between the number of knife-cavity modules and leakage for developed cavity flows is given by

$$G_r/G_{r1} = N^{-0.4}$$

where G_r = mass flux, G_{r1} is the mass flux through a single throttle, and N the number of throttles or cavity-throttle modules[60]; for gas throttles only, see Egli[61] for an equivalent relation (Egli's interest was steam, yet applicable to gases in general). Conditions relating the sharpness of the tooth to the ability to restrict flows are given by Mahler[35] (Fig. 29) and more recently explored by computational fluid dynamics (CFD).[62]

Labyrinth seals are good in restricting the flow but do not respond well to dynamics and often lead to turbomachine instabilities. These problems have been addressed by several investigators starting with Thomas[63] and Alford.[64] They recognized that the dynamic forces drove instabilities and heuristically determined stable operating configurations (Fig. 30). Benckert and Wachter,[66] Childs et al.[67] and Muszynska[68] addressed the root causes and introduced the swirl brake at the seal inlet to mitigate the circumferential velocity component within the cavities (Fig. 31). More recently circumferential flow blocks and flow slots have been introduced to mitigate the circumferential velocity component (Figs. 32 and 33).[69]

Labyrinth seals have a lengthy history of proven reliability with robust operation and developed technology and are well suited for abradable interfaces. Their tendency to engender instabilities can be controlled by swirl brakes or intracavity slots or blocks and drum dampers. Nearly all turbomachines rely on labyrinth seals or labyrinth sealing principle (Egli,[61] Trutnovsky,[70] Stocker et al.,[33] and Stocker[34]). In general, nearly all sealing applications rely heavily on the essential features of sharp-edge flow restrictors [e.g., the aspirating seal (see Sec. V.E) has a labyrinth tooth and the face-sealing dam,[71] Figs. 34a and 34b and the inlet throttle confining flows to the honeycomb land (Fig. 35)].

Table 5 Typical operating limits for state-of-the-art brush seals

Parameter	Units	S_1
Differential pressure	Up to 300 psid per stage	2.1 MPa
Surface speed	Up to 1200 ft/s	400 m/s
Operating temperature	Up to 1200°F	600°C
Size (diameter range)	Up to 120 in.	3.1 m

D. Brush Seals

As described by Ferguson,[72] the brush seal is the first simple, practical alternative to the finned labyrinth seal that offers extensive performance improvements. Benefits of brush seals over labyrinth seals include 1) reduced leakage compared to labyrinth seals (upwards of 50% possible); 2) accommodation of shaft excursions as a result of stop/start operations and other transient conditions (labyrinth seals often incur permanent clearance increases under such conditions, degrading seal and machine performance); 3) significantly less axial space than labyrinth seal required; and 4) more stable leakage characteristics over long operating periods.

Brush seals have matured significantly over the past 20 years. Typical operating conditions of state-of-the-art brush seals are shown in Table 5.¶

Brush seal construction is deceptively simple, requiring the well-ordered layering or tufting of fine-diameter bristles into a dense pack that compensates for circumferential differences between inside and outside diameters (Figs. 36 and 37). This pack is sandwiched and

¶Data available online at http://www.fluidsciences.perkinelmer.com/turbomachinery.

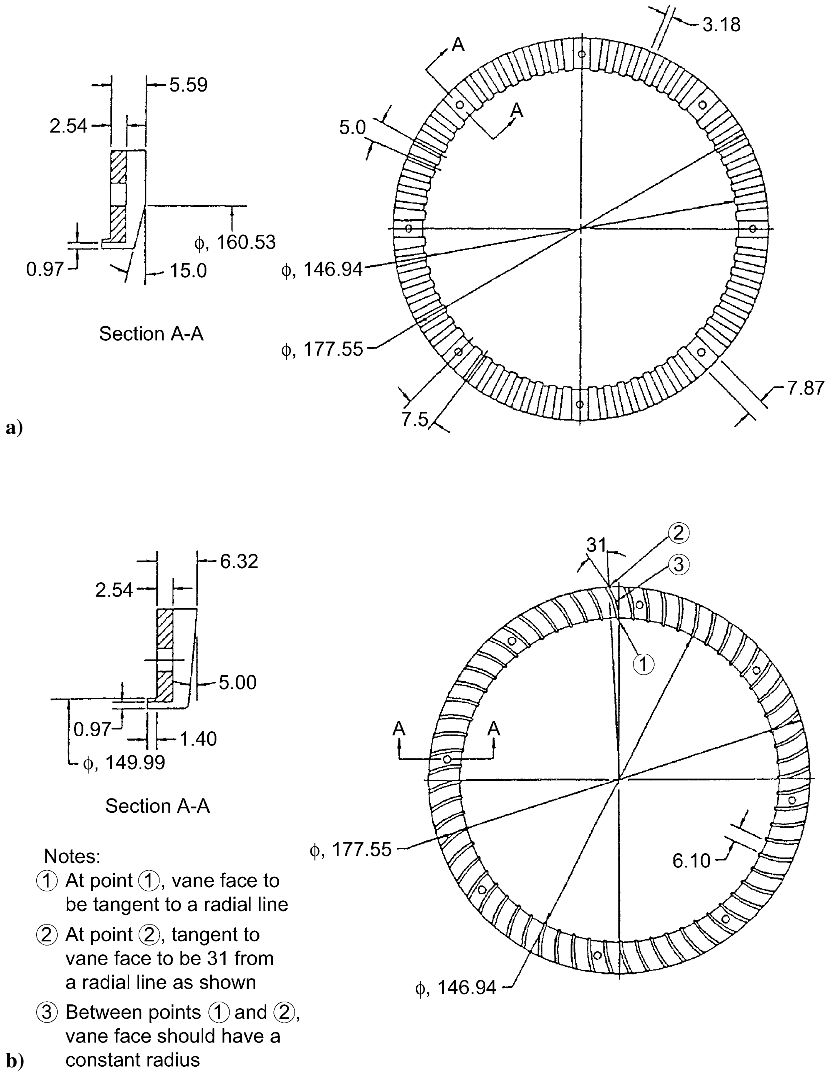

Fig. 31 Typical swirl brake configurations applied at the inlet to a labyrinth seal: a) radial swirl brake and b) improved swirl brake.[67]

welded between a backing ring (downstream side) and sideplate (upstream side), then stress relieved to ensure stability and flatness. The weld on the seal outer diameter is machined to form a close-tolerance outer-diameter sealing surface to fit into a suitable housing. The wire bristles protrude radially inward (shaft rotor) or outward (drum rotor) and are machined to fit the mating rotor, with slight interference. Brush seal interferences (preload) must be properly selected to prevent catastrophic overheating of the rotor and excessive rotor thermal growths.

To accommodate anticipated radial shaft movements, the bristles must bend. To allow the bristles to bend without buckling, the wires are oriented at an angle (typically 45 to 55 deg) to a radial line through the rotor. The bristles are canted in the direction of rotor rotation. The bristle lay angle also facilitates seal installation because of the slight interference between the bristle pack and the rotor. The backing ring provides structural support to the otherwise flexible bristles and assists the seal in limiting leakage. To minimize brush seal hysteresis caused by brush bristle binding on the backplate, new features have been added to the backing ring. These include reliefs of various forms. An example design is shown in Fig. 36 and includes the recessed pocket and seal dam. The recessed pocket assists with pressure balancing of the seal, and the relatively small contact area at the seal dam minimizes friction allowing the bristles to follow the speed-dependent shaft growths. The bristle free-radial-length and packing pattern are selected to accommodate radial shaft movements while operating within the wire's elastic range at temperature.

A number of brush seal manufacturers** include some form of flow deflector (e.g., see flexi-front plate in Fig. 36) on the high-pressure side of the wire bristles. This element aids in mitigating the radial pressure closing loads (e.g., sometimes known as "pressure closing") caused by air forces urging the bristles against the shaft. This element can also aid in reducing installation damage, bristle flutter in highly turbulent flowfields, and FOD.

Brush seals, initially developed for aero gas turbines, have also been used in industrial gas and steam turbines since the 1990s. Design similitude, analysis, and modeling of brush and woven seals were established earlier in the works of Flower[73] and Hendricks et al.[22] Within in the confines of this paper, we are only able to address a few sealing types, their locations, and material constraints. For further details, see Hendricks and coworkers[25,74,75] and NASA conference publications.[76,77] An extensive summary of brush seal research and development work through 1995 has been published[78,79] and updated in a more recent summary.[37]

1. *Brush Seal Design Considerations*

To properly design and specify brush seals for an application, many design factors must be considered and traded off. Comprehensive brush seal design algorithms have been proposed by Chupp et al.,[37] Dinc et al.,[80] Hendricks et al.,[22] and Holle and Krishan.[81] An iterative process must be followed to satisfy seal

**Data available online at http://www.crossmanufacturing.com.

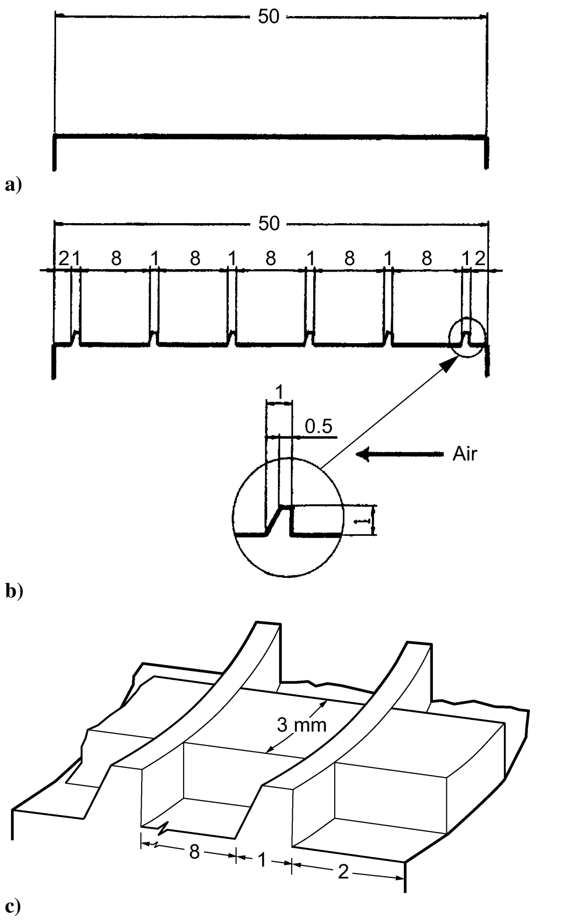

Fig. 32 Labyrinth circumferential flow blocks: a) annular seal, b) labyrinth seal, and c) flow blocks.[69]

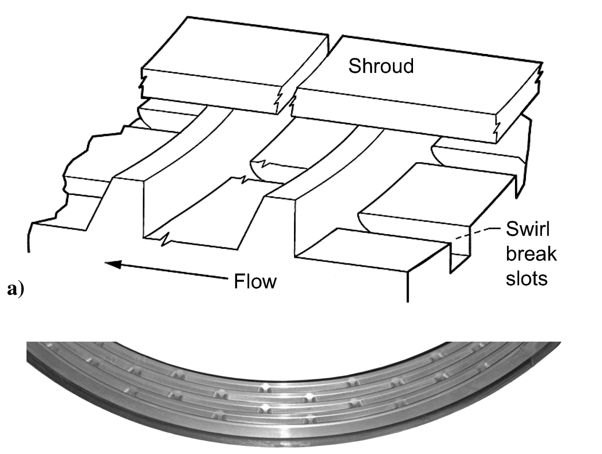

Fig. 33 Web seal with circumferential flow blocking slots: a) conceptual web seal sketch and b) photograph of web seal.[12]

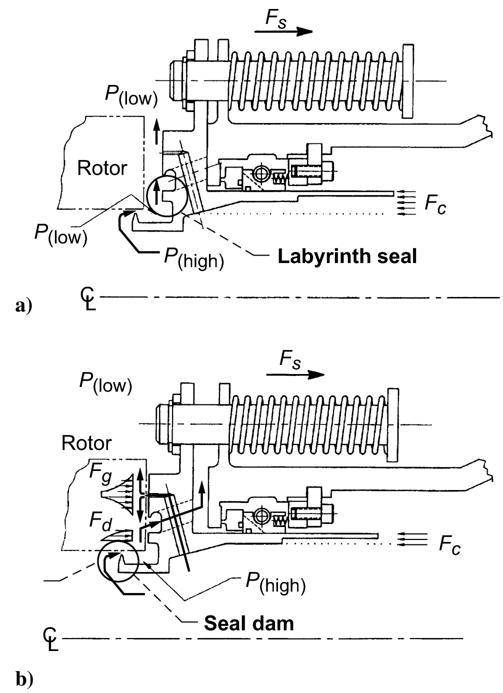

Fig. 34 Aspirating seal labyrinth tooth and seal dam sharp-edge flow restrictor: a) at shutdown phase and b) at steady-state operation.[71]

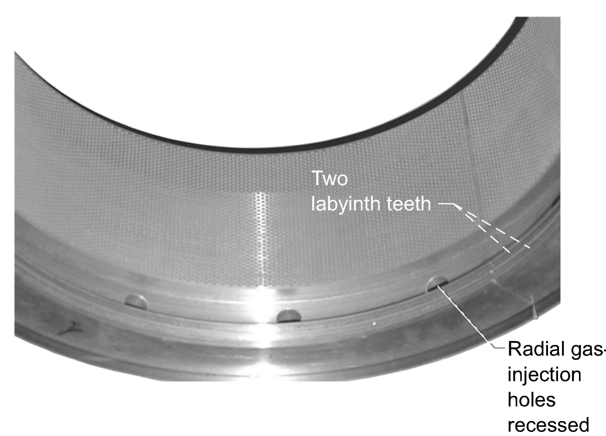

Fig. 35 Primary labyrinth throttle confining flows to the honeycomb journal land.[12]

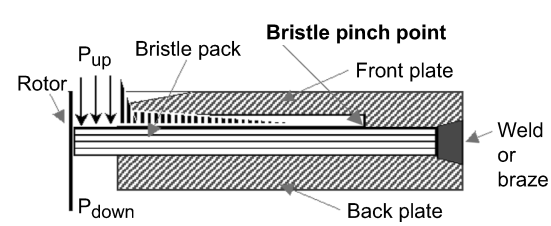

Fig. 36 Typical brush seal configuration and geometric features.

basic geometry, stress, thermal (especially during transient rub conditions), leakage, and life constraints to arrive at an acceptable design many of the characteristics that must be considered and understood for a successful brush seal design are given here[80]: pressure capability, seal upstream protection, frequency, seal high- and low-cycle fatigue (HCF, LCF) analysis, seal leakage, seal oxidation, seal stiffness, seal creep, seal blowdown (e.g., pressure closing effect), seal wear, bristle-tip forces and pressure stiffening effect, solid particle erosion, seal heat generation, reverse rotation, bristle-tip temperature, seal life/long-term considerations, rotor dynamics, performance predictions, rotor thermal stability, oil sealing, secondary flow and cavity flow (including swirl flow), and shaft considerations (e.g., coating, etc.). Design criteria are required for each of the different potential failure modes including stress, fatigue life, creep life, wear life, oxidation life, among others. Several important designs parameters are discussed next.

a) Material selection. Materials in rubbing contact in brush seal installations must have sufficient wear resistance to satisfy engine durability requirements. A proper material selection requires knowledge of the rotor and seal materials and their interactions. In

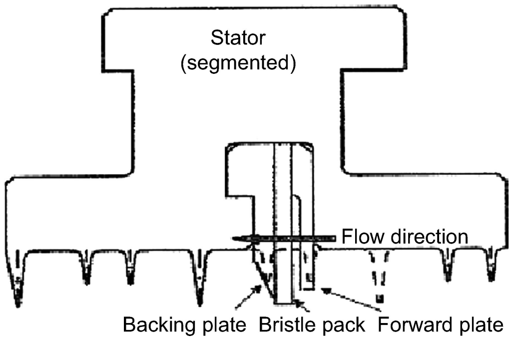

Fig. 37 Brush seal design for steam-turbine applications.

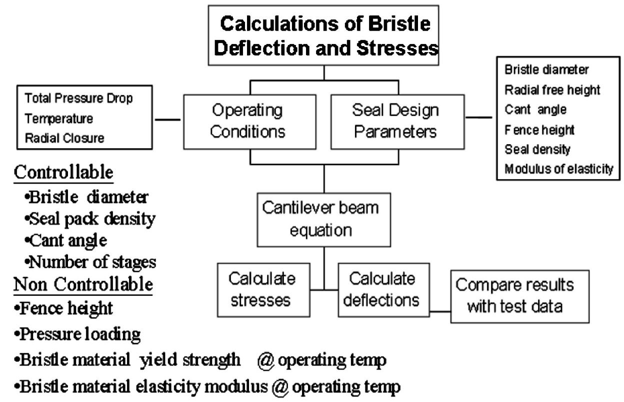

Fig. 38 Bristle stress/deflection analysis.

addition to good wear characteristics, the seal material must have acceptable creep and oxidation properties.

Metallic bristles: Brush seal wire bristles range in diameter from 0.071 mm (0.0028 in.) (for low pressures) to 0.15 mm (0.006 in.) (for high pressures). The most commonly used material for brush seals is the cobalt-based alloy Haynes 25 based on its good wear and oxidation characteristics. Brush seals are generally run against a smooth, hard-face coating to minimize shaft wear and the chances of wear-induced cracks from affecting the structural integrity of the rotor. The usual coatings selected for aircraft applications are ceramic, including chromium carbide and aluminum oxide. Selecting the correct mating wire and shaft surface finish for a given application can reduce frictional heating and extend seal life through reduced oxidation and wear. There is no general requirement for coating industrial gas- and steam-turbine rotor surfaces, where the rotor thicknesses are much greater than aircraft applications.

Nonmetallic bristles: High-speed turbine designers have long wondered if brush seals could replace labyrinth seals in bearing sump locations. Brush seals would mitigate traditional labyrinth seal clearance opening and corresponding increased leakage. Issues slowing early application of brush seals in these locations included coking (carburization of oil particles at excessively high temperatures), metallic particle damage of precision rolling element bearings, and potential for fires. Development efforts have found success in applying aramid bristles for certain bearing sump locations.[82,83] Advantages of the aramid bristles include stable properties up to 300°F (150°C) operating temperatures, negligible amount of shrinkage and moisture absorption, lower wear than Haynes 25 up to 300°F, lower leakage (because of smaller 12-μ-diam fibers), and resistance to coking.[82] Based on laboratory demonstration, the aramid fiber seals were installed in a GE 7EA frame (#1) inlet bearing sealing location. Preliminary field data showed that the nonmetallic brush seal maintained a higher pressure difference between the air and bearing drain cavities and enhanced the effectiveness of the sealing system allowing less oil particles to migrate out of the bearing.

b) Seal fence height. A key design issue is the required radial gap (fence height) between the backing ring and the rotor surface. Following detailed secondary flow, heat transfer, and mechanical analyses, fence height is determined by the relative transient growth characteristics of the rotor vs the stator and rotordynamic considerations. This backing ring gap is designed to avoid contact with the rotor surface during any operating condition with an assumed set of dimensional variations. Consequently, the successful design of an effective brush seal hinges on a thorough knowledge of the turbine behavior, operating conditions, and design of surrounding parts.

c) Brush pack considerations. Depending on required sealing pressure differentials and life, wire bristle diameters are chosen in the range of 0.0028 to 0.006 in. (Ref. 84). Better load and wear properties are found with larger bristle diameters. Bristle pack widths also vary depending on application: the higher the pressure differential, the greater the pack width. Higher-pressure applications require bristle packs with higher axial stiffness to prevent the bristles from blowing under the backing ring. Dinc et al.[80] have developed brush seals that have operated at air pressures up to 2.76 MPa (400 psid) in a single stage. Brush seals have been made in very large diameters. Large brush seals, especially for ground power applications, are often made segmented to allow easy assembly and disassembly, especially on machines where the shaft stays in place during refurbishment.

d) Seal stress/pressure capability. Pressure capacity is another important brush seal design parameter. The overall pressure drop establishes the seal bristle diameter, bristle density, and the number of brush seals in series. In a bristle pack, all bristles are essentially cantilever beams held at the pinch point by a front plate and supported by the backplate. From a loading point of view, the bristles can be separated into two regions (see Fig. 36): the lower part, fence region, between the rotor surface and the backplate inner diameter (i.d.), and the upper part from the back plate i.d. to the bristle pinch point. The innermost radial portion carries the main pressure load and is the main source of the seal stress.[85] In addition to the mean bending stress, contact stress at the bristle-backplate interface must be considered. Furthermore, bristle stress is a very strong function of the fence height set by the expected relative radial movement of the rotor and seal. Figure 38 shows a diagram illustrating design considerations for seal stress and deflection analysis and includes a list of the controllable and noncontrollable design parameters. As a word of caution, care must be taken in using multiple brush configurations as pressure drop capability becomes more nonlinear with fluid compressibility and most of the pressure drop or bristle pressure loading is carried by the downstream brush.

e) Heat generation/bristle-tip temperature. As the brush seal bristles rub against the rotor surface, frictional heat is created that must be dissipated through convection and conduction and is quite similar to the classic Blok problem,[86] where extensive heating occurs at the sliding interface. Brush seal frictional heating was addressed by Hendricks et al.[22,87] and modeled as fin in crossflow with a heat source at the tip by Dogu and Aksit.[88] If the seal is not properly designed, this heating can lead to premature bristle loss, or worst, the rotor/seal operation could become thermally unstable. The latter condition occurs when the rotor grows radially into the stator increasing the frictional heating, leading to additional rotor growth, until the rotor rubs the seal backing plate resulting in component failure. In some turbine designs, brush seals are often assembled with a clearance to preclude excessive interference and heating during thermal and speed transients. These mechanical design issues significantly affect the range of feasible applications for brush seals. Many of these issues have been addressed by Dinc et al.[80] and Soditus.[89]

f) Seal leakage. Leakage characterization of brush seals typically consists of a series of tests at varying levels of bristle-to-rotor interference or clearance, as shown in Figs. 39 and 40. Static (nonrotating) tests are run to get an approximate level of seal leakage and pressure capability. They are followed by dynamic (rotating) tests to provide a more accurate simulation of seal behavior. Rotating tests also reveal rotor dynamics effects, an important consideration for steam-turbine rotors and turbomachines in general, which can be sensitive to radial rubs caused by nonuniform heat generation.

Proctor and Delgado studied the effects of speed [up to 365 m/s (1200 ft/s)], temperature [up to 650°C (1200°F)] and pressure [up

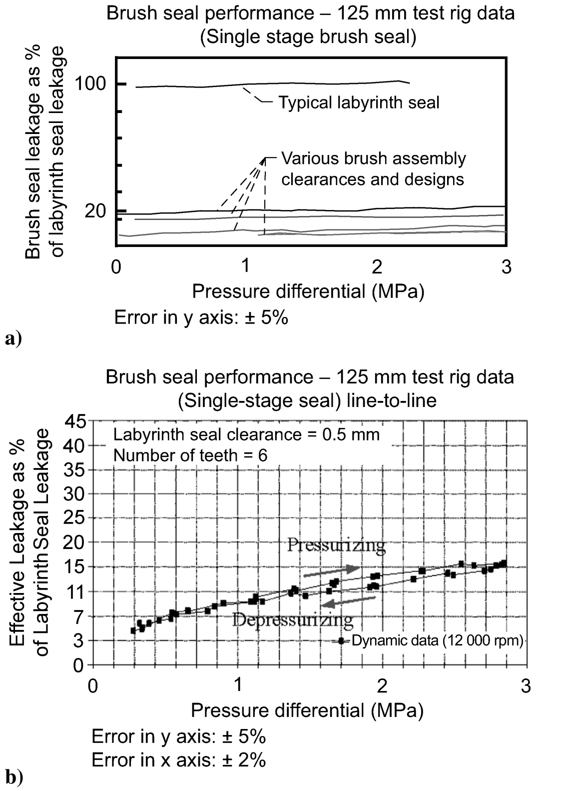

Fig. 39 Brush seal performance as compared to labyrinth seal. Representative brush seal leakage data compared to a typical, 15-tooth, 0.5-mm (20-mil) clearance labyrinth seal. Measured brush seal leakage characteristic with increasing and decreasing pressure drop compared to a typical, six-tooth, 0.5-mm (20-mil) clearance labyrinth seal.[37]

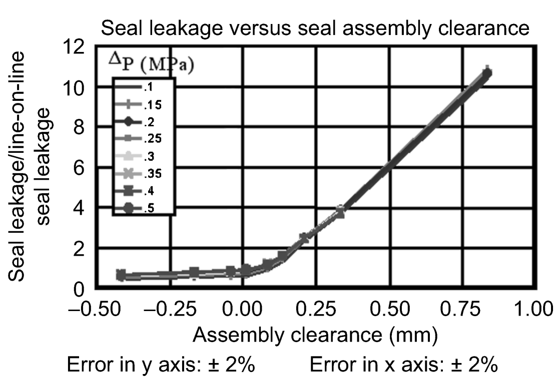

Fig. 40 Measured brush seal leakage for interference and clearance conditions.[37]

to 0.52 MPa (75 psid)] on brush seal and finger seal leakage and power loss.[90] They determined that leakage generally decreased with increasing speed. Leakage decreases somewhat with increasing surface speed because circumferential flow is enhanced and the rotor diameter increases; changes in diameter cause both a decrease in the effective seal clearance and an increase in contact stresses (important in wear and surface heating).

g) Other considerations. If not properly considered, brush seals can exhibit three other phenomena deserving some discussion. These include seal "hysteresis," "bristle stiffening," and "pressure closing." As described by Short et al.[84] and Basu et al.,[91] after the rotor moves into the bristle pack (caused by radial excursions or thermal growths) the displaced bristles do not immediately recover against the frictional forces between them and the backing ring. As a result, a significant leakage increase (more than double) was observed following rotor movement.[91] This leakage hysteresis exists until after the pressure load is removed (e.g., after the engine is shut down). Furthermore if the bristle pack is not properly designed, the seal can exhibit a considerable stiffening effect with application of pressure. This phenomenon results from interbristle friction loads, making it more difficult for the brush bristles to flex during shaft excursions. Air leaking through the seal also exerts a radially inward force on the bristles, resulting in what has been termed pressure closing or bristle blowdown. This extra contact load, especially on the upstream side of the brush, affects the life of the seal (upstream bristles are worn in either a scalloped or coned configuration) and higher interface contact pressure. By measuring baseline seal leakage in a line-to-line (zero clearance) assembly configuration, bristle blowdown for varying loads of assembly clearance can be inferred from leakage data (see Fig. 40).

2. *Brush Seal Flow Modeling*

Brush seal flow modeling is complicated by several factors unique to porous structures, in that the leakage depends on the seal porosity, which depends on the pressure drop across the seal. Flow through the seal travels perpendicular to the brush pack through the annulus formed between the backing ring bore and the shaft diameter. The flow is directed radially inward towards the shaft as it flows around individual bristles and collides with the bristles downstream in adjacent rows of the pack and finally between the bristle tips and the shaft.

A flow model proposed by Holle et al.,[92] uses a single-parameter, effective brush thickness, to correlate the flows through the seal. Variation in seal porosity with pressure difference is accounted for by normalizing the varying brush thicknesses by a minimum or ideal brush thickness. Maximum seal flow rates are computed by using an iterative procedure that has converged when the difference in successive iterations for the flow rate is less than a preset tolerance.

Flow models proposed by Hendricks et al.[22,87,93] are based on a bulk average flow through the porous media. These models account for brush porosity, bristle loading and deformation, brush geometry parameters, and multiple flow paths. Flow through a brush configuration is simulated using an electrical analog with driving potential (pressure drop), current (mass flow), and resistance (flow losses, friction, and momentum) as the key variables. All of the just-mentioned brush flow models require some empirical data to establish correlation constants. Once the constants are established, the models can predict brush seal flow reasonably well.

A number of researchers have applied numerical techniques to model brush seal flows and bristle pressure loadings.[94–97] Though these models are more complex, they permit a more detailed investigation of the subtleties of flow and stresses within the brush pack.

3. *Applications*

a) Aero-gas-turbine engines. Brush seals are seeing extensive service in both commercial and military turbine engines. Lower leakage brush seals permit better management of cavity flows and significant reductions in specific fuel consumption when compared to competing labyrinth seals. Allison Engines has implemented brush seals for the Saab 2000, Cesna Citation-X, and V-22 Osprey. General Electric (GE) has implemented a number of brush seals in the balance piston region of the GE90 engine for the Boeing 777 aircraft. Pratt and Whitney has entered revenue service with brush seals in three locations on the PW1468 for Airbus aircraft and on the PW4084 for the Boeing 777 aircraft.[98]

b) Ground-based-turbine engines. Brush seals are being retrofitted into ground-based turbines both individually and combined with labyrinth seals to greatly improve turbine power output and heat rate.[37,80,99–103] Dinc et al. report that incorporating brush seals in a GE Frame 7EA turbine in the high-pressure packing location increased output by 1.0% and decreased heat rate by 0.5% (Ref. 80). Figure 41 is a photo of a representative brush seal taken during a routine inspection. The seal is in good condition after nearly three years of operation (~22,000 h). To date, more than 200 brush seals have been installed in GE industrial gas turbines in the compressor discharge high-pressure packing (HPP), middle bearing, and turbine

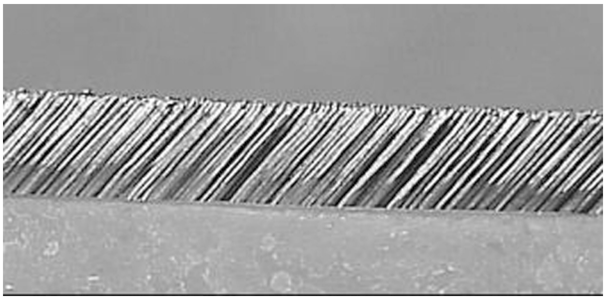

Fig. 41 7EA Gas-turbine high-pressure packing brush seal in good condition after 22,000 h of operation.

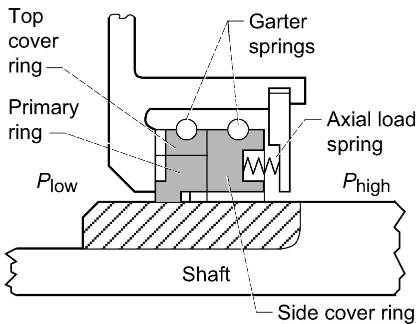

Fig. 42 Shaft riding or circumferential contact seal.[104]

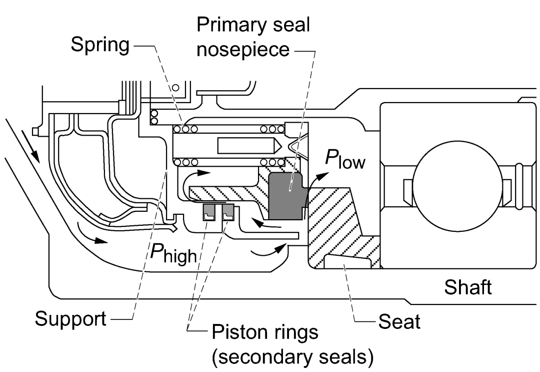

Fig. 43 Positive contact face seal.[106]

interstage locations. Field data and experience from these installations have validated the brush seal design technology. Using brush seals in the interstage location resulted in similar improvements. Brush seals have proven effective for service lives of up to 40,000 h (Ref. 80).

E. Face Seals

Labyrinth seals are less impacted by FOD debris than other type seals, yet also pass that debris to other components such as bearing cavities. One of the major functions of face and buffer sealing is to preclude debris from entering the bearing or gear-box oil, yet an equally important function is to prevent oil vapors from leaking into the wheel space and from entering the cabin airstream. Debris in the bearing or gear-box oil can radically shorten life, and oil vapor in the wheel space can cause fire or explosions. Oil vapors in the cabin are unacceptable to the consumer-traveler.

Face seals are classified as mechanical seals. They are pressure balanced contact or self-acting seals. The key components are the primary ring (stator) or nosepiece, seat or runner (rotor), spring or bellows preloader assembly, garter or retainer springs, secondary seal and housing (Figs. 42 and 43).[105,106] There is a wealth of information on experimental, design, and application of mechanical seals in the literature, including Ludwig[4] to books by, for example, Lebeck.[107]

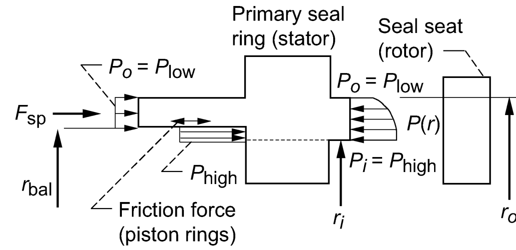

Fig. 44 Pressure balancing forces in face sealing.[108]

For the face seal, the geometry of the ring or nosepiece becomes critical. For successful face sealing, the forces caused by system pressure, sealing dam pressure, and the spring or bellows must be properly balanced and stable over a range in operating parameters (pressure, temperature, surface speed) (Fig. 44.)[108]

Contact seals wear and are generally limited to surface speeds less than 76 m/s (250 ft/s). To mitigate the wear, prolonging life and decreased leakage, Ludwig[109] and Dini[110] promoted the self-acting Rayleigh step and spiral groove seal (Figs. 45–47). A labyrinth seal or a simple projection representing a single throttle is used for presealing to control excessive leakage should the dam of the face seal "pop" open as, for example, the labyrinth preseal is illustrated in Fig. 45 (and aspirating seal of Sec. V.E). Spiral groove (Fig. 47), slot, and T-grooving (bidirectional) are more commonly used than Rayleigh steps to provide more lift at less cost to manufacture.

Self-acting seals permit tighter clearances and better control of the sealing dam geometry as sealing pressure drops are increased, providing lower leakage. Figure 48 provides a comparison of the leakage rates between labyrinth, face-contact and self-acting seals. Whereas self-acting face sealing greatly reduces leakage, surface speeds are generally limited to less than 213 m/s (700 ft/s), but nearly triple the limits of contact face sealing 61–91 m/s (200–300 ft/s).

F. Oil Seals

Gas-turbine shaft seals are used to restrict leakage from a region of gas at high pressure to a region of gas at low pressure. A common use of mechanical seals is to restrict gas leakage into bearing sumps. Oil sealing of bearing compartments of turbomachines is difficult. A key is to prevent the oil side of the seal from becoming flooded. Still, oil-fog and oil-vapor leakage can occur by diffusion of oil as a result of concentration gradients and oil transport as a result of vortical flows within the rotating labyrinth cavities (crude distillation columns). Bearing sumps contain an oil-gas mixture at near-ambient pressure, and a minimal amount of gas leakage through the seal helps prevent oil leakage and maintains a minimum sump pressure necessary for proper scavenging. Bearing sumps in the HPT are usually the most difficult to seal because the pressure and temperatures surrounding the sump can be near compressor discharge conditions.

1. Radial Face Seals

Conventional rubbing-contact seals (shaft-riding and radial face types) are also used to seal bearing sumps. Because of their high wear rates, shaft-riding and circumferential seals (Fig. 42) have been limited to pressures less than 0.69 MPa (100 psi); and successful operation has been reported at a sealed pressure of 0.58 MPa (85 psi), a gas temperature of 370°C (700°F), and sliding speed of 73 m/s (240 ft/s) (Ref. 105).

2. Ring Seals

The ring seal, as described by Whitlock[111] and Brown,[106] is essentially an expanding or contracting piston ring. The expanding design is simpler and is illustrated in Fig. 49. Other designs that can be grouped in the ring seal family include the circumferential segmented ring seal and the floating or controlled-clearance ring, as described by Ludwig.[4] The material requirements for these seals are essentially the same as those for the expanding ring seal. The ring seals are carbon, and they seal radially against the inside diameter

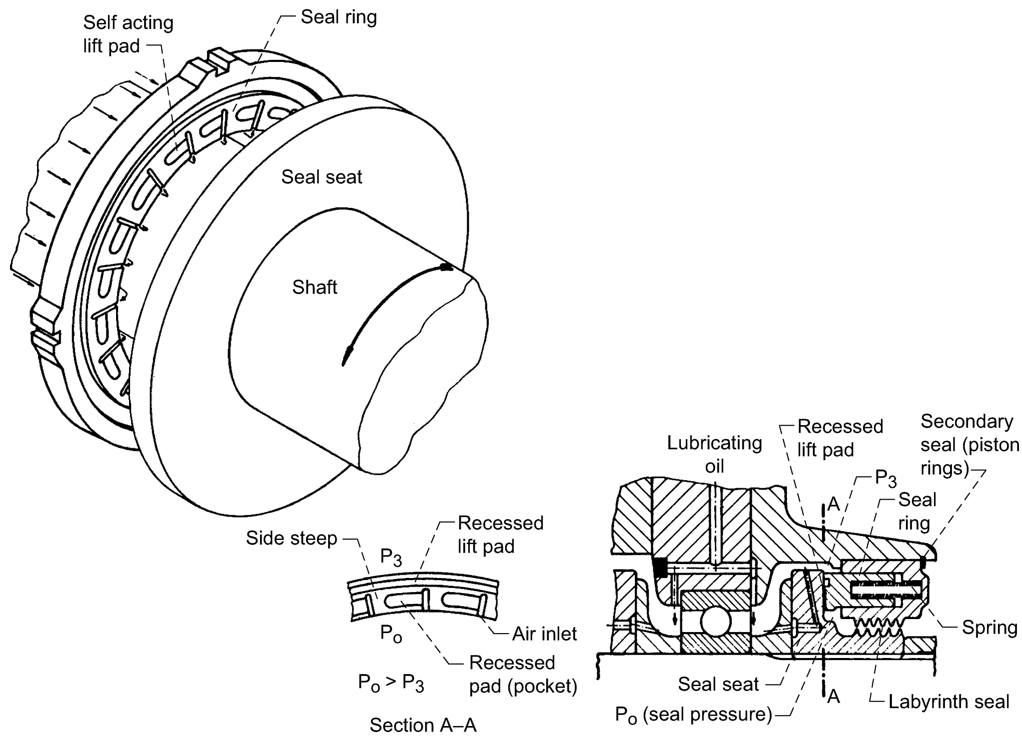

Fig. 45 Self-acting face seal with labyrinth seal presealing.[110]

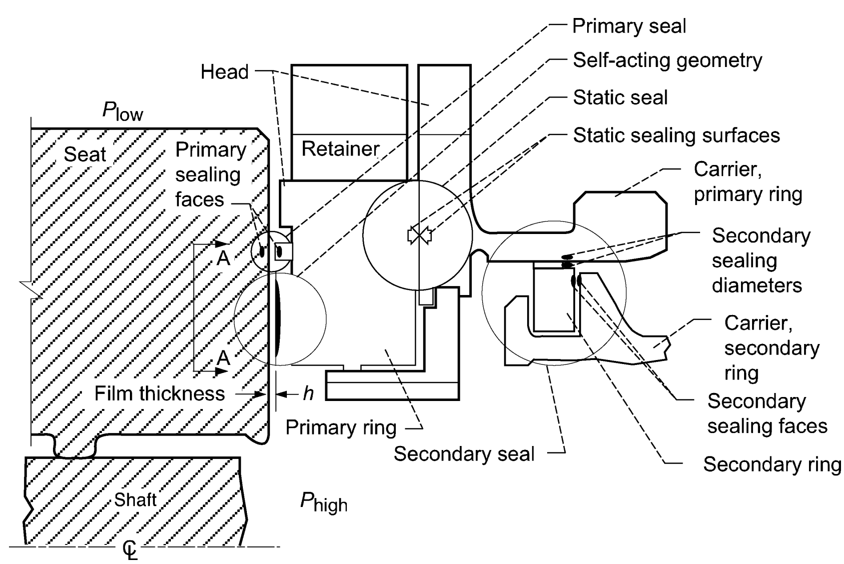

(a) Nomenclature

Fig. 46 Component schematic Rayleigh pad self-acting face seal.[109]

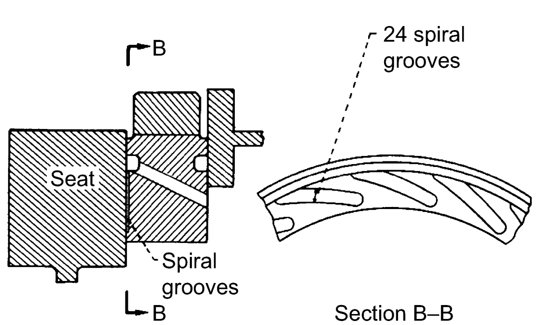

Fig. 47 Spiral groove sealing schematic.[109]

of the stationary cylindrical surface as well as axially against the faces of the adjacent metal seal seats (Fig. 49). The metal seal seats are fixed to, and rotate with, the shaft. The sealing closing force is provided by a combination of spring forces and gas pressures. Ring seals are employed where there is a large relative axial movement as a result of thermal mismatch between the shaft and the stationary structure. Ring seals are limited to operation at air pressure drops and sliding speeds considerably lower than those allowed for face seals. However, they can be used to gas temperature levels in the same range as for positive-contact face seals, approximately to 480°C (900°F). Generally, a minimum pressure differential of 14 kPa (2 psid) must be maintained to prevent oil leakage from the bearing compartment.

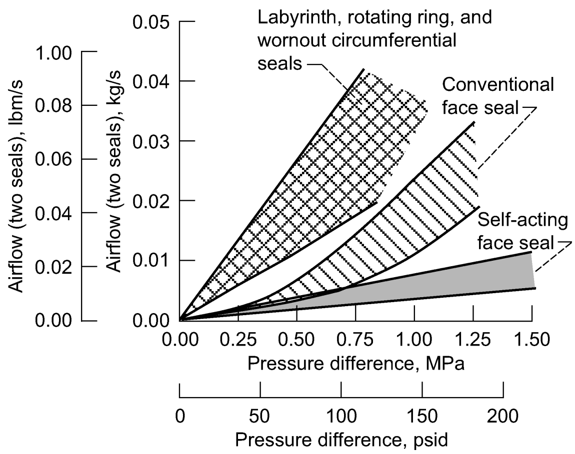

Fig. 48 Comparison of leakage characteristics for labyrinth, conventional (contact) face seal and self-acting face seals.[109]

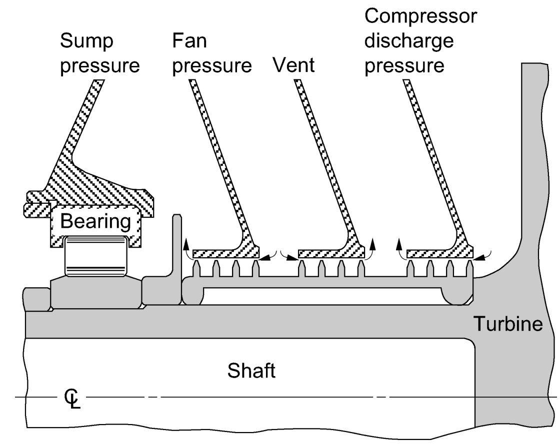

Fig. 51 Schematic of aero-gas-turbine buffer sealing of oil cavity.[109]

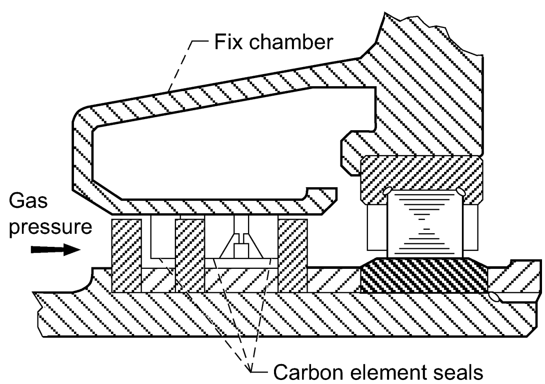

Fig. 49 Expanding ring seal.[106]

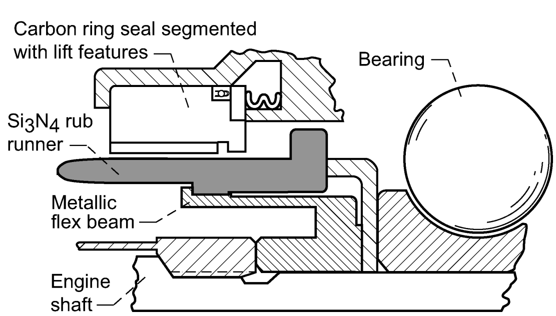

Fig. 50 Hybrid ceramic carbon ring seal.[112]

Carbon ring and face sealing of the sumps described by Ludwig,[4] Whitlock,[111] and Brown[106] are fairly standard. Boyd et al.[112] have investigated a hybrid ceramic shaft seal, which is composed of a segmented carbon ring with lifting features as the outer or housing ring and a silicon-nitride tilt-support arched rub runner mounted on a metal flex beam as the inner ring (Fig. 50). The flex beam added sufficient damping for stability, and no oil seepage was seen at idle speed down to pressure differentials of 0.7 kPa (0.1 psia), air to oil.

3. *Materials*

Selecting the correct materials for a given seal application is crucial to ensuring desired performance and durability. Seal components for which material selection is important from a tribological standpoint are the stationary nosepiece (or primary seal ring) and the mating ring (or seal seat), which is the rotating element. Brown[106] described the properties considered ideal for the primary seal ring as shown here: 1) mechanical—high modulus of elasticity, high tensile strength, low coefficient of friction, excellent wear characteristics and hardness, and self-lubrication; 2) thermal—low coefficient of expansion, high thermal conductivity, thermal shock resistance, and thermal stability; 3) chemical—corrosion resistance, and good wetability; and 4) miscellaneous—dimensional stability, good machinability, and low cost and readily available.

Because of its high ranking in terms of satisfying these properties, carbon graphite is used extensively for one of the mating faces in rubbing contact shaft seals. However, in spite of its excellent properties, the carbon material must be treated in order for it to satisfy the operational requirements of sealing applications in the main rotor bearing compartment of jet engines.

Seal failures are driven by thermal gradient fatigue or axial and radial thermal expansions during maximum power excursions. Bearing compartment carbon seals will fail from the heat generated in frictional rub. Excessive face wear occurs during transients, and, as mentioned, labyrinth seals can allow oil transport out of the seal and oil contamination by the environment (moisture, sand, etc.).[113]

G. Buffer Sealing

Public awareness of environmental hazards, well-publicized effect of hazardous leakages (Three Mile Island, *Challenger*), and a general concern for the environment have precipitated emissions limits that drive the design requirements for sealing applications. Of paramount concern are the types of seals, barrier fluids, and the necessity of thin lubricating films and stable turbomachine operation to minimize leakages and material losses generated by rubbing contacts.[104]

A zero-leakage seal is an oxymoron. Industrial practice is to introduce a buffer fluid between ambient seals and those seals confining the operational fluid (Fig. 51) with proper disposal of the buffered fluid mixture.[109,111] A second example is for shaft sealing as shown in Fig. 52 where buffer fluids are introduced. In the case of oil sumps, the buffered mixture is vented to the hot-gas exhaust stream and is presumed to be consumed. Within the nuclear industry, this becomes a containment problem where waste storage now becomes an issue. In the case of rocket engines, the use of buffering or inerting fluids (e.g., helium) is commonplace to separate fuel and oxidizer-rich environments for example in the space shuttle main engine turbomachinery.

H. Rim Sealing and Disk Cavity Flows

Turbomachine blade-vane interactions engender unsteady seal and cavity flows in multiply connected cavities with conjugate heat transfer and rotordynamics. A comprehensive review of seals secondary flow system developments are documented by Hendricks et al.[114,115] and NASA Seals Code and Secondary Flow Systems Development publications.[77]

Unsteady flows perturb both the power and the secondary flow streams.[2] A T1 turbine (first stage of the HPT) can have 76 blades and 46 stators all interacting with unsteady loadings (Fig. 53).[116] Cavity

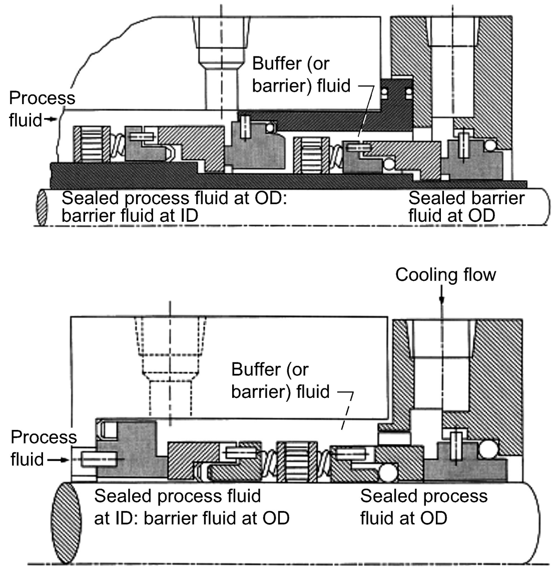

Fig. 52 Schematic of buffer fluid use in system sealing.[104]

ingestion of rapidly pulsating hot gases induces cavity heating and increases disk temperature, which in turn limits disk life and can compromise engine safety. Proper sealing confines these gases to the blade platform regions.

Rotordynamic issues further complicate rim seal and interface seal designs. These issues are addressed in Thomas,[63] Alford,[64,117,118] Benckert and Wachter,[66] NASA conference publications,[76] Abbott,[65] von Pragenau,[119] Vance,[120] Childs,[121] Muszynska,[68] Bently and Hatch,[122] Hendricks,[115] and Temis.[123]

Cavity and sealing interface requirements differ between industrial and aeroturbomachines. Major differences include split casings and through-bolted disks and compressors and turbines with common drive shafts for industrial machines vs cylindrical casings and drum rotors on multiple spools for aeromachines. Figure 53 shows a typical aeromultistage turbine cavity section. Several experimental studies that consider both simplified and complex disk cavity configurations have been reported (e.g., Chen,[124] Chew et al.,[125,126] Graber et al.,[127] and Johnson et al.[128,129]). Cavity sealing is complex and has a significant effect on component and engine performance and life. However, several analytical and numerical tools are available to help guide the designer, experimenter, and field engineer in addressing these challenges (see Appendix).

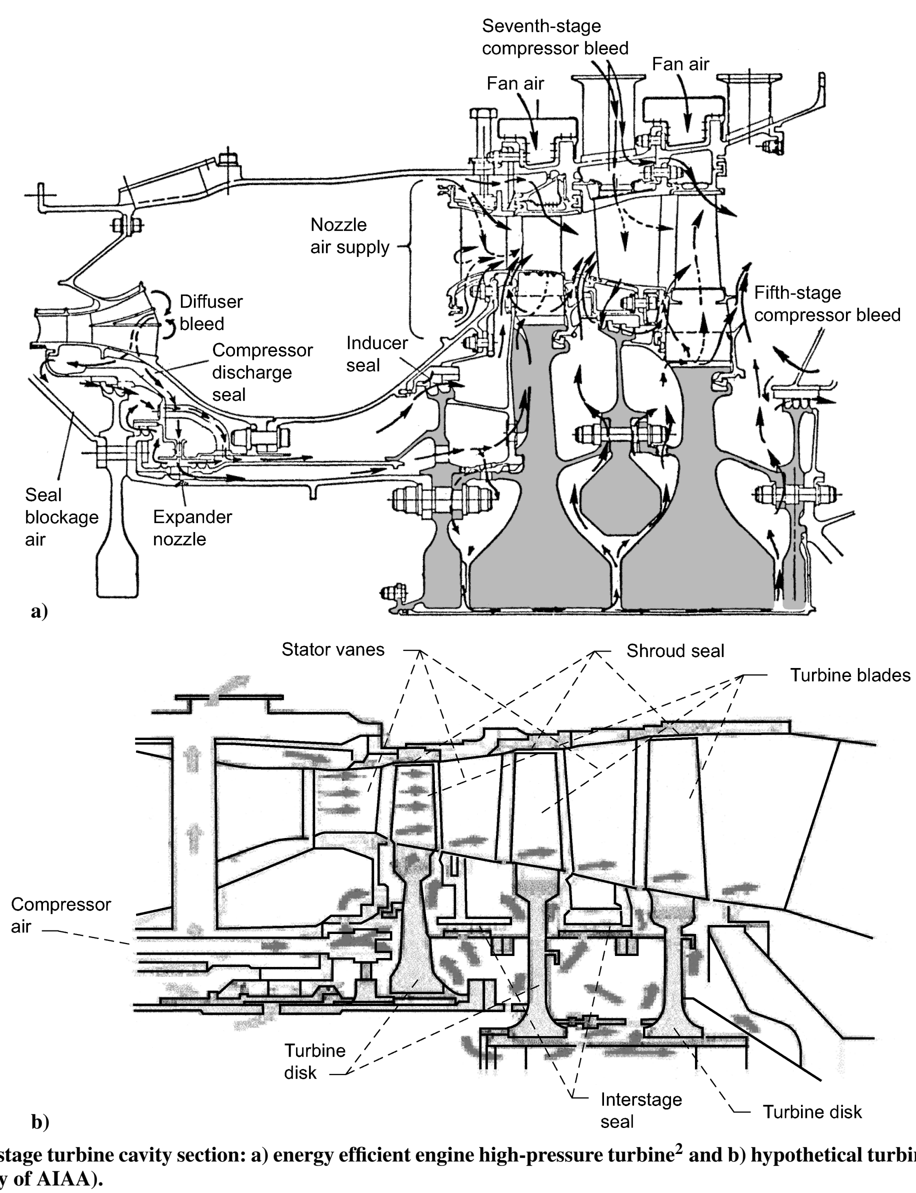

Fig. 53 Typical multistage turbine cavity section: a) energy efficient engine high-pressure turbine[2] and b) hypothetical turbine secondary air cooling and sealing[116] (courtesy of AIAA).

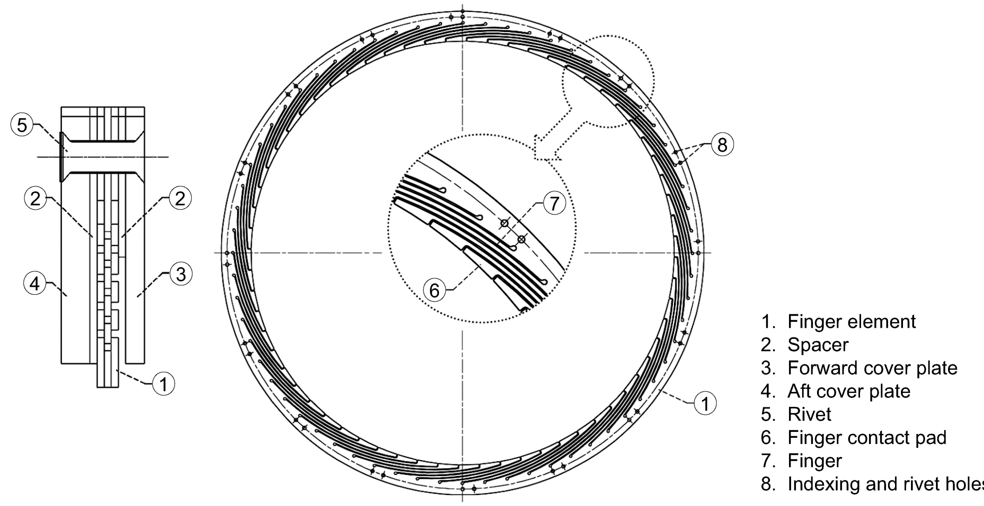

Fig. 54 Finger seal and detailed components.[132]

V. Advanced Seal Designs

A. Finger Seal

The finger seal is a relatively new seal technology developed for air-to-air sealing for secondary flow control and gas-path sealing in gas-turbine engines.[130–132] It can easily be used in any machinery to minimize airflow along a rotating or nonrotating shaft. Measured finger seal air leakage is $\frac{1}{3}$ to $\frac{1}{2}$ of conventional labyrinth seals. Finger seals are compliant contact seals. The power loss is similar to that of brush seals.[133] It is reported that the cost of finger seals is estimated to be 40 to 50% of the cost to produce brush seals.

The finger seal is composed of a stack of several precisely machined sheet stock elements that are riveted together near the seal outer diameter as shown in Fig. 54. The outer elements of the stack, called the forward and aft coverplates, are annular rings. Behind the forward coverplate is a forward spacer, then a stack of finger elements, the aft spacer and then the aft coverplate. The forward spacer is an annular ring with assembly holes and radial slots around the seal inner diameter that align with feed-through holes for pressure balancing. The finger elements are fundamentally an annular ring with a series of cuts around the seal inner diameter to create slender curved beams or fingers with an elongated contact pad at the tip. Each finger element has a series of holes near the outer diameter, which are spaced such that when adjacent finger elements are alternately indexed to the holes, the spaces between the fingers of one element are covered by the fingers of the adjacent element. Some of the holes create a flowpath for high pressure upstream of the seal to reach the pressure balance cavity formed between the last finger element, the aft spacer and seal dam, and the aft coverplate. The aft spacer consists of two concentric, annular rings. One is like the forward spacer. The second is smaller with an inner diameter the same as the aft coverplate and forms the seal dam. It is connected to the outer annular ring by a series of radial spokes.

The fingers provide the compliance in this seal and act as cantilever beams, flexing away from the rotor during centrifugal or thermal growth of the rotor or during rotordynamic deflections. The pressure balance cavity reduces the axial load reacted by the seal dam and hence minimizes the frictional forces that would cause the fingers to stick to the seal dam and cause hysteresis in the finger seal leakage performance. In this seal there are two leakage paths. One is through the fingers at the seal/rotor interface. The other is a radial flow across the seal dam. When a pressure differential exists across the seal, the fingers tend to move radially inward towards the rotor. Test results confirm this pressure closing effect. The pressure closing effect is largely caused by the pressure gradient under the finger contact pads. The bulk of the radial pressure loads on the curved beam of the finger balance out to a zero net load. Ideally, one would design finger seals to have a line-to-line fit during operation. However, most applications involve a range of operating conditions and seal-to-rotor fits and clearances change caused by different coefficients of thermal expansion, centrifugal rotor growth, pressure closing effects, and dynamics of the rotor. Depending on the requirements of the application, it might be desirable to start with an interference fit at build and allow the seal to wear in, or it might be desirable to have a clearance between the seal and rotor at build and allow the gap to close up.

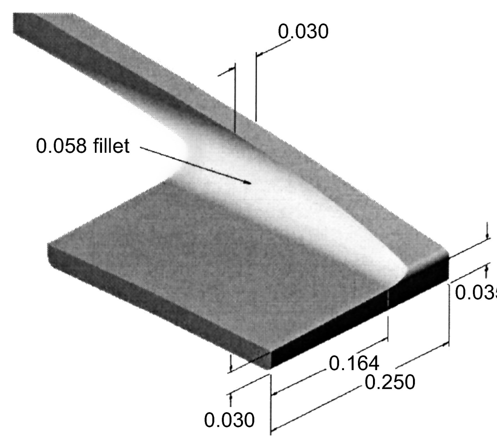

Fig. 55 Illustration of a noncontacting finger seal downstream padded finger.[134]

Finger seals are contacting seals, and wear of the finger contact pad is expected. Life is dependent on the materials selected and operating conditions. Arora et al.[131] reported the seal and rotor were in excellent condition after a 120-h endurance test. Testing of Haynes-25 fingers against a Cr_3C_2-coated rotor resulted in a wear track on the rotor 0.0064 mm (0.00025 in.) deep. The finger seal wore quickly to a near line-to-line fit with the rotor.[132]

B. Noncontacting Finger Seal

Altering the geometry of the basic finger seal concept, Braun et al.[134] and Proctor and Steinetz[135] developed a new seal that combines the features of a self-acting shaft seal lift pad as an extension of the downstream finger with an overlapping row of noncontacting upstream fingers (Figs. 55 and 56). These lift pads are in very close proximity to the rotor outer diameter so that hydrodynamic lift can be generated during shaft rotation. The seal geometry is designed such that the hydrostatic pressure between the downstream lift pad and the shaft is slightly greater than that above the pad. Depending on the application and operating conditions, the designer can choose to integrate hydrodynamic lift geometries on either the rotor or pads (e.g., taper, pockets, steps, etc.) to further increase liftoff forces. The overlapping fingers reduce the axial and radial flows along the compliant fingers that allow for radial motion of the shaft-seal interface. These seals respond to both radial and axial shaft perturbations and some degree of misalignment with minimal hysteresis. This technology is still being developed, but some experimental and analytical work has shown its feasibility.[136] It is expected that noncontacting finger seals will have leakage performance approximately 20% higher than a contact finger seal, which is still significantly better than conventional labyrinth seals, but have near infinite life because they will not rub against the rotor, except very briefly at start and stop. Both the finger seal and noncontacting finger seal are in the development stage. To the authors' knowledge, neither seal has been tested in an engine.

C. Leaf and Wafer Seals

The leaf seal, as described by Flower[137] and Nakane,[138] (Fig. 57) is an adaptation of the wafer seal advanced by Steinetz and Sirocky[139] with principles of operation delineated by Hendricks et al.,[22,87] Steinetz and Hendricks,[108] and Nakane et al.[138] The leaf and wafer seals have similar encapsulation but differ in root attachment and moments of inertia or cross section. The stacked leaves (or wafers) are relatively free to move in the radial direction and are deformable along the length or circumference providing a compliant restrained two-dimensional motion as opposed to the brush seal bristle, which deforms in three-dimensions.

Nakane et al.[138] reported leakage performance of a leaf seal at less than $\frac{1}{3}$ that of an equivalent four-stage, 0.5-mm-gap labyrinth seal geometry when run back to back on the same test rotor, with little wear at the smooth coated rotor interface. Variations in front- and backplate gaps are used to control lift of the leaves based on pressure drop and rotor speed. Modeling of a leaf or wafer sealing is similar (Fig. 58), where pressure balances, thickness, length, inclination, housing gaps and attachment points all require proper treatment for flexure and gap spacing. The latter are difficult to assess, and flow coefficients are most often determined experimentally. With that in mind, computations provided by Nakane et al.[138] are in good agreement with experimental data and CFD results, with little interface wear. Leaf-seal, leakage, endurance, and reliability are being evaluated in a M501G in-house industrial gas turbine. Both leaf and wafer seals provide for radial, circumferential, and axial motions. Even though the wafer seal is depicted with a low mobility wall, this restraint is not required. Evaluation of the rotordynamic stability coefficients for these seals is still required. Stiffness and damping is similar to brush configuration modeling but with an altered cross section. These seals will not respond well to grooved or rough surfaces, which are alleviated when lift off occurs.

An alternate form of the leaf seal has been advanced by Gardner.[140] The seal is composed of overlapping shaft-riding leaves

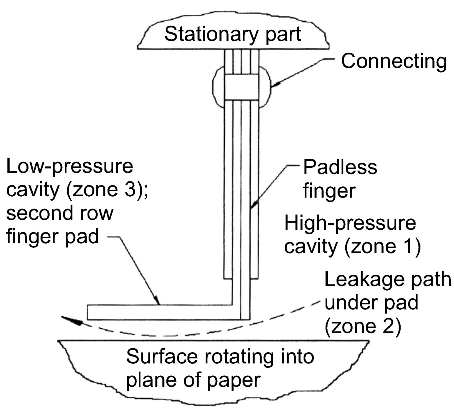

Fig. 56 Cross section of noncontacting finger seal with two rows of padded low-pressure and padless high-pressure fingers.[134]

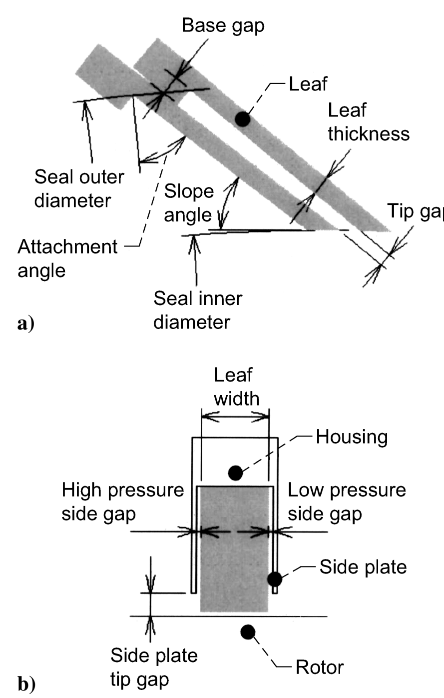

Fig. 58 Leaf-seal configuration parameters: a) front view and b) side view.[138]

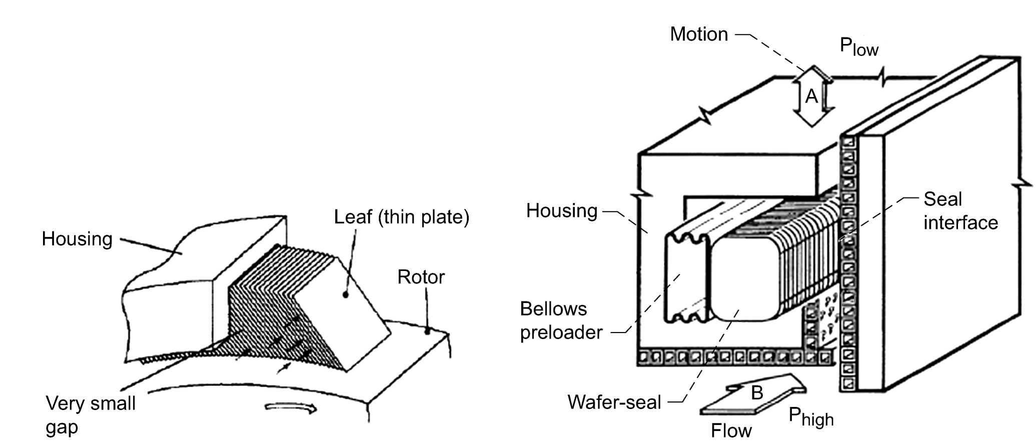

Fig. 57 Basic elements of leaf and wafer seals: a) leaf seal[138] and b) wafer seal.[139]

(thin metallic sheets), which extend from the sealing inlet about the shaft, forming shaft-riding fingers (Fig. 59). The cantilevered inner leaves form lifting pads that are overlapped by outer leaves that appear as cantilevered J springs. The outer leaf, which sees system pressure, seals the cavity and permits compliant radial excursions. It is similar in configuration to a film riding compliant foil bearing. This design also allows for hydrostatic operation, namely, when pressure is applied, the interface deforms to maintain an operating film, even without rotation. The overlapping shingled elements float on the fluid film providing excellent sealing with virtually no wear, yet can be somewhat limited by their ability to handle large system pressure and radial excursions without damaging the leaves. Gardner[140] reported hydrostatic and hydrodynamic performance results for a 121-mm (4.75-in.)-diam seal. The pressure-balanced seal permitted hydrostatic liftoff independent of rotor speed with total liftoff and no shaft torque with a 0.48-MPa (70-psid) pressure differential. The seal produced a torque of 0.028 N-m (0.25 in.-lb) at 1200 rpm with a 0.42-MPa (60-psid) pressure differential and a radial displacement of 0.23 mm (0.009 in.). When compared to typical industrial and an aerospace four-tooth labyrinth seal, with a 0.152-mm (0.006-in.) clearance and 1995 vintage-brush seal configurations, the leaf seal had leakage characteristics $\frac{1}{4}$ to that of the industrial labyrinth at design conditions (Fig. 60).[140]

D. Hybrid Brush Seals

Justak[141,142] combined a brush seal with tilt pad-bearing concepts to eliminate bristle wear. He introduced two designs: 1) the bristles are attached to the pads and 2) the pads are supported via beam elements and the bristle tips remain in contact with the outer surface of the pads (see Figs. 61 and 62, respectively). The brush seal stiffness is based on the design flow conditions and rotational speed. In the spring beam design, the beam elements are sized to allow radial movement and restrict axial displacements. In either design, seal leakage is controlled by the brush and liftoff by the pads, but leakage is more constant than a conventional brush seal and can accommodate reverse rotation with no bristle wear. Testing with rotor offsets up to 0.51 mm (0.020 in.) showed no wear or temperature rise and $\frac{1}{3}$ less torque to maintain speed when compared to a conventional brush seal.[142]

Shapiro[143] combined shaft, face, and brush sealing concepts to form a film riding seal with L-shaped annular segments (pads), which are preloaded onto the shaft via the brush seal and held in place by a garter spring (Fig. 63). The brush seal is separated axially from the brim of the cylindrical segments via a spring. This design allows the axial position of the brush seal to alter the preload and hence stiffness of the cylindrical seal segments. Analytical studies show low leakage, compliance, stability, and low wear during seal operation, yet development is required.

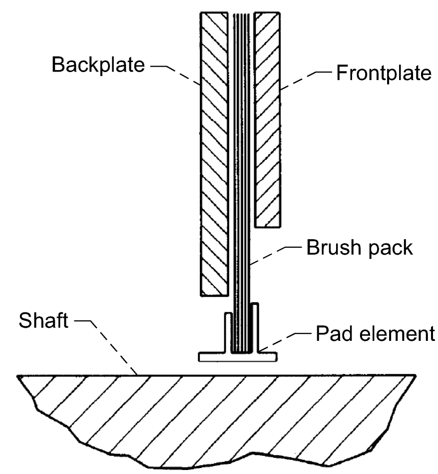

Fig. 61 Illustration of hydrodynamic brush seal (pad elements attached to bristles).[141]

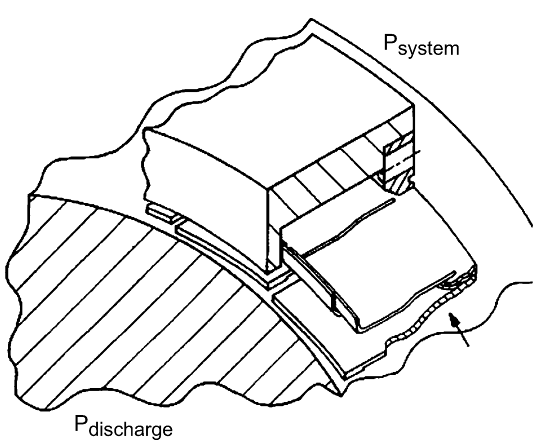

Fig. 59 Pressure-balanced compliant film riding leaf seal.[140]

Fig. 62 Hydrodynamic brush seal (spring beam elements).[142]

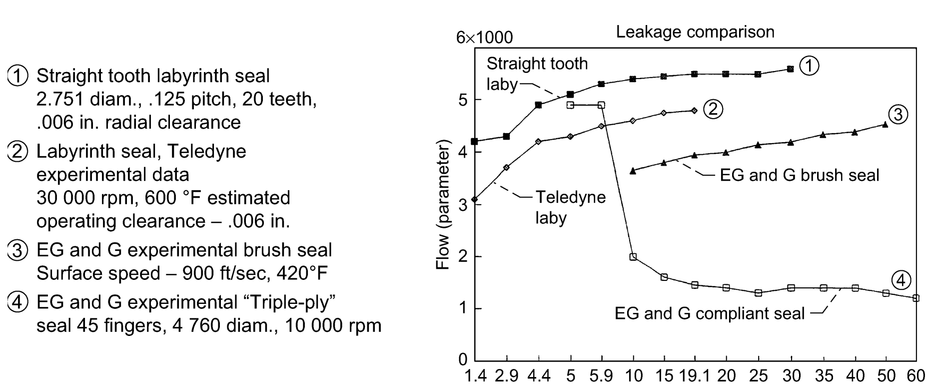

Fig. 60 Leaf seal leakage comparison with labyrinth and brush seals.[140]

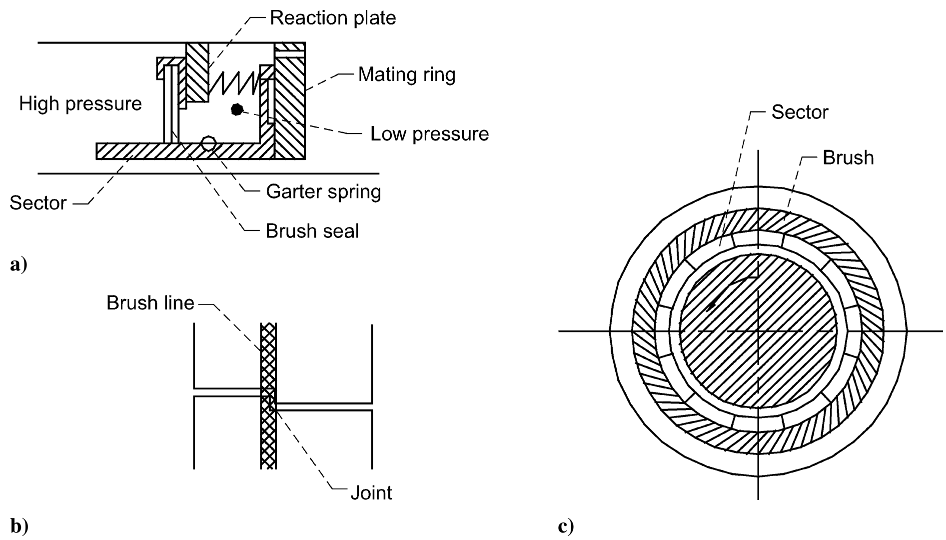

Fig. 63 Schematic of film riding brush seal: a) assembly, b) joint, and c) installed.[143]

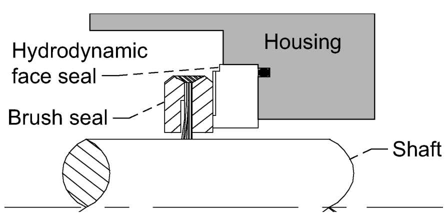

Fig. 64 Hybrid Floating Brush Seal (HFBS).[146]

The Hybrid Floating Brush Seal (HFBS) (Fig. 64) combines a brush seal and a film riding face seal that allows both axial and radial excursions mitigating interface problems of friction, heat, and wear.[144] The brush seal forms the primary seal, rotates with the shaft, while floating against a secondary face seal that acts as a thrust bearing. The HFBS relies on a high interference fit or preload. Major advantages include elimination of wear between rotating and stationary components, improved sealing performance, and the ability to handle large axial and radial shaft excursions while maintaining sealing integrity. For a 71-mm (2.8-in.)-diam HFBS that allowed up to 6.4-mm (0.25-in.) axial travel, experimental results showed $\frac{1}{6}$ the leakage of a standard brush seal at the same operating pressure ratios and rotational speed and an order of magnitude less than numerical predictions of a standard labyrinth seal (see Fig. 65).[145–147]

E. Aspirating Seals

An aspirating seal is a hydrostatic face seal with a narrow gap to control the leakage flow and a labyrinth tooth to control leakage flow at elevated clearances (Fig. 34a) and forms a high-pressure cavity for the diffused-injected flow in the engine cavity at operating conditions (Fig. 34b).[71]

Conventional labyrinth seals are typically designed with a seal/rotor radial clearance that increases proportionally with diameter. Aspirating face seals are noncontacting seals that are designed to establish an equilibrium position within close proximity [typically 0.038 to 0.076 mm (0.0015 to 0.003 in.) of the rotor surface regardless of the seal diameter].[148–153] Aspirating seals have a potentially significant performance advantage over conventional labyrinth seals, particularly at large diameters. In addition, these seals are inherently not prone to wear, owing to their noncontacting nature, and so their performance is not expected to degrade over time. Figures 34a and 34b show a cross section of the seal design, which is enhanced by the presence of a flow deflector on the rotor face.

During operation, the aspirating face seal performs as a hydrostatic gas bearing. The gas bearing on the sealing face provides a thin, stiff air film at the interface; as the clearance between the seal face and the rotor decreases, the opening force of the gas bearing increases. The seal face geometry is designed to give an operating clearance of 0.038 to 0.076 mm (0.0015 to 0.003 in.). In operation, the spring forces play a minor role; thus, the seal is free to follow the rotor on axial excursions. Tolerances between the primary face seal ring and the housing allow the ring to tilt relative to the housing; the seal can thus follow the rotor even if there is an angle between the face and the rotor, such as during a maneuver or due to rotor runout.

When there is an insufficient pressure drop across the seal to maintain an adequate film thickness (such as during startup and shutdown, periods when conventional face seals would touchdown), springs retract the seal from the rotor face (Fig. 34a). This ensures that the seal never contacts the rotor, thus providing for long seal life. In the retracted position, the pressure drop across the seal occurs at the aspirator tooth. During startup, as the pressure drop rises, the pressure balance across the primary face seal ring aspirates the seal to a closed position (Fig. 34b). The labyrinth tooth provides the required pressure drop to close the seal as well as a fail-safe seal in case of failure of the aspirating face seal.

Tests have been conducted to evaluate prototype performance under a variety of conditions that the seal might be subjected to in an aircraft engine application, including cases of rotor runout and seal/rotor tilt.[148,154] The tests were executed on a full-scale 36-in.-diam rotary test rig. Analyses were performed using three-dimensional CFD in order to validate test data and to establish the seal design. The full-scale tests demonstrated that with the flow isolation tip a hydrostatic film forms at the air bearing resulting in a seal/rotor clearance of 0.025 to 0.038 mm (0.001 to 0.0015 in.)., with correspondingly low leakage rates. The seal performs effectively with rotor runouts as great as 0.25 mm (0.010 in.) total indicator reading, and the seal was able to accommodate the expected angular misalignment (tilt) of 0.27 deg.

F. Microdimple

Laser surface texturing, termed microdimples (Fig. 66),[155] is a further extension of the damper-bearing and seal-bearing work established by von Pragenau[156,157] and extended by Yu and Childs,[158] who found that a hole-area to surface-area ratio of 0.69 is a more effective seal than honeycomb. For the microdimpled seal (Fig. 66), where diameter is 125 ± 5 μm (4900 ± 200 μ-in.) and depth 2.5 ± 0.5 μm (98 ± 20 μ-in.) with 0.2 μm (8 μ-in.) surface finish, the hole/surface area ratio is 0.3, indicating some potential for improvement. Diamond-like graphite or antifouling coatings were not used, but afford potential improvements.

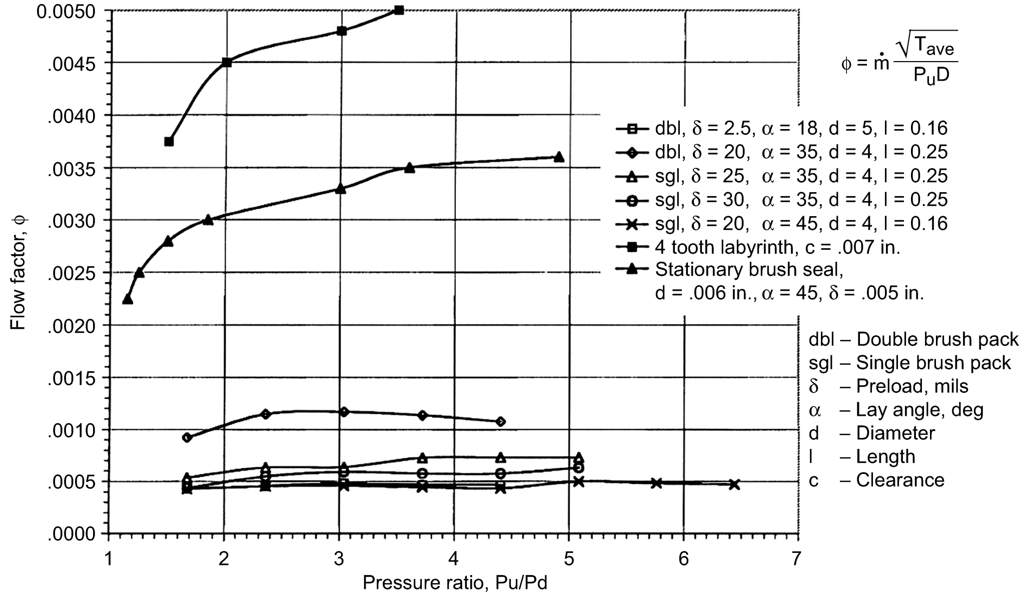

Fig. 65 HFBS performance compared to a stationary brush seal and a labyrinth seal: $\dot{m}$ is the mass flow rate of air (pps), T_{ave} is the average upstream air temperature (°R), P_u is the average upstream air pressure (psia), and D is the shaft outer diameter (in.) (Ref. 146).

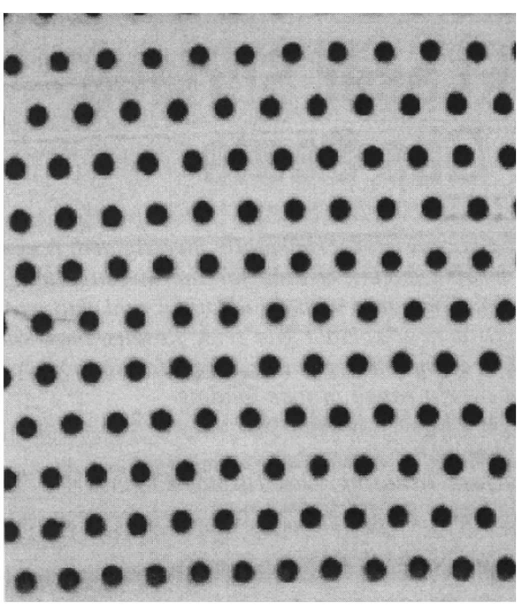

Fig. 66 Microdimpled surface by laser texturing.[155]

G. Wave Interfaces

Etsion[159] also developed a wave pumping face seal, modified by Young and Lebeck[160] to a wave interface; these concepts have been combined and further improved by Flaherty et al.[161] and are considered more debris tolerant (Fig. 67).

H. Seal Bearing

Munson et al.[7] describe and provide operations data for room-temperature testing of a seal-bearing concept. The basic concept was advanced by von Pragenau.[119,157] In Munson et al.'s seal configuration, the foil thrust bearing is combined with a mating flat interface to make a device called a foil face seal (Fig. 68). Multiple wave bump foils support the interface foils. With pressure drop and rotation, this interface gives rise to a compliant hydrodynamic film-riding face seal. For a 20,000-lb (89-kN)-thrust class engine, with this technology, an estimated mission fuel burn reduction of 1.85%

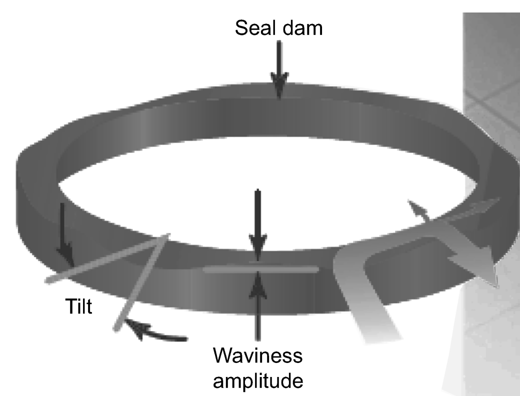

Fig. 67 Wave face seal.[161]

for a fixed engine and rubber airframe and 3.17% for both engine and airframe being "rubber" was reported. (Here "rubber" refers to allowing for design parameter changes.)

I. Compliant Foil Seal

Expanding upon Gardner's leaf seal concept,[140] Salehi and Heshmat[162] proposed an extension of their foil bearing work as a seal (Fig. 69).

Forming an inexpensive, close tolerance, bell-mouth smooth interface foil, similar to a nozzle inlet, is not an easy task, yet can be accomplished by flow form or shear form spinning.[67] However, Salehi and Heshmat[162] and Heshmat[163] chose to form the bellmouth-nozzle inlet by cutting radial relief slots to account for the difference between inner and outer circumference (diameters) and bending the tabs to form the bell-mouth or L-shaped foil section. The resulting foil is then attached to the housing at one end opposing rotation. The slot relief spacing is dependent on stresses in the bend radius, foil thickness, and seal diameter to prevent significant "pleating" of the seal-interface foil. The resulting near-smooth compliant, noncontacting foil interface rides on a fluid film, typically <0.0127 mm (<500 μ-in.) thickness. The L-shaped section provides blockage for the bump foil opening and must be carefully contoured at the shoulder and spring pressed against the support structure forming the necessary secondary seal. Overlapping leaves

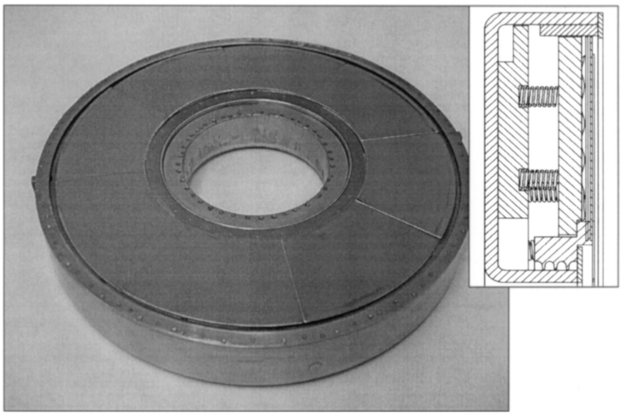

Fig. 68 Proof-of-concept foil face seal[7] (courtesy of Rolls-Royce/Allison).

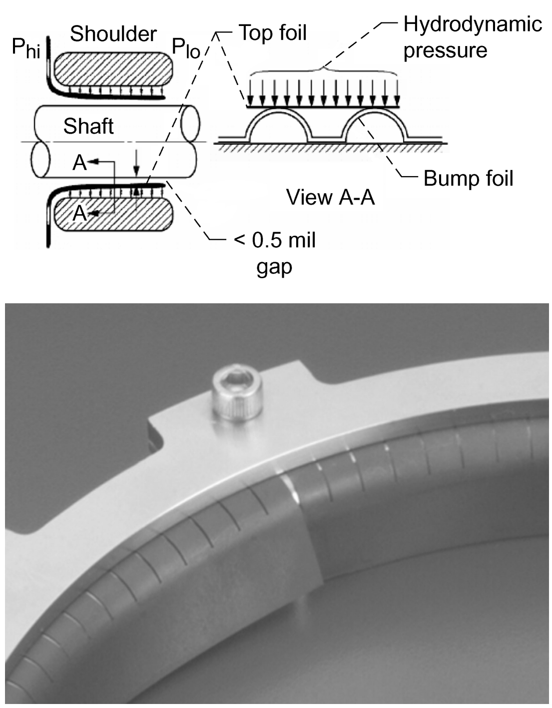

a)

b)

Fig. 69 Foil seal: a) schematic illustrating foil and bump-foil support and b) foil seal nozzle inlet or L-shaped interface at attached and free end.

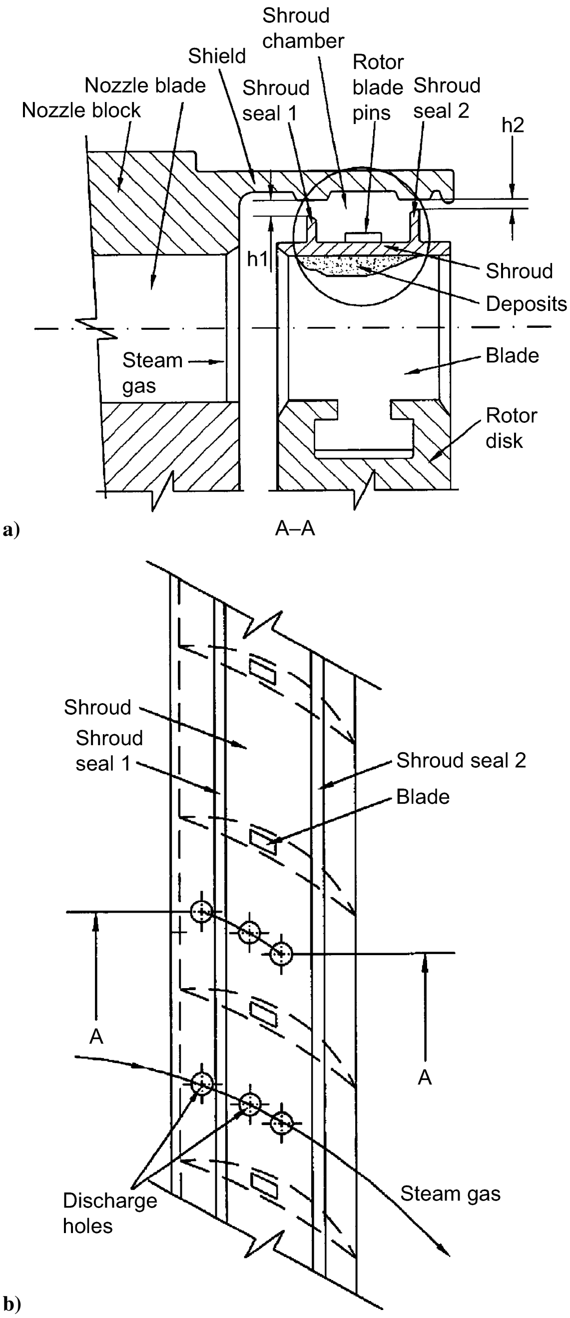

a)

b)

Fig. 70 Turbine shroud ring for deposit control: a) deposits build up in turbine passage and b) shroud discharge hole locations.[164]

can assist to minimize these slot leakages, yet it is a difficult area to seal. The interface foil (or foils) is in turn supported on a series of bump foils that provide variable stiffness in response to radial shaft excursions. The foils are usually coated with a solid lubricant to minimize startup and shutdown interface contact wear while permitting radial leaf sliding at the inlet.

Such seals are low leakage fluid film devices that are capable of operating at high surface velocities and temperature and pressure loadings limited by the foil materials used in the construction, for example, 365 m/s (1200 fps) and 600°C (1100°F).

J. Deposits Control

For turbines operating in high salt environments, Nalotov[164] introduces strategically placed holes within the turbine shroud ring to provide equalization of circumferential pressures within the labyrinth interface. The concept is shown in Figs. 70a and 70b. Figure 70a is a sketch representing the cross section of a nozzle and shrouded turbine stage where salt and metal oxides have built up on the shroud. Figure 70b shows the location of the discharge holes. The pressure equalization induces stability inside the shroud chamber, which allows for reduced shroud seal clearance. The flow through the shroud ring produces an obstacle effect to prevent deposits from building up and hence reduces blade passage blockage by accumulated salts. The concept has the net effects of increasing turbine engine efficiency as well as service life.

K. Active Clearance Control (ACC)

Most modern turbomachines have variable geometry controls. The compressor, for example, uses inlet guide vanes that are rotated to enhance efficiency at off-design conditions [usually designed to handle takeoff (TO) and set for cruise]. In large aeroengines, case clearance control is used in the turbine. Today's larger commercial engines control HPT blade-tip clearances by impinging fan air on the outer case flanges. Systems such as those shown in Figs. 71a and 71b scoop air from the fan bypass duct to cool the outer case flanges, reducing the case diameter and hence shroud clearance. Other engines use a mixture of fan and compressor air to achieve finer HPT tip clearance control. Because these thermal systems are

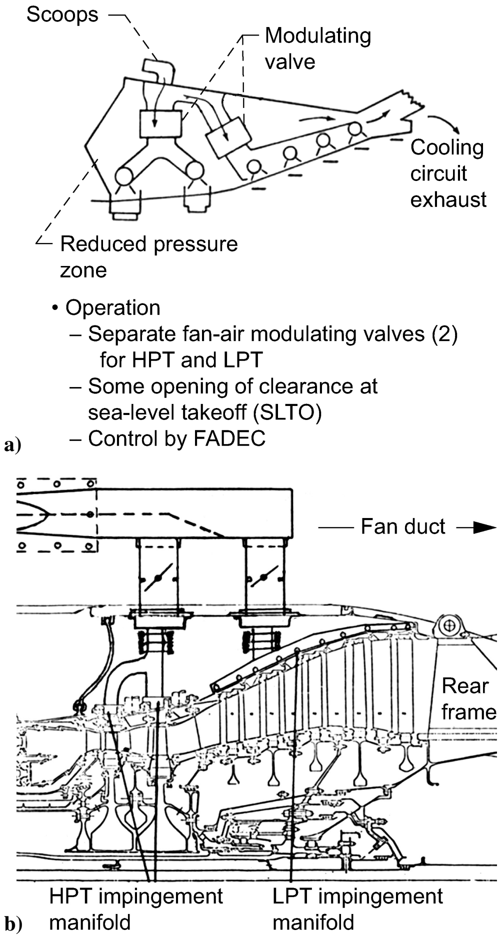

Fig. 71 Thermal ACC system: a) scoop design and b) HPT impingement manifold[2] (FADEC-full authority digital engine controller).

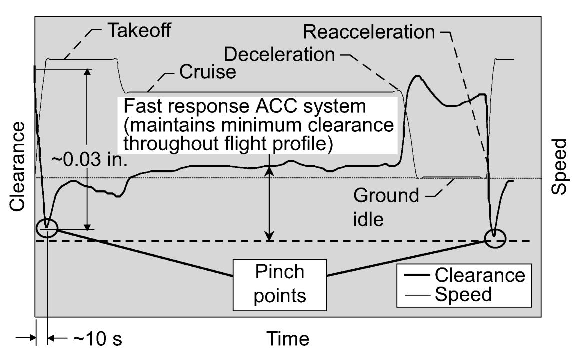

Fig. 72 High-pressure turbine blade-tip clearance over given mission profile.[6]

relatively slow, they cannot be used during transient events such as TO and reaccel. As such, they are generally scheduled for operation during cruise conditions. Lattime and Steinetz[165] are developing fast-response systems that utilize clearance measurement feedback control, enabling true active clearance control at engine startup and throughout the flight envelope (Fig. 72). Active clearance control is not usually used in the compressor; rather, the efficiency is enhanced through varying the vane angle and vortex control through fluid injection. Without these systems several points in efficiency are lost. Yet such close control is not without potential blade shroud and vane-rotor rubbing where the cited efficiency can be lost.

VI. Life and Limitations

System design conditions for seal-controlled component cooling are driven by compliance to regulatory agencies, reliability, and safety standards.[166] The mean time between failures (MTBF) is highly dependent on the thermal loading (Fig. 73) and the aeroengine and flight operations profile (Figs. 74 and 75).

For engine component life modeling, the time τ_i and the life L_i under thermomechanical load from the environmental temperature (Fig. 76) and flight envelope profile (Figs. 74 and 75) are used to determine the cumulative loss of component life according to the linear damage rule of Palmgren, Langer, and Miner.[167]

Zaretsky et al.[168] applied Weibull-based life and reliability analysis to rotating engine structures. The NASA E^3 engine design data served as the basis for the analysis.[2,169] When limits are placed on stress, temperature, and time for a component's design, the criterion that will define the component's life and thus the engine's life will be either high-cycle or low-cycle fatigue.

Knowing the cumulative statistical distribution (Weibull function) of each engine component is a prerequisite to accurately predicting the life and reliability of an entire engine. Table 6 shows how some of the hot section component lives correlate to aeroengine maintenance practices without and with refurbishment, respectively. That is, it can be reasonably anticipated that at one of these time intervals, 5% of the engines in service will have been removed for repair or refurbishment for cause.

Within the open literature there is a dearth of data for seals and their functional life and for basic materials. The classic approach

Table 6 E3 engine flight propulsion system life based on 1985 technology and experience[169]

Component	Service life, h	Total life with repair, h
Combustor	9,000	18,000
HPT rotating structure	18,000	36,000
HPT blading	9,000	18,000
Remainder of engine	——	36,000

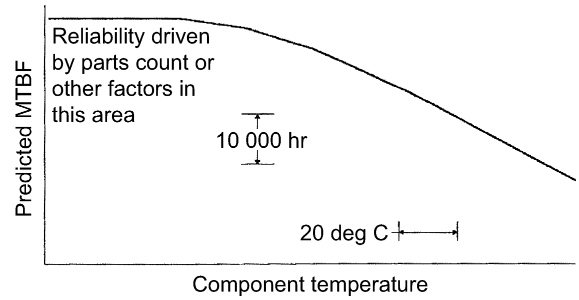

Fig. 73 Effect of component temperature on predicted mean time between failures for typical engine-mounted electronic device[166] (courtesy of The Boeing Company).

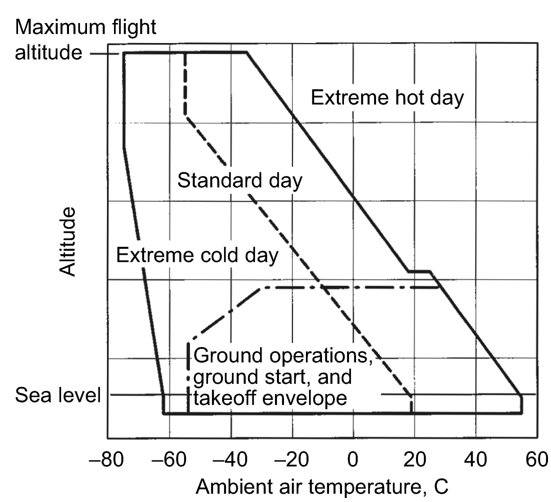

Fig. 74 Engine operating envelope[167] (courtesy of Pratt and Whitney).

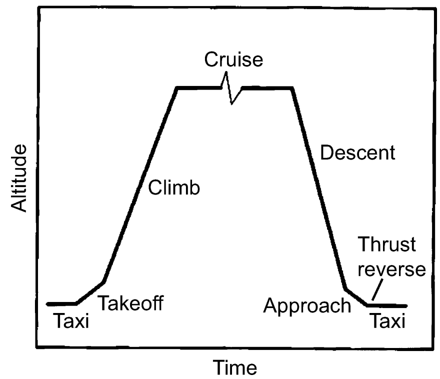

Fig. 75 Flight profile[167] (courtesy of Pratt and Whitney).

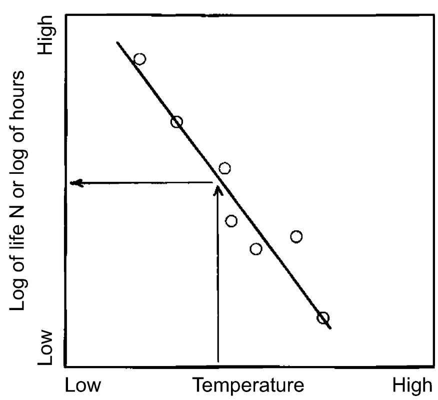

Fig. 76 Material life as a function of temperature relation[167] (courtesy of Pratt and Whitney).

is deterministic and assumes that full and certain knowledge exists for the service conditions and the material strength. Specific equations define sealing conditions are coupled with experience-based safety factors. Variations with loading can have a significant effect on component reliability. The Weibull-based analysis addresses these issues, but until a sealing database is established, MTBF will continue to be based on field experience.

VII. Summary

Turbine engine cycle efficiency, operational life, and systems stability depend on effective clearance control. Designers have put renewed attention on clearance control, as it is often the most cost-effective method to enhance system performance. Advanced concepts and proper material selection continue to play important roles in maintaining interface clearances to enable the system to meet design goals. No one sealing geometry or material is satisfactory for general use. Each interface must be assessed in terms of its operational requirements. Insufficient clearances limit coolant flows, cause interface rubbing, and engender turbomachine instabilities and system failures. Excessive clearances lead to losses in cycle efficiency, flow instabilities, and hot-gas ingestion into disk cavities. Hot-gas ingestion in the turbine reduces critical disk life and in the bearing sump location engenders bearing and materials failures. Reingestion of flow along the compressor drum interface causes unnecessary blockage and can lead to compressor stall.

Materials play a major role in maintaining interface clearances. Abradable materials for the fan are usually polymers; for the LPC compressor, ambient to 400°C (750°F): fiber metals and AlSi + filler can be used, but for the midrange LPC and HPC, ambient to 760°C (1400°F): Ni or Co base can be used (titanium blade fire protection limits); and if the blades are Ni-based superalloys, NiCrAl-Bentonite might be a choice. In the HPT, 760°C (1400°F) to 1150°C (2100°F), yttria-stabilized zirconia (YSZ) with controlled porosity and cBN or preferably SiC blade-tip abrasive grits can be used, depending on how hot the engine runs; in general, air plasma spray thermal barrier coatings (APS-TBCs) are used in the combustor, and for some engines first vanes (nozzles) and second-stage blades of the HPT. Electron beam plasma vapor deposition (EB-PVD) TBCs are used on the HPT T1 or first-stage blades, some second-stage blades, and some first-stage vanes (nozzles). TBCs are not commonly used in the LPT because of lower heat flux and are less effective in decreasing component temperature. APS ceramics are also used on shroud seals (blade outer air seals) where they function as both a thermal barrier for the metallic shroud and abradable seal.

Component life and reliability are closely coupled with the duty cycle. But as energy demands (and emissions regulations) necessitate more time-responsive-controlled engines, the industrial and aeroengine duty cycles become similar.

Appendix: Further Discussion on Rim Sealing and Disk Cavity Flows

Coupling of the power stream, seals, and cavity flows is a necessary aspect of multistage compressor and turbine design. Athavale et al.[170,171] have reported detailed descriptions of these tools and representative simulations (see also Janus and coworkers[172,173]). These works include the gas-path flows through the stages (blades and vanes) interacting with those under the platform and within the cavity as well as the sealing interface (shaft to platform) (Fig. A1).[174] Interstage-labyrinth-rim seal interface design goals are to keep leakage small, reduce windage and blockage, and mitigate ingestion and reintroduction of leakage flows.

Teramachi et al.[175] investigated turbine rim interface sealing (Figs. A1 and A2), providing data and some CFD results on four rim seal configurations: (0) T-on rotor, (1) T-on rotor with overlap T-on stator, (2) T-on stator with overlap T-on rotor; and (3) fish mouth on rotor with overlap T-on stator. Dummy stators were introduced, but there were no blades on the rotor. Carbon-dioxide concentration measurements [similar to the work of Johnson[129] (Graber et al.[127])] defined seal effectiveness in terms of the ratio of purge gas to ingested gas.

Figure A3 shows the seal effectiveness of these configurations, where flow coefficient $C_w = Q/\nu b$ and $Re_m = Vb/\nu$, where b is the cavity outer radius, V is the mean flow speed, Q is the purge flow rate, and ν is the kinematic viscosity. Configuration (3) is the least affected by changes in overlap and configuration and (0) the most; configuration (2) is quite sensitive to overlap. The high effectiveness of configuration (3) is related to the buffer cavity between the two rotor seal teeth with a stator tooth between the rotor teeth. The lowest effectiveness of configuration (1) is because of the large clearance

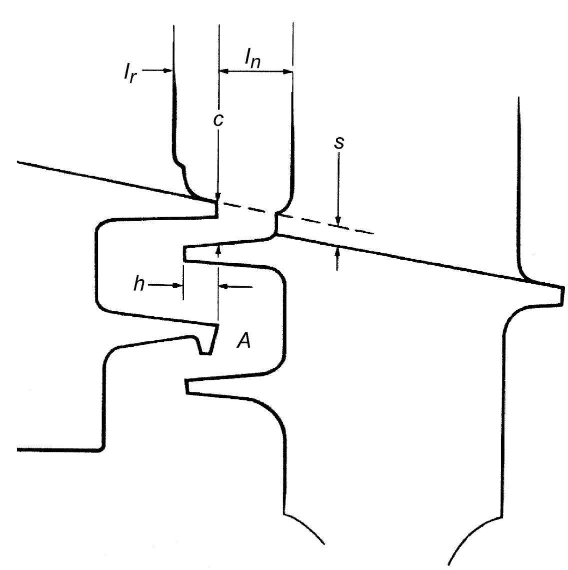

Fig. A1 Generic turbine nozzle rotor gap configuration.[174]

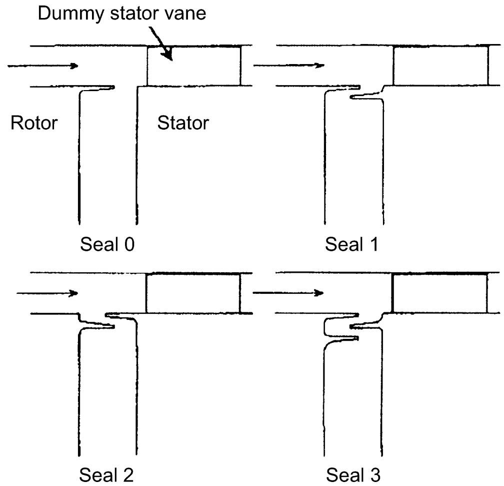

Fig. A2 Experimental rim seal configurations.[175] (courtesy of AIAA).

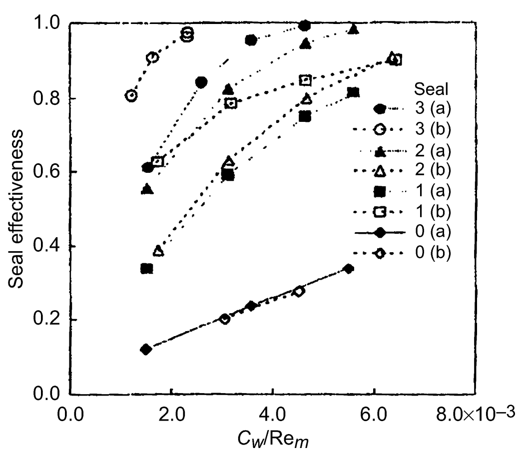

Fig. A3 Comparison of experimental rim seal data at Reynolds numbers: a) 2.4E6 and b) 1.1E6[175] (courtesy of AIAA).

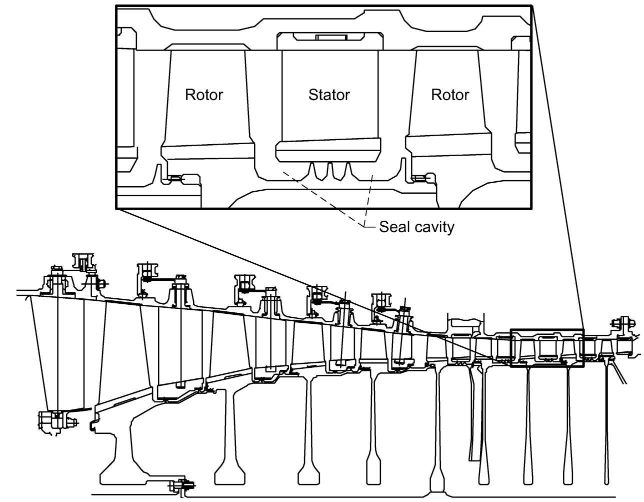

Fig. A4 Schematic of typical high-speed axial compressor with close-up view of seal cavity region under inner-banded stator.[59]

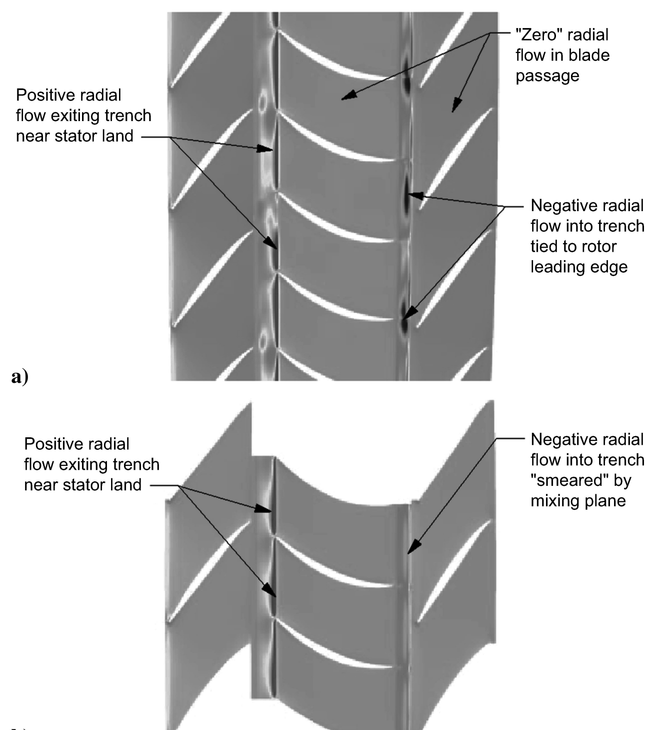

Fig. A5 Contours of radial velocity located one computational cell above hub (rotor) surface for course mesh: a) unsteady and b) mixing plane rotor/stator/rotor ADPAC solutions.[59]

gap, although the ingestion is nearly zero. CFD results show the gap recirculation zone where power-stream gas is ingested at on-pitch positions and ejected at midpitch positions (i.e., flow ingestion at the vane leading edge partially returns in the midpitch region mixing with the purge air; see also Wellborn and Okiishi[176]).

Wellborn and Okiishi[30,176] investigated the effect of leakage in a four-stage, LPC with blading design based on the NASA E3 engine. Seal leakages did not affect upstream stages but did progressively degrade performance of the downstream stages. For each 1% change in clearance/span ratio, the pressure rise penalty was nearly 3% with a 1% drop in efficiency. Hall and Delaney[177–179] simulated the low-speed axial compressor experiments with Adamczyk's analysis package.[180] They also completed sensitivity studies but did not address the effects on rotordynamics.

Heidegger et al.[59] presented three-dimensional solutions of the interaction between the power stream and seal cavity flow in a typical multistage compressor (Fig. A4). Using the Allison/NASA-developed ADPAC code, they performed a parametric study on a three-tooth labyrinth seal/cavity configuration and a sensitivity study to various sealing parameters. Their study shows that the leakage flow out of the seal cavities can affect the power stream significantly, mainly by altering the inlet flow near the stator blade root area, and can potentially affect the performance of the overall compressor (Fig. A5).

Feiereisen et al.[181] completed an experimental study of the primary and secondary flow in a turbine rig. It represents a first attempt at understanding this interaction and at generating data for validation. CFD techniques provide detailed flowfield information on complex cavity shapes that cannot be treated with analytical methods (e.g., Athavale et al.,[182,183] Chew,[125] Virr et al.,[184] and Ho et al.[185]).

Ho et al.[185] and Athavale et al.[186] in studying the Allison 501D turbine found that ingested fluid could work its way well into the disk space, even though purge fluid flows were substantial. Figures A6–A8 show the calculated interaction between power stream and secondary flows. Without conjugate heat transfer, the calculations would not match the Allison 501D turbine design data. It is most important at power-stream interfaces where the thermal gradient from the platform to the hub is significant. These aerothermomechanical loads can drastically affect disk and engine life.

The coupled codes SCISEAL and MS–TURBO[62] have been applied to several experimental test rig data sets showing conditions under which ingested flow can be controlled. The configuration

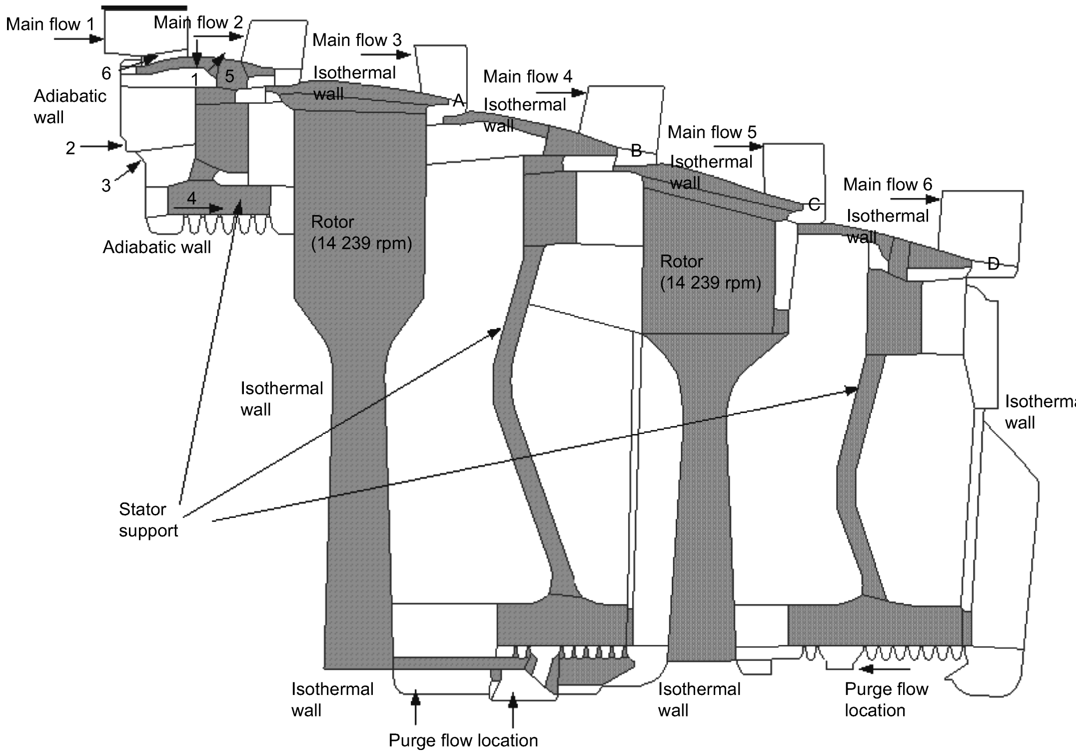

Fig. A6 Flow domain and conjugate heat-transfer calculations of all inner disk cavity pairs. Shaded areas denote conjugate heat transfer. Static pressures are specified at six main flow exits.[186]

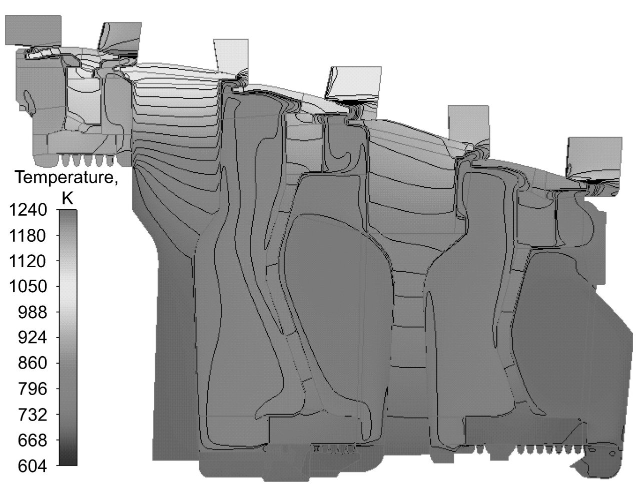

Fig. A7 Temperature field in fluid and solid parts of turbine cavities (absolute frame).[186]

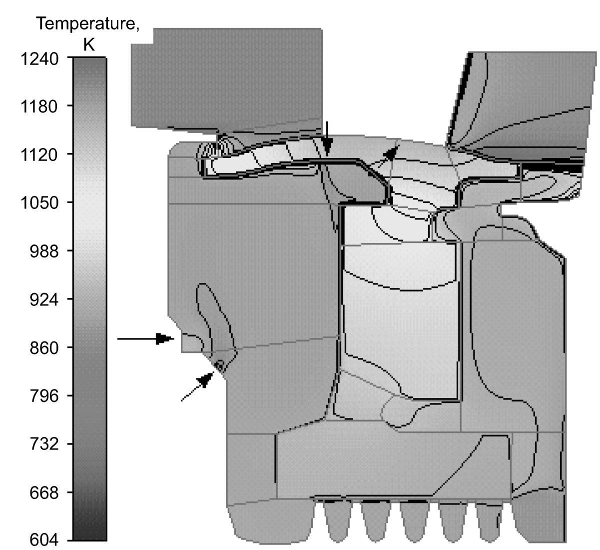

Fig. A8 Details of streamlines and temperatures in stage 1-2 cavities with conjugate heat transfer (absolute frame).[186]

(Figs. A9 and A10) is a 30-deg pi-sector with four vanes (stators) and five blades (rotors) simulating the stator/rotor set (48/58) with a three-tooth labyrinth seal and overlap rim seals.[62,181] Athavale et al.[62] found that a recirculation zone in the rim seal was present at the lower purge flow rate but was absent at the higher purge flow rate. The recirculation allows some gas ingestion into the rim seal area. This gas can then travel inside the cavity by both diffusion and convection (Fig. A11). Two important observations can be made:

1) The interface velocities show a tangential component that is lower than the rotor speed. This slow fluid alters the angle of attack near the roots of the rotor blades and can cause loss of power (turbine) and stall (compressor).

2) The rotor blades have the expected upstream pressure rise, which affects the flow in the rim seal and the cavity (enhances ingestion), although this disturbance is rather small.

Smout et al.[187] in a CFD analysis of rim sealing cite some collaborative efforts involved in investigating rotating cavity ventilation, bearing cavity purge and cooling, pressure balance, and sealing rotor/stator gaps. The turbine slinger determines the preswirl of cooling air entering the HPT blades. Controlling preswirl in power and secondary flow streams becomes very important for rotordynamics and power-on-demand cycling. For preswirl analysis and control methods, see Thomas,[63] Benckert and Wachter,[66] NASA conference publications,[76] von Pragenau,[119] Childs,[121] Muszynska,[68] Bently and Hatch,[122] and Hendricks.[115]

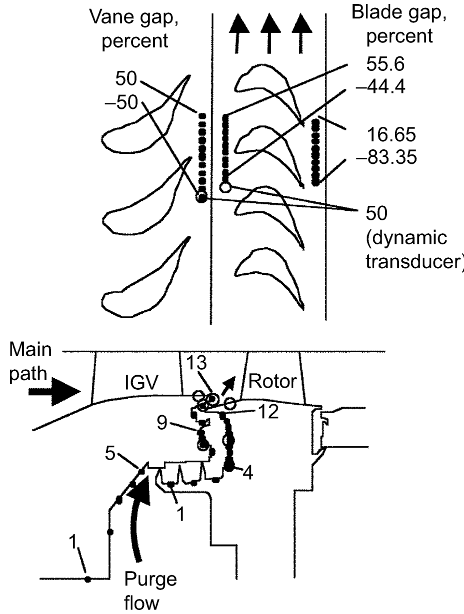

Fig. A9 Locations of pressure taps in United Technologies Research Corporation experimental rig: ●, steady pressure, ○, transient pressure measurements.[62]

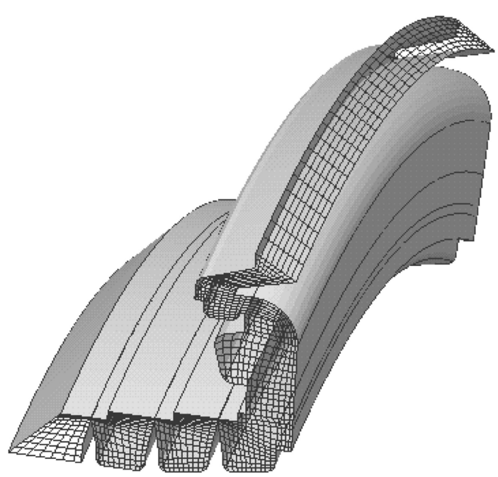

Fig. A10 Computational grid in disk cavity of high-pressure rig.[62]

Acknowledgments

Sealing in turbomachinery has been the focus of numerous development efforts. Many of these developers have been cited here. The authors would like to especially acknowledge contributors to this review paper: Mahmut Aksit (cloth static seals and extensively reviewing this paper), Margaret Proctor (finger seals), Norm Turnquist (aspirating seals), Saim Dinc and Mehmet Demiroglu (brush seals), Stephen Stone and Greg Moore (metallic static seals), and Farshad Ghasripoor (abradables). We also wish to thank our sponsoring organizations for the time and resources to prepare this paper.

References

[1]Miller, M., Colehour, J., and Dunkleberg, K., "Engine Case Externals, Challenges and Opportunities," *Proceedings of the 7th International Symposium on Transport Phenomena and Dynamics of Rotating Machinery*, ISROMAC-7, edited by A. Muszynska, J. A. Cox, and D. T. Nosenzo, Oct. 1998.

[2]Halila, E. E., Lenahan, D. T., and Thomas, T. T., "Energy Efficient Engine High Pressure Turbine Test Hardware: Detailed Design Report," NASA CR-167955, June 1982.

[3]Hendricks, R. C., Griffin, T. A., Kline, T. R., Csavina, K. R., Pancheli, A., and Sood, D., "Relative Performance Comparison Between Baseline Labyrinth and Dual Brush Compressor Discharge Seals in a T-700 Engine Test," Paper 94-GT-266, June 1994.

[4]Ludwig, L. P., and Bill, R. C., "Gas Path Sealing in Turbine Engines," ASLE Transactions, Vol. 23, No. 1, 1980, pp. 1–22.

[5]Moore, A., "Gas Turbine Engine Internal Air Systems. A Review of the Requirements and the Problems," American Society of Mechanical Engineers, Paper 75-WA/GT-1, Nov. 1975.

[6]Lattime, S. B., and Steinetz, B. M., "Turbine Engine Clearance Control Systems: Current Practices and Future Directions," *Journal of Propulsion and Power*, Vol. 20, No. 2, 2004, pp. 302–311.

[7]Munson, J., Grant, D., and Agrawal, G., "Foil Face Seal Proof-of-Concept Demonstration Testing," AIAA Paper 2002-3791, July 2002.

[8]Chupp, R. E., Ghasripoor, F., Moore, G. D., Kalv, L. S., and Johnston, J. R., "Applying Abradable Seals to Industrial Gas Turbines," AIAA Paper 2002-3795, July 2002.

[9]Bill, R. C., "Wear of Seal Materials Used in Aircraft Propulsion Systems," *Wear*, Vol. 59, No. 1, 1980, pp. 165–189.

[10]Aksit, M. F., Chupp, R. E., Dinc, O. S., and Demiroghu, M., "Advanced Seals for Industrial Turbine Applications: Design Approach and Static Seal Development," *Journal of Propulsion and Power*, Vol. 18, No. 6, 2002, pp. 1254–1259; also "Advanced Flexible Seals for Gas Turbine Shroud Applications," AIAA Paper 99-2827, June 1999.

[11]Camatti, M., Vannini, G., Baldassarre, L., Fulton, J., and Forte, P., "Full Load Test Experience on the Instability of a High Speed Back to Back Compressor Equipped with a Honeycomb Seal," *Proceedings of the 2nd International Symposium on Stability Control of Rotating Machinery*, ISCORMA-2, edited by A. Gosiewski and A. Muszynska, MAX MEDIA, Warsaw, Aug. 2003, pp. 617–626.

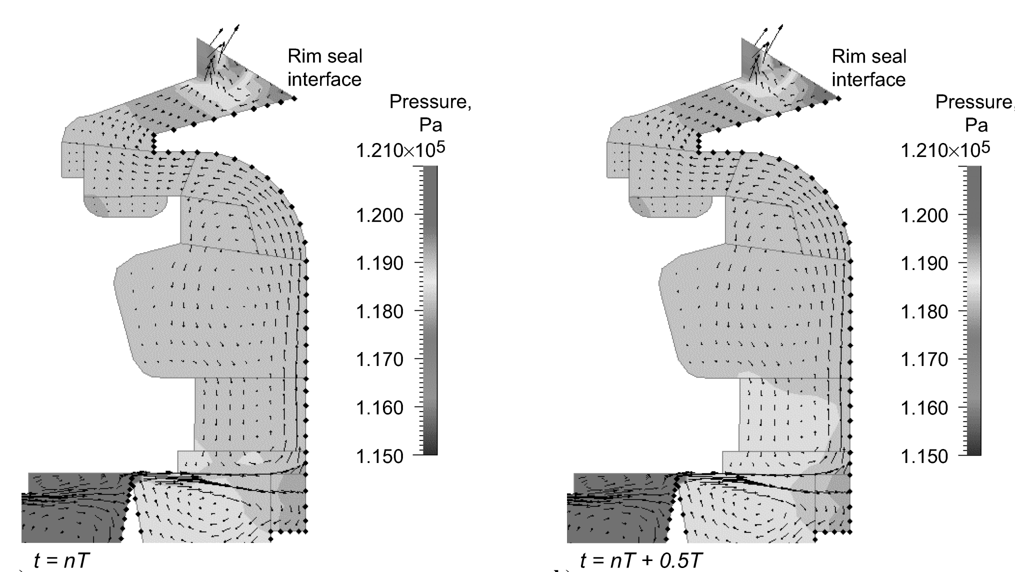

Fig. A11 Time-dependent cavity flows for 0.69% purge flow (absolute frame): a) time-transient pressures and b) velocity vectors in cavity, where $\eta = Re_{\text{feed}}/Re^{0.8}_{\text{turbine}} = 0.005$; t is time; n is cycle number; and T is cycle time.[62]

[12]Camatti, M., Vannini, G., Fulton, J., and Hopenwasser, F., "Instability of a High Pressure Compressor Equipped with Honeycomb Seals," *Proceedings of the 32nd Turbomachinery Symposium*, Turbomachinery Lab., Texas A&M Univ., College Station, TX, 2003.

[13]Shiembob, L. T., "Development of Abradable Gas Path Seals," PWA-TM-5081, Pratt and Whitney Aircraft, East Hartford, CT, 1974; also NASA Contract NAS3-18023, NASA CR-134689.

[14]More, D. G., and Datta, A., "Ultra High Temperature Resilient Metallic Seal Development for Aero Propulsion and Gas Turbine Applications," *2003 NASA Seal/Secondary Air System Workshop*, NASA/CP-2004-212963, Washington, DC, Vol. 1, pp. 359–370.

[15]Layer, J., *Advanced Metallic Seal for High Temperature Applications*, NASA CP-10198, Washington, DC, 1997, pp. 307–328.

[16]Aksit, M. F., Bagepalli, B. S., Demiroglu, M., Dinc, O. S., Keelock, I., and Farrell, T., "Advanced Flexible Seals for Gas Turbine Shroud Applications," AIAA Paper 99-2827, June 1999.

[17]Bagepalli, B. S., Aksit, M. F., and Farrell, T. R., "Gas-Path Leakage Seal for a Turbine," U.S. Patent 5934687, 10 Aug. 1999.

[18]Tompkins, T. L., "Ceramic Oxide Fibers Building Blocks for New Applications," *Ceramic Industry Publications*, Business News Publishing, April 1995.

[19]Steinetz, B. M., and Adams, M. L., "Effects of Compression, Staging, and Braid Angle on Braided Rope Seal Performance," *Journal of Propulsion and Power*, Vol. 14, No. 6, 1998, pp. 934–940; also NASA TM-107504, June 1997.

[20]Steinetz, B. M., "High Temperature Braided Rope Seals for Static Sealing Applications," NASA TM-107233, 1997; also *Journal of Propulsion and Power*, Vol. 13, No. 5, 1997, pp. 675–682.

[21]Opila, E. J., Lorincz, J. A., and Demange, J. J., "Oxidation of High-Temperature Alloy Wires in Dry Oxygen and Water Vapor," *High Temperature Corrosion and Materials Chemistry V*, Electrochemical Society, Inc., Pennington, NJ, 2005, pp. 67–80.

[22]Hendricks, R. C., Braun, M. J., Canacci, V., and Mullen, R. L., "Brush Seals in Vehicle Tribology," *17th-Leeds-Lyon Symposium on Tribology*, Paper IX, Tribology Series 18, Elsevier, Amsterdam, 1991, pp. 231–242.

[23]Dunlap, P. H., Steintez, B. M., Curry, D. M., DeMange, J. J., Rivers, H. K., and Hsu, S. Y., "Investigation of Control Surface Seals for Re-Entry Vehicles," *Journal of Spacecraft and Rockets*, Vol. 40, No. 4, 2003, pp. 570–583.

[24]Steinetz, B. M., and Dunlap, P. H., "Rocket Motor Joint Construction Including Thermal Barrier," U.S. Patent No. 6,446,979 B1 (LEW 16,684-1), Sept. 2002.

[25]Hendricks, R. C., Steinetz, B. M., Zaretsky, E. V., Athavale, M. M., and Przekwas, A. J., "Reviewing Turbomachine Sealing and Secondary Flows Parts A, B, C," *The 2nd International Symposium on Stability Control of Rotating Machinery, ISCORMA-2003*, MAX MEDIA, Warsaw, Aug. 2003, pp. 40–91; also unabridged versions NASA/TM-2004-211991/PART1, PART2, PART3.

[26]Van Zante, D. E., Stazisar, A. J., Wood, J. R., Hathaway, M. D., and Okiishi, T. H., "Recommendations for Achieving Accurate Numerical Simulation of Tip Clearance Flows in Transonic Compressor Rotors," *Journal of Turbomachinery*, Vol. 122, Oct. 2000, pp. 733–742.

[27]Lakshminarayana, B., *Fluid Dynamics and Heat Transfer of Turbomachinery*, Wiley, New York, 1996.

[28]Copenhaver, W. W., Mayhew, E. R., Hah, C., and Wadia, A. R., "The Effect of Tip Clearance on a Swept Transonic Compressor Rotor," *Journal of Turbomachinery*, Vol. 118, No. 2, 1996, pp. 230–239.

[29]Strazisar, A. J., Wood, J. R., Hathaway, A. D., and Suder, K. L., "Laser Anemometer Measurements in a Transonic Axial-Flow Fan Rotor," NASA TP-2879, Nov. 1989.

[30]Wellborn, S. R., and Okiishi, T. H., "The Influence of Shrouded Stator Cavity Flows on Multistage Compressor Performance," *Journal of Turbomachinery*, Vol. 121, No. 3, 1999, pp. 486–498.

[31]Bill, R. C., and Wisander, D. W., "Friction and Wear of Several Compressor Gas-Path Seal Materials," NASA TP-1128, Jan. 1978.

[32]Bill, R. C., Wolak, J., and Wisander, D. W., "Effects of Geometric Variables on Rub Characteristics of Ti-6Al-4V," NASA TP-1835 (AVRADCOM TR 80-C-19), April 1981.

[33]Stocker, H. L, Cox, D. M., and Holle, G. F., "Aerodynamic Performance of Conventional and Advanced Design Labyrinth Seals with Solid-Smooth, Abradable, and Honeycomb Lands," NASA CR-135307 (EDR9339), Nov. 1977.

[34]Stocker, H. L., "Determining and Improving Labyrinth Seal Performance in Current and Advanced High Performance Gas Turbines," AGARD-CP-237 (AGARD-AR-123), Paper 13, Aug. 1978.

[35]Mahler, F. H., "Advanced Seal Technology," Pratt and Whitney Aircraft, Report PWA-4372 (Contract No. AD-739922), 1972.

[36]Morrell, P., Betridge, D., Greaves, M., Dorfman, M., Russo, L., Britton, C., and Harrison, K., "A New Aluminum-Silicon/Boron Nitride Powder for Clearance Control Application," *Proceedings of the International Thermal Spray Conference*, ITSC 98, ASM Thermal Spray Society, 1998, pp. 1187–1192.

[37]Chupp, R. E., Ghasripoor, F., Turnquist, N. A., Demiroglu, M., and Aksit, M. F., "Advanced Seals for Industrial Turbine Applications: Dynamic Seal Development," *Journal of Propulsion and Power*, Vol. 18, No. 6, 2002, pp. 1260–1266.

[38]Schmid, R. K., Ghasripoor, F., Dorfman, M., and Wei, X., "An Overview of Compressor Abradables," *Proceedings of the International Thermal Spray Conference*, ITSC 2000, ASM International, 2000, pp. 1087–1093.

[39]Guilemany, J. M., Navarro, J., Lorenzana, C., Vizcanio, S., and Miguel, J. M., "Tribological Behaviour of Abradable Coatings Obtained by Atmospheric Plasma Spraying (APS)," *Proceedings of the International Thermal Spray Conference*, ITSC 2001, ASM International, May 2001, pp. 1115–1118.

[40]Ghasripoor, F., Schmid, R. K., Dorfman, M., and Russo, L., "A Review of Clearance Control Wear Mechanisms for Low Temperature Aluminum Silicon Alloys," *Proceedings of the International Thermal Spray Conference*, ITSC 1998, ASM International, 1998, pp. 139–144.

[41]Nava, Y., Mutasim, Z., and Coe, M., "Abradable Coatings for Low-Temperature Applications," *Proceedings of the International Thermal Spray Conference*, ITSC 2001, ASM International, May 2001, pp. 119–126 (263–268).

[42]Schmid, R., "New High Temperature Abradables for Gas Turbines," Ph.D. Dissertation, Dept. of Materials, Swiss Federal Inst. of Technology, Zurich, 1997.

[43]Borel, M. O., Nicoll, A. R., Schlaepfer, H. W., and Schmid, R. K., "Wear Mechanisms Occurring in Abradable Seals of Gas Turbines," *Surface Coating Technology*, 1989, pp. 117–126.

[44]Chappel, D., Vo, L., and Howe, H., "Gas Path Blade Tip Seals: Abradable Seal Material Testing at Utility Gas and Steam Turbine Operating Conditions," American Society of Mechanical Engineers, Paper 2001-GT-0583, June 2001.

[45]Chappel, D., Howe, H., and Vo, L., "Abradable Seal Testing: Blade Temperatures During Low Speed Rub Event," AIAA Paper 2001-3479, July 2001.

[46]Ghasripoor, F., Schmid, R., and Dorfman, M., "Abradables Improve Gas Turbine Efficiency," *Journal of the Institute of Materials*, Vol. 5, No. 6, 1997, pp. 328–330.

[47]Ghasripoor, F., Schmid, R., Dorfman, M., and Wei, X., *Optimizing the Performance of Plasma Control Coatings up to 850C*, Surface Modification Technologies XII, ASME International, Rosemont, IL, 1998.

[48]Shell, J. D., and Farr, H. J., "Abrasive Ceramic Matrix Turbine Blade Tip and Method for Forming," U.S. Patent No. 5,952,110, Sept. 1999.

[49]Ghasripoor, F., Schmid, R. K., and Dorfman, M., "Silicon Carbide Composition for Turbine Blade Tips," U.S. Patent No. 5,997,248, Dec. 1999.

[50]Benoit, R., Beverly, E. M., Love, C. M., and Mack, G. J., "Abrasive Blade Tip," U.S. Patent No. 5,603,603, Feb. 1997.

[51]Draskovich, B. S., Frani, N. E., Joseph, S. S., and Narasimhan, D., "Abrasive Tip/Abradable Shroud System and Method for Gas Turbine Compressor Clearance Control," U.S. Patent No. 5,704,759, Jan. 1998.

[52]Johnson, G. F., and Schilke, P. W., "Alumina Coated Silicon Carbide Abrasive," U.S. Patent No. 4,249,913, Feb. 1981.

[53]Pan, Y., and Baptista, J., "Chemical Stability of Silicon Carbide in Presence of Transition Metals," *Journal of the American Ceramics Society*, Vol. 79, No. 8, 1996, pp. 2017–2026.

[54]Hutchings, I. M., "Erosion By Solid Particle Impact," *Tribology; Friction and Wear of Engineering Materials*, Edward Arnold, London, 1992, Sec. 6.4, pp. 171–197.

[55]Biesiadny, T. J., McDonald, G. E., Hendricks, R. C., Little, J. K., Robinson, R. A., Klann, G. A., and Lassow, E., "Experimental and Analytical Study of Ceramic-Coated Turbine-Tip Shroud Seals for Small Turbojet Engines," NASA TM X-86881, Jan. 1985.

[56]Wei, X., Mallon, J. R., Correa, L. F., Dorfman, M., and Ghasripoor, F., "Microstructure and Property Control of CoNiCrAlY Based Abradable Coatings for Optimal Performance," *Proceedings of the International Thermal Spray Conference*, ITSC 2000, ASM International, 2000, pp. 407–412.

[57]Burcham, R. E., and Keller, R. B., Jr., "Liquid Rocket Engine Turbopump Rotating-Shaft Seals," NASA SP-8121, Feb. 1979.

[58]Alford, J. S., "Labyrinth Seal Designs Have Benefited From Development and Service Experience," Society of Automotive Engineers, Paper 710435, Feb. 1971.

[59]Heidegger, N. J., Hall, E. J., and Delaney, R. A., "Parameterized Study of High-Speed Compressor Seal Cavity Flow," NASA CR-198504, 1996; also AIAA Paper 96-2807, July 1996.

[60]Hendricks, R. C., and Stetz, T. T., "Flow Rate and Pressure Profiles for One to Four Axially Aligned Orifice Inlets," NASA TP-2460, May 1985.

[61]Egli, A., "Leakage of Steam Through Labyrinth Seals," *Transactions of the ASME*, Vol. 57, No. 3, 1935, pp. 115–122.

[62]Athavale, M. M., Steinetz, B. M., and Hendricks, R. C., "Gas Turbine Primary-Secondary Flow Path Interaction: Transient, Coupled Simulation and Comparison with Experiments," AIAA Paper 2001-3627, July 2001.

[63]Thomas, R. J., "Unstable Oscillations of Turbine Rotors due to Steam Leakage in the Clearances of the Sealing Glands and the Buckets," *Bulletin Scientifique*, Vol. 71, 1958, pp. 1039–1063; also NASA CP-2133, Jan. 1980.

[64]Alford, J. S., "Protection of Labyrinth Seals From Flexural Vibration," American Society of Mechanical Engineers, Paper 63-AHGT-9, 1963; also *Journal of Engineering for Power*, Vol. 86, Series A, April 1964, pp. 141–148.

[65]Abbott, D. R., "Advances in Labyrinth Seal Aeroelastic Instability Prediction and Prevention," *Journal of Engineering for Power*, Vol. 103, April 1981, pp. 308, 312.

[66]Benckert, H., and Wachter, J., "Rotordynamic Instability Problems in High-Performance Turbomachinery," NASA CP-2133, Jan. 1980, pp. 189–212.

[67]Childs, D. W., Baskharone, E., and Ramsey, C., "Test Results for Rotordynamic Coefficients of the SSME HPOTP Turbine Interstage Seal with Two Swirl Brakes," NASA CP-3122, Oct. 1991, pp. 165–178.

[68]Muszynska, A., "The Fluid Force Model in Rotating Machine Clearances Identified by Modal Testing and Model Applications: An Adequate Interpretation of the Fluid-Induced Instabilities, Invited Lecture," *Proceedings of the 1st International Symposium on Stability Control of Rotating Machinery (ISCORMA-1)*, edited by D. Bently, A. Muszynksa, and J. A. Cox, Bently Pressurized Bearing Corp., Mendin, NV, Aug. 2001.

[69]Kanki, H., Shibabe, S., and Goshima, N., "Destabilizing Force of Labyrinth Seal Under Partial Admission Condition," *Proceedings of the 2nd International Symposium on Stability Control of Rotating Machinery (ISCORMA-2)*, edited by A. Gosiewski and A. Muszynska, MAX MEDIA, Warsaw, Aug. 2003, pp. 278–288.

[70]Trutnovsky, K., "Contactless Seals, Foundations and Applications of Flows Through Slots and Labyrinths," NASA TT F 17, 352, 1977; also Beruhrungsfreie Diechtungen, *Grundlagen und Anwendungen der Stromung durch Spalte und Labyrinthe*, VDI-Verlag GmbH, Dusseldorf, Germany, 1964, pp. 1–300; also NASA TT F 17, 352, April 1977.

[71]Tseng, T., McNickel, A., Steinetz, B., and Turnquest, N., "Aspirating Seal GE90 Test," *2001 NASA Seal/Secondary Air System Workshop*, NASA/CP-2002-211911/Vol. 1, 2002, pp. 79–93.

[72]Ferguson, J. G., "Brushes as High Performance Gas Turbine Seals," American Society of Mechanical Engineers, International Inst., Paper 88-GT-182, Amsterdam, June 1988.

[73]Flower, R., "Brush Seal Development Systems," AIAA Paper 90-21443, July 1990.

[74]Stenietz, B. M., Hendricks, R. C., and Munson, J., "Advanced Seal Technology Role in Meeting Next Generation Turbine Engine Goals," NATO Research and Technology Agency, AVT-PPS-Paper 11, NASA/TM-1998-206961, E-11109, May 1998.

[75]Hendricks, R. C., Chupp, R. E., Lattime, S. B., and Steinetz, B. M., "Turbomachine Interface Sealing," *International Conference on Metallurgical Coatings and Thin Films*, American Vacuum Society, Paper 608, May 2005.

[76]Childs, D. W., Vance, J. M., and Hendricks, R. C. (eds.), "Rotordynamic Instability Problems in High-Performance Turbomachinery," *NASA Conference Publications*, NASA CP-2133, 1980; NASA CP-2250, 1982; NASA CP-2338, 1984; NASA CP-2409, 1985; NASA CP-2443, 1986; NASA CP-3026, 1988; NASA CP-3122, 1990; NASA CP-3239, 1993; NASA CP-3344, 1997; and "Instability in Rotating Machinery," NASA CP-2409, 1985.

[77]Hendricks, R. C., Liang, A. D., and Steinetz, B. M. (eds.), *Seals Code Development and Seal and Secondary Air Systems Workshops Conference Publications*, NASA CP-10124, 1992; CP-10136, 1993; CP-10181, 1995; CP-10198, 1996; CP-208916, 1998; CP-210472, 2000; CP-211208, 2001; CP-211911, 2002; CP-212458, 2003; and CP-211963, 2004.

[78]Chupp, R. E., and Holle, G. F., "Generalizing Circular Brush Seal Leakage Through a Randomly Distributed Bristle Bed," *Journal of Turbomachinery*, Vol. 118, Jan. 1996, pp. 153–161.

[79]Hendricks, R. C., Liang, A. D., Childs, D. W., and Proctor, M. P., "Development of Advanced Seals for Space Propulsion Turbomachinery," SAE TP Series 921028, Society of Automotive Engineers, April 1992; also NASA TM105659.

[80]Dinc, S., Demiroglu, M., Turnquist, N., Toetze, G., Maupin, J., Hopkins, J., Wolfe, C., and Florin, M., "Fundamental Design Issues of Brush Seals for Industrial Applications," *Journal of Turbomachinery*, Vol. 124, April 2002, pp. 293–300.

[81]Holle, G. F., and Krishnan, M. R., "Gas Turbine Engine Brush Seal Applications," AIAA Paper 90-2142, July 1990.

[82]Bhate, N., Thermos, A. C., Aksit, M. F., Demiroglu, M., and Kizil, H., "Non-Metallic Brush Seals for Gas Turbine Bearings," American Society of Mechanical Engineers, Paper GT-2004-54296, June 2004.

[83]Aksit, M. F., Dogu, Y., and Gursoy, M., "Hydrodynamic Lift of Brush Seals in Oil Sealing Applications," AIAA Paper 2004-3721, July 2004.

[84]Short, J. F., Basu, P., Datta, A., Loewenthal, R. G., and Prior, R. J., "Advanced Brush Seal Development," AIAA Paper 96-2907, July 1996.

[85]Chen, L. H., Wood, P. E., Jones, T. V., and Chew, J. W., "Detailed Experimental Studies of Flow in Large Scale Brush Seal Model and a Comparison with CFD Predictions," *Journal of Engineering for Gas Turbines and Power*, Vol. 122, No. 4, 1999, pp. 672–679; also American Society of Mechanical Engineers, Paper 99-GT-218, June 1999.

[86]Carslaw, H. S., and Jaeger, J. C., *Conduction of Heat in Solids*, 2nd ed., Oxford Press, Oxford, England, U.K., 1959, pp. 269, 270.

[87]Hendricks, R. C., Schlumberger, J., Braun, M. J., Choy, F. S., and Mullen, R. L., "A Bulk Flow Model of a Brush Seal System," American Society of Mechanical Engineers, Paper 91-GT-325, June 1991.

[88]Dogu, Y., and Aksit, M. F., "Brush Seal Temperature Distribution Analysis," American Society of Mechanical Engineers, TGTI Paper GT2005-69120, June 2005.

[89]Soditus, S. M., "Commercial Aircraft Maintenance Experience Relating to Current Sealing Technology," AIAA Paper 98-3284, July 1998.

[90]Proctor, M. P., and Delgado, I. R., "Leakage and Power Loss Test Results for Competing Turbine Engine Seals," American Society of Mechanical Engineers, Paper GT-2004-53935, June 2004.

[91]Basu, P., Datta., P., Johnson, A., Loewenthal, R., and Short, J., "Hysteresis and Bristle Stiffening Effects of Conventional Brush Seals," *Journal of Propulsion and Power*, Vol. 10, No. 4, 1994, pp. 569–575.

[92]Holle, G. F., Chupp, R. E., and Dowler, C. A., "Brush Seal Leakage Correlations Based on Effective Thickness," *Proceedings of the Fourth International Symposium on Transport Phenomena and Dynamics of Rotating Machinery*, Vol. A, Begell House, New York, 1992, pp. 296–304.

[93]Hendricks, R. C., Carlile, J. A., Yoder, D., and Braun, M. J., "Investigation of Flows in Bristle and Fiberglass Brush Seal Configurations," *Proceedings of the Fourth International Symposium on Transport Phenomena and Dynamics of Rotating Machinery*, Vol. A, Begell House, New York, 1992, pp. 315–325.

[94]Braun, M. J., and Kudriavtsev, V. V., "A Numerical Simulation of a Brush Seal Section and Some Experimental Results," *Transactions of the ASME*, Vol. 117, Jan. 1995, pp. 190–202.

[95]Turner, M. T., Chew, J. W., and Long, C. A., "Experimental Investigation and Mathematical Modeling of Clearance Brush Seals," American Society of Mechanical Engineers, Paper 97-GT-282, June 1997.

[96]Chen, L. H., Wood, P. E., Jones, T. V., and Chew, J. W., "An Iterative CFD and Mechanical Brush Seal Model and Comparisons with Experimental Results," American Society of Mechanical Engineers, Paper 98-GT-372, June 1998; see also *Journal of Engineering for Gas Turbines and Power*, Vol. 121, No. 4, 1999, pp. 656–661.

[97]Aksit, M. F., "Analysis of Brush Seal Bristle Stresses with Pressure Friction Coupling," American Society of Mechanical Engineers, Paper GT-2003-38718, June 2003.

[98]Mahler, F., and Boyes, E., "The Application of Brush Seals in Large Commercial Jet Engines," AIAA Paper 95-2617, July 1995.

[99]Chupp, R. E., Johnson, R. P., and Loewenthal, R. G., "Brush Seal Development for Large Industrial Gas Turbines," AIAA Paper 95-3146, July 1995.

[100]Chupp, R. E., Prior, R. J., and Loewenthal, R. G., "Update on Brush Seal Development for Large Industrial Gas Turbines," AIAA Paper 96-3306, July 1996.

[101]Bancalari, E., Diakunchak, I. S., and McQuiggan, G., "A Review of W501G Engine Design, Development and Field Operating Experience," American Society of Mechanical Engineers, Paper GT-2003-38843, June 2003.

[102]Diakunchak, I. S., Gaul, G. R., McQuiggan, G., and Southall, L. R., "Siemens Westinghouse Advanced Turbine Systems Program Final Summary," American Society of Mechanical Engineers, Paper GT-2002-30654, June 2002.

[103]Ingistov, S., "Compressor Discharge Brush Seal for Gas Turbine Model 7EA," *Journal of Turbomachinery*, Vol. 124, No. 2, April 2002, pp. 301–305.

[104]Hendricks, R. C., *Environmental and Customer Driven Seal Requirements*, NASA CP-10136, 1994, pp. 67–78.

[105]Schweiger, F. A., "The Performance of Jet Engine Contact Seals," *Lubrication Engineering*, Vol. 19, No. 6, 1963, pp. 232–238.

[106]Brown, P. F., *Status of Understanding for Seal Materials Tribology in the 80's*, NASA CP-23000-Vol-2, 1984, pp. 811–829.

[107]Lebeck, A. O., *Principles and Design of Mechanical Face Seals*, Wiley, New York, 1991.

[108]Steinetz, B. M., and Hendricks, R. C., "Aircraft Engine Seals," *Tribology for Aerospace Applications*, edited by E. V. Zaretsky, STLE SP-37, Society of Tribologists and Lubrication Engineers, Park Ridge, 1997, Chap. 9.

[109]Ludwig, L. P., "Self-Acting Shaft Seals," AGARD-CP-237, Paper 16, July 1978; also AGARD-AR-123 and NASA TM-73890, Jan. 1978.

[110]Dini, D., "Self Active Pad Seal Application for High Pressure Engines," AGARD-CP-237, Paper 17, Aug. 1978; also AGARD-AR-123, July 1978.

[111]Whitlock, D. C., "Oil Sealing of Aero Engine Bearing Compartments," AGARD-CP-237, Paper 7, Aug. 1978; also AGARD-AR-123, July 1978.

[112]Boyd, G. L., Fuller, F., and Moy, J., "Hybrid-Ceramic Circumferential Carbon Ring Seal," SAE Transactions, Vol. 111, Pt. 1, 2002, p. 522.

[113]Smith, C. R., "American Airlines Operational and Maintenance Experience with Aerodynamic Seals and Oil Seals in Turbofan Engines," AGARD-CP-237, Paper 5, Aug. 1978; also AGARD-AR-123, July 1978.

[114]Hendricks, R. C., Steinetz, B. M., Athavale, M. M., Przekwas, A. J., Braun, M. J., Dozozo, M. I., Choy, F. K., Kudriavtsev, V. V., Mullen, R. L., and von Pragenau, G. L., "Interactive Developments of Seals, Bearings, and Secondary Flow Systems with the Power Stream," *International Journal of Rotating Machinery*, Vol. 1, No. 3–4, 1995, pp. 153–185.

[115]Hendricks, R. C., et al., "Turbomachine Sealing and Secondary Flows Parts A, B and C," *Proceedings of the 2nd International Symposium on Stability Control of Rotating Machinery (ISCORMA-2)*, edited by A. Gosiewski and A. Muszynska, Aug. 2003, pp. 40–91; Unabridged versions NASA/TM-2004-211991/Part1, Part2, Part3, July 2004.

[116]Allcock, D. C. J., Ivey, P. C., and Turner, J. R., "Abradable Stator Gas Turbine Labyrinth Seals: Part 2 Numerical Modelling of Differing Seal Geometries and the Construction of a Second Generation Design Tool," AIAA Paper 2002-3937, July 2002.

[117]Alford, J. S., "Protecting Turbomachinery from Self-Excited Rotor Whirl," *Journal of Engineering for Power*, Series A, Vol. 87, Oct. 1965, pp. 333–344.

[118]Alford, J. S., "Protecting Turbomachinery From Unstable and Oscillatory Flows," *Journal of Engineering for Power*, Series A, Vol. 89, Oct. 1967, pp. 513, 528.

[119]von Pragenau, G. L., "Damping Seals for Turbomachinery," NASA TP-1987, March 1982.

[120]Vance, J., *Rotordynamics of Turbomachinery*, Wiley, New York, 1988.

[121]Childs, D. W., *Turbomachinery Rotordynamics Phenomena, Modeling, and Analysis*, Wiley, New York, 1993.

[122]Bently, D. E., Hatch, C. T., and Grissom, B., (eds.), *Fundamentals of Rotating Machinery Diagnostics*, Bently Pressurized Bearings Press, Minden, NV, 2002.

[123]Temis, Y. M., and Temis, M. Y., "Influence of Elastohydrodynamic Contact Deformations in Fluid Film Bearing on High-Speed Rotor Dynamics," *Proceedings of the 2nd International Symposium on Stability Control of Rotating Machinery (ISCORMA-2)*, edited by A. Gosiewski and A. Muszynska, Bently Pressurized Bearings Press, Minden, NV, 2003, pp. 150–159.

[124]Chen, J. P., "Unsteady Three-Dimensional Thin-Layer Navier–Stokes Solutions for Turbomachinery in Transonic Flows," Ph.D. Dissertation, Dept. of Aerospace Engineering, Mississippi State Univ., MS, Dec. 1991.

[125]Chew, J. W., "Predictions of Flow in Rotating Disk Systems Using the k-e Turbulence Model," American Society of Mechanical Engineers, Paper 88-GT-229, June 1988.

[126]Chew, J. W., Green, T., and Turner, A. B., "Rim Sealing of Rotor-Stator Wheelspaces in the Presence of External Flow," *Journal of Turbomachinery*, Vol. 114, April 1992, pp. 426–432, 439–445.

[127]Graber, D. J., Daniels, W. A., and Johnson, B. V., "Disk Pumping Test," AFWAL-TR-87-2050, Sept. 1987.

[128]Johnson, B. V., Daniels, W. A., Kaweki, E. J., and Martin, R. J., "Compressor Drum Aerodynamic Experiments with Coolant Injected at Selected Locations," *Journal of Turbomachinery*, Vol. 113, April 1991, pp. 272–280; see also Vol. 114, April 1992, pp. 426–432.

[129]Johnson, B. V., Mack, G. J., Paolillo, R. E., and Daniels, W. A., "Turbine Rim Seal Gas Path Flow Ingestion Mechanisms," AIAA Paper 94-2703, June 1994.

[130]Johnson, M. C., and Medlin, E. G., "Laminated Finger Seal with Logarithmic Curvature," U.S. Patent 5,108,116, April 1992.

[131]Arora, G. K., Proctor, M. P., Steinetz, B. M., and Delgado, I. R., "Pressure Balanced, Low Hysteresis, Finger Seal Test Results," NASA/TM-1999-209191, June 1999; also ARL-MR-457, AIAA Paper 99-2686, June 1999.

[132]Proctor, M. P., Kumar, A., and Delgado, I. R., "High-Speed, High-Temperature Finger Seal Test Results," *Journal of Propulsion and Power*, Vol. 20, No. 2, 2004, pp. 312–318.

[133]Proctor, M. P., and Delgado, I. R., "Leakage and Power Loss Test Results for Competing Turbine Engine Seals," NASA/TM-2004-213049, June 2004; also American Society of Mechanical Engineers, Paper GT-2004-53935.

[134]Braun, M., Pierson, H., Deng, D., Choy, F., Proctor, M., and Steinetz, B., "Structural and Dynamic Considerations Towards the Design of a Padded Finger Seal," AIAA Paper 2003-4698, July 2003.

[135]Proctor, M. P., and Steinetz, B. M., "Non-Contacting Finger Seal," U.S. Patent 6,811,154, Nov. 2004.

[136]Braun, M., Pierson, H., Deng, D., Choy, F., Proctor, M., and Steinetz, B., "Non-Contacting Finger Seal Developments," NASA/CP-2005-213655, Vol. 1, Nov. 2004, pp. 181–208.

[137]Flower, R. F. J., "Brush Seal with Asymmetrical Elements," U.S. Patent No. 5135237, Aug. 1992.

[138]Nakane, H., Maekawa, A., Akita, E., Akagi, K., Nakano, T., Nishimoto, S., Hashimoto, S., Shinohara, T., and Uehara, H., "The Development of High-Performance Leaf Seals," *Journal of Engineering and Gas Turbines and Power*, Vol. 126, April 2004, pp. 342–350.

[139]Steinetz, B. M., and Sirocky, P. J., "High Temperature Flexible Seal," U.S. Patent No. 4,917,302, April 1990.

[140]Gardner, J., "Pressure Balanced, Radially Compliant Non-Contact Shaft Riding Seal," *Seal/Secondary Flows Workshop*, Vol. 1, NASA CP 10198, Oct. 1997, pp. 329–348.

[141]Justak, J., "Hydrodynamic Brush Seal," U.S. Patent No. 6,428,009 B2, Aug. 2001.

[142]Justak, J., "Non-Contacting Seal Developments," NASA CP-2005-213655, Sept. 2005, pp. 101–114.

[143]Shapiro, W., "Film Riding Brush Seal," *2002 NASA Seal/Secondary Air System Workshop*, NASA/CP-2003-212458/Vol. 1, 2003, pp. 247–265.

[144]Braun, M. J., and Choy, F. K., "Hybrid Floating Brush Seal," U.S. Patent No. 5,997,004, 7 Dec. 1999.

[145]Kudriavtsev, V. V., Braun, M. J., and Choy, F. K., "Floating Brush Seal: Concept Feasibility Study," NASA SBIR Contract NAS3-27528, June 1995.

[146]Lattime, S. B., "A Hybrid Floating Brush Seal for Improved Sealing and Wear Performance in Gas Turbine Applications," Ph.D. Dissertation, Dept. of Mechanical Engineering, Univ. of Akron, OH, Dec. 2000.

[147]Lattime, S. B., Braun, M. J., Choy, F. K., Hendricks, R. C., and Steinetz, B. M., "Rotating Brush Seal," *The International Journal of Rotating Machinery*, Vol. 8, No. 2, 2002, pp. 153–160.

[148]Pope, A. N., "Gas Bearing Sealing Means," U.S. Patent No. 5,284,347, 8 Feb. 1994.

[149]Hwang, M. F., Pope, A. N., and Shucktis, B., "Advanced Seals for Engine Secondary Flowpath," *Journal of Propulsion and Power*, Vol. 12, No. 4, 1996, pp. 794–799.

[150]Wolfe, C. E., Bagepalli, B., Turnquist, N. A., Tseng, T. W., McNickle, A. D, Hwang, M. F., and Steinetz, B. M., "Full Scale Testing and Analytical Validation of an Aspirating Face Seal," AIAA Paper 96-2802, July 1996.

[151]Bagepalli, B., Imam, I., Wolfe, C. E., Tseng, T., Shapiro, W., and Steinetz, B., "Dynamic Analysis of an Aspirating Seal for Aircraft Engine Application," AIAA Paper 96-2803, July 1996.

[152]Turnquist, N. A., Bagepalli, B., Reluzco, G., Wolfe, C. E., Tseng, T. W., McNickle, A. D., Dierkes, J. T., Athavale, M., and Steinetz, B. M., "Aspirating Face Seal Modeling and Full Scale Testing," AIAA Paper 97-2631, July 1997.

[153]Turnquist, N. A., Tseng, T. W., McNickle, A. D., Dierkes, J. T., Athavale, M., and Steinetz, B. M., "Analysis and Full Scale Testing of an Aspirating Face Seal with Improved Flow Isolation," AIAA Paper 98-3285, July 1998.

[154]Turnquist, N. A., Tseng, T. W., McNickle, A. D., and Steinetz, B. M., "Angular Misalignment Analysis and Full Scale Testing of an Aspirating Seal," AIAA Paper 99-2682, June 1999.

[155]McNickel, A. D., and Etsion, I., *Improved Main Shaft Seal Life in Gas Turbines Using Laser Surface Texturing*, NASA/CP-2002-211911/Vol. 1, Oct. 2002, pp. 111–126.

[156]von Pragenau, G. L., "Damping Seals for Turbomachinery," NASA CP-2372, April 1985, pp. 438–451.

[157]von Pragenau, G. L., "From Labyrinth Seals to Damping Seals/Bearings," *Proceedings of the 4th International Symposium on Transport Phenomena and Dynamics of Rotating Machinery (ISROMAC-4)*, CRC Press, Boca Raton, FL, 1993, pp. 234–242.

[158]Yu, Z., and Childs, D., "A Comparison of Experimental Rotordynamic Coefficients and Leakage Characteristics for Hole Pattern Gas Damper Seals and a Honeycomb Seal," NASA CP-3344, 1997, pp. 77–93.

[159]Etsion, I., "A New Concept of Zero-Leakage Noncontacting Mechanical Face Seal," *Journal of Tribology*, Vol. 106, July 1984, pp. 338–343.

[160]Young, L. A., and Lebeck, A. O., *Lubrication Engineering*, Vol. 45, No. 5, May 1989, pp. 322–329.

[161]Flaherty, A., Young, L., and Key, B., "Seals Developments at Flowserve Corporation," NASA/CP-2004-212963, Vol. 1, 2004, pp. 229–238.

[162]Salehi, M., Heshmat, H., Walton, J. F., and Cruszen, S., "The Application of Foil Seals to a Gas Turbine Engine," AIAA Paper 99-2821, June 1999.

[163]Heshmat, H., "Compliant Foil Seal," U.S. Patent 6505837 B1, 14 June 2003; 19 Aug. 2003.

[164]Nalotov, O., "Step of Pressure of the Steam and Gas Turbine with Universal Belt," U.S. Patent 6,632,069 B1, 14 Oct. 2003.

[165]Lattime, S. B., and Steinetz, B. M., "Test Rig for Evaluating Active Turbine Blade Tip Clearance Control Concepts," NASA/TM-2003-212533, 2003; *Journal of Propulsion and Power*, Vol. 21, No. 3, 2005, pp. 552–563.

[166]Dunkelberg, K., "Commercial Airplane Nacelle Component (Engine Externals) Certification and Typical Temperature Exposure," *Proceedings of the 7th International Symposium on Transport Phenomena and Dynamics of Rotating Machinery (ISROMAC-7)*, edited by A. Muszynska, J. A. Cox, and D. T. Nosenzo, Bird Rock Publ., Minden, NV, Feb. 1998; also NASA Advanced Subsonic Technology (AST) 028, Oct. 1998.

[167]Stoner, B. L., "The Importance of Engine Externals' Health," *Proceedings of the 7th International Symposium on Transport Phenomena and Dynamics of Rotating Machinery (ISROMAC-7)*, edited by A. Muszynska, J. A. Cox, and D. T. Nosenzo, Bird Rock Publ., Minden, NV, Feb. 1998, p. 572.

[168]Zaretsky, E. V., Hendricks, R. C., and Soditus, S., "Weibull-Based Design Methodology for Rotating Aircraft Engine Structures," *Proceedings of the 9th International Symposium on Transport Phenomena and Dynamics of Rotating Machinery (ISROMAC-9)*, edited by Y. Tsujimoto, Pacific Center of Thermal-Fluids Engineering, Honolulu, HI, Feb. 2002.

[169]Davis, D. Y., and Stearns, E. M., "Energy Efficient Engine Flight Propulsion System Final Design and Analysis," NASA CR-168219, Aug. 1985.

[170]Athavale, M. M., Przekwas, A. J., Hendricks, R. C., and Steinetz, B. M., "Development of a Coupled, Transient Simulation Methodology for Interaction Between Primary and Secondary Flowpaths in Gas Turbine Engines," AIAA Paper 97-2727, July 1997.

[171]Athavale, M. M., Przekwas, A. J., Hendricks, R. C., and Steinetz, B. M., "Coupled Transient Simulations of the Interaction Between Power and Secondary Flowpaths in Gas Turbines," AIAA Paper 98-3290, July 1998.

[172]Janus, J. M., "Advanced 3-D CFD Algorithm for Turbomachinery," Ph.D. Dissertation, Dept. of Aerospace Engineering, Mississippi State Univ., MS, May 1989.

[173]Janus, J. M., and Horstman, H. Z., "Unsteady Flow-Field Simulation of Ducted Prop-Fan Configurations," AIAA Paper 92-0521, Jan. 1992.

[174]Campbell, D. A., "Gas Turbine Disk Sealing System Design," AGARD-CP-237 (AGARD-AR-123), Paper 18, July 1978.

[175]Teramachi, K., Manabe, T., Yanagidani, N., and Fujimura, T., "Effect of Geometry and Fin Overlap on Sealing Performance of Rims Seals," AIAA Paper 2002-3938, July 2002.

[176]Wellborn, S. R., and Okiishi, T. H., "Effects of Shroud Stator Cavity Flows on Multistage Axial Compressor Performance," NASA CR-198536, Oct. 1996.

[177]Hall, E. J., and Delaney, R. A., "Investigation of Advanced Counterrotation Blade Configuration Concepts for High Speed Turboprop Systems," *Task 5—Unsteady Counterrotation Ducted Propfan Analysis Computer Program User's Manual*, NASA CR-187125, Jan. 1993.

[178]Hall, E. J., and Delaney, R. A., "Investigation of Advanced Counterrotation Blade Configuration Concepts for High Speed Turboprop Systems," *Task 5—Unsteady Counterrotation Ducted Propfan Analysis Final Report*, NASA CR-187126, Jan. 1993.

[179]Hall, E. J., and Delaney, R. A., "Investigation of Advanced Counterrotation Blade Configuration Concepts for High Speed Turboprop Systems," *Task 7—ADPAC User's Manual*, NASA CR-195472 (NASA Contract NAS3-25270), April 1996.

[180]Adamczyk, J. J., Celestina, M. L., and Greitzer, E. M., "The Role of Tip Clearance in High-Speed Fan Stall," *Journal of Turbomachinery*, Vol. 115, No. 1, 1993, pp. 29–39.

[181]Feiereisen, J. M., Paolillo, R. E., and Wagner, J., "UTRC Turbine Rim Seal Ingestion and Platform Cooling Experiments," AIAA Paper 2000-3371, July 2000.

[182]Athavale, M. M., Przekwas, A. J., and Hendricks, R. C., "A Numerical Study of the Flow-Field in Enclosed Turbine Disk-Cavities in Gas Turbine Engines," *Proceedings of the 4th International Symposium on Transport Phenomena and Dynamics of Rotating Machinery (ISROMAC-4)*, Vol. 1, edited by W.-J. Yang and J. H. Kim, Begell House, Boca Raton, New York, 1992, pp. 92–101.

[183]Athavale, M. M., Przekwas, A. J., Hendricks, R. C., and Steinetz, B. M., "Numerical Analysis of Intra-Cavity and Power-Stream Flow Interaction in Multiple Gas-Turbine Disk-Cavities," American Society of Mechanical Engineers, Paper 95-GT-325, June 1995.

[184]Virr, G. P., Chew, J. W., and Coupland, J., "Application of Computational Fluid Dynamics to Turbine Disc Cavities," *Journal of Turbomachinery*, Vol. 116, No. 4, 1994, pp. 701–708.

[185]Ho, Y. H., Athavale, M. M., Forry, J. M., Hendricks, R. C., and Steinetz, B. M., "Numerical Simulation of Secondary Flow in Gas Turbine Disc Cavities, Including Conjugate Heat Transfer," American Society of Mechanical Engineers, Paper 96-GT-67, June 1996.

[186]Athavale, M. M., Ho, Y. H., and Przekwas, A. J., "Analysis of Coupled Seals, Secondary and Powerstream Flow Fields in Aircraft and Aerospace Turbomachines," NASA Contract NAS3-27392, Final Report, Dec. 1999.

[187]Smout, P. D., Chew, J. W., and Childs, P. R. N., "ICAS–GT: A European Collaborative Research Programme on Internal Cooling Air Systems for Gas Turbines," Paper GT-2002-30479, June 2002.